NORTHWESTERN UNIVERSITY

EFFECT OF CRACK WIDTH ON CARBONATION: IMPLICATIONS FOR CRACK-DATING

A THESIS

SUBMITTED TO THE GRADUATE SCHOOL IN PARTIAL FULFILLMENT OF THE REQUIREMENTS

For the Degree of

MASTERS OF SCIENCE

Field of Civil Engineering

By
Laura E. Sullivan-Green

Evanston, IL
March, 2005

Abstract

**Effects of Crack Width on Carbonation Penetration:
Implications for Crack-Dating**

Laura E. Sullivan-Green

Carbonation, a neutralizing reaction in cement paste, can be used to date cracks in cementitious materials. Currently, comparison between two cracks is the only method available to predict a relative age with carbonation. These two crack studies require a crack of known age in a similar material with similar exposure to the crack of unknown age. This thesis presents measurements of the extent of carbonation in cracks of varying width as a first step in laying a quantitative formulation for the use of carbonation in crack dating. This information will allow comparisons between two cracks of more similar exposure, but different crack width, which can expand the applicability of this dating method. Accelerated reaction rates were produced with a pure carbon dioxide environment and cement mixes with high contents of fly ash and are evaluated for economy and applicability. Relationships between carbonation penetration and crack width were established from these measurements.

Acknowledgements

I would first like to thank my advisor, Dr. Charles H. Dowding. The road to completing this project and thesis was quite long and a bit bumpy, but in the end the product was superb. This paper wouldn't be what it is without your guidance and support. Thank you for helping me find my way.

In addition, a very special thanks to Mr. Bill Hime. Your continuous support during this project is indescribable. This project would have been even more difficult without your expertise and willingness to share it with a student who called you out of the blue one day. Your assistance on this project and those to follow is greatly appreciated.

Any project has those who work behind the scenes. I want to thank them for their part in this work. Each had a seemingly small, but vital role in the progression of this work. Thank David Ventre, John Chirayil, Margaret Reed, and Steve Albertson, for all their hard work and patience with my endless questions.

My experience at Northwestern have left a lasting impression on my life and helped me realize the type of engineer and professor I want to be. I want to especially thank professors Dr. Charles H. Dowding, Dr. Richard J. Finno and Dr. Raymond J. Krizek for encouraging me to think outside the box. Also, thanks to my classmates, past and present, for being there to share in the chaos that is graduate school.

On a personal note, I would like to thank my parents, Con and Linda Sullivan. They instilled in me the drive to achieve and the encouragement to see it through. For that I am truly grateful. Finally, I want to say thank you to my husband, Chris Green. Without your support and love, I wouldn't be here today. I love you.

Table of Contents

Title	Page
Abstract	ii
Acknowledgements	iii
List of Figures	vi
List of Tables	viii
Chapter 1: Introduction	1
Chapter 2: Background	6
Chemistry of Carbonation	7
Measuring Carbonation	8
Factors Affecting Carbonation	10
Time-Rate Relationships	13
Chapter 3: Experiment	15
Laboratory Setup	15
Cement Mixes	20
Sample Preparation	21
Incubation Conditions	24
Testing Procedure	28
Experimental Improvements	37
Error Analysis- Round 2	43
Chapter 4: Results	46
Round 1- Taped, Test Surface Parallel to Material Face	46
Carbonation Penetration and Crack Depth	59
Round 2- Painted, Testing Surface Perpendicular to Material Surface	61
Analysis of Continuous Carbonation Fronts	69
Chapter 5: Analysis	72
Overall Observations	72
Statistical Significance of Observations	73
Trends in Carbonation Penetration with Depth	74
Precision of Data	86
Relationship Between Laboratory and Field Conditions	87
Linearity of Relationships	90
Chapter 6: Conclusions	94
Experimental Technique: Effect of Humidity	95
Wider Cracks Facilitate Carbonation Penetration	96
Applicability of Carbonation as an Age-Dating Technique	96
Future Work	97

Table of Contents, cont.

References 99

Appendices 101
- a. Round 1 Data 102
- b. Round 2 Data 110
- c. Relative Humidity Data 116
- d. Gas Chromatography Data 118
- e. Concrete Strength Data 119

List of Figures

Figure	Title	Page
2.1	Photo Showing Phenolphthalein Coloring on Concrete.	9
2.2	Schiessl's Figures Showing Carbonation in a Crack.	14
3.1	Laboratory Set-up.	17
3.2	Sample Set-up, Round 1.	18
3.3	Sample Set-up, Round 2.	19
3.4	Gas Flow for Round 2 Set-up.	19
3.5	Cubes Showing Saw Cut and Crack Locations.	22
3.6	Photo Showing Saw Cut Samples.	22
3.7	Wire Location in Samples.	23
3.8	Photo of Wire Placement.	23
3.9	Paint Coverage for Round 2.	24
3.10	Drawdown Curve for CO_2 Concentration.	25
3.11	Relative Humidity Changes in Round 1.	26
3.12	Relative Humidity Changes in Round 2.	27
3.13	Variation in Carbonation Penetration with Depth into Crack.	29
3.14	Break Locations for Round 1 Samples.	30
3.15	Break-Away Showing Testing Surface for Round 1.	31
3.16	Photo of Round 1 Readings.	31
3.17	Regression of Carbonation Fronts in Round 1 Samples.	32
3.18	Photo with Area Calculations Shown.	32
3.19	Break Locations for Round 2 Samples.	33
3.20	Break-Away Showing Testing Surface for Round 2.	34
3.21	Photo of Round 2 Readings.	35
3.22	Round 2 Sample Showing Inward Curve Carbonation Front.	36
3.23	Round 2 Sample Showing Outward Curve Carbonation Front.	37
3.24	Variation in Break Location in Round 1 Samples.	39
3.25	Variation in Carbonation Front over Small Distances.	39
3.26	Paint Cover, Break Locations, and Wire Placement in Round 2.	42
3.27	Variation in Crack Location in Round 2 Samples.	45
4.1	Average Carbonation Penetration vs. Crack Width, 10 mm Depth, Round 1.	48
4.2	Average Carbonation Penetration vs. Crack Width, 10 mm Depth, Round 1, Minus H/L.	48
4.3	Average Carbonation Penetration vs. Crack Width, 20 mm Depth, Round 1.	51
4.4	Average Carbonation Penetration vs. Crack Width, 20 mm Depth, Round 1, Minus H/L.	51
4.5	Maximum Carbonation Penetration vs. Crack Width, 10 mm Depth, Round 1.	53
4.6	Maximum Carbonation Penetration vs. Crack Width, 10 mm Depth, Round 1, Minus H/L.	53

List of Figures, cont.

4.7	Maximum Carbonation Penetration vs. Crack Width, 20 mm Depth, Round 1.	54
4.8	Maximum Carbonation Penetration vs. Crack Width, 20 mm Depth, Round 1, Minus H/L.	54
4.9	Minimum Carbonation Penetration vs. Crack Width, 10 mm Depth, Round 1.	56
4.10	Minimum Carbonation Penetration vs. Crack Width, 10 mm Depth, Round 1, Minus H/L.	56
4.11	Carbonated Area as Percentage of Total Area vs. Crack Width, Round 1.	58
4.12	Carbonation Front Progression as Depth into the Crack Increases, Round 1.	60
4.13	Average Carbonation Penetration vs. Crack Width, 0 mm Depth, Round 2.	62
4.14	Average Carbonation Penetration vs. Crack Width, 3 mm Depth, Round 2.	62
4.15	Average Carbonation Penetration vs. Crack Width, 5 mm Depth, Round 2.	64
4.16	Average Carbonation Penetration vs. Crack Width, 5 mm Depth, Round 2, Minus H/L.	64
4.17	Average Carbonation Penetration vs. Crack Width, 10 mm Depth, Round 2.	66
4.18	Average Carbonation Penetration vs. Crack Width, 10 mm Depth, Round 2, Minus H/L.	66
4.19	Maximum Carbonation Penetration into Crack vs. Crack Width, Round 2.	68
4.20	Maximum Carbonation Penetration into Crack vs. Crack Width, Round 2, Minus H/L.	68
4.21	Carbonation Front Progression as Depth into the Crack Increases, Round 2.	70
5.1	Comparison of Trends With and Without Extreme Values.	73
5.2	Average Carbonation Penetration lines from Round 1 and Round 2.	75
5.3	Comparison of Linear and Exponential Best-Fit Lines for Carbonation Fronts.	78
5.4	Reduction of Standard Deviation When Rectangular-Shaped Fronts are Eliminated.	80
5.5	Differences in Exposure due to Saw Cut Location.	82
5.6	Comparison of Carbonation Penetration vs. Crack Width between Rounds 1 and 2.	83
5.7	Drawing Comparing Carbonation Penetration between Round 1 and Round 2.	85
5.8	‘S’ Shaped Carbonation Penetration Curve for Infinite Samples.	92
5.9	Carbonation Front Shape When Carbonation Rates Reach Near Zero.	92

List of Tables

Table	Title	Page
5.1	Variation in Standard Deviation about Linear and Exponential Best Fit Lines.	77
5.2	Data Ranges at 10 mm Below the Material Face for Round 1 and Round 2.	81
5.3	Data Ranges for all Depths Below Material Face for Round 2.	86

Chapter 1
Introduction

Research described herein lays the foundation for the use of the process of carbonation of cementitious construction materials as a means of determining the age of cracks. Crack age is significant because billions of dollars are being spent on damage claims, alleging that cracking was produced by some recent adjacent anthropomorphic activity such as traffic, construction, blasting, etc. or some recent natural phenomena, such as earthquake, hurricane, flood, etc. Some time after the disturbance the concerned party inspects the facility and notices cracks. The observer often seeks compensation for the cracks from those who caused the disturbance or those who insure against associated perils or hazards.

Cracking is natural in most construction materials. Often cracking is inappropriately defined as ‘damage’, leading many to believe that cracking is caused by

an event in proximity to the structure and that any cracking has a negative impact on a structure's integrity. Most cracking present in structures can be categorized as threshold or cosmetic cracking, indicating that the cracks are small, hairline sized cracks that do not have any impact on the performance of the structure, but are a nuisance to the owner.

Billions of dollars are allocated for damage when natural disasters strike, such as the $15 billion allocated when the Northridge earthquake struck southern California in 1994 (Aurelius, 1994). It is unclear how much of that $15 billion was dispensed for minor damage to residential and commercial buildings, but even if only a small portion of that money was allocated for minor damage, it is still a considerable amount. Blasting companies spend millions more on insurance premiums and pre-blasting investigation to protect themselves from lawsuits claiming blasting events caused cracking in homes. If one damage-related lawsuit is assumed for every four million people in the United States and that each case costs an average $500,000, $35 million more is spent on investigation, arbitration, and litigation each year.

Once cracking becomes the issue, attention then turns to what caused the crack, and the age of the crack more often than not plays a central role in the investigation. Unfortunately, crack-dating methods are limited and those that are most often used are subjective and limited to certain materials. The most-often employed technique for crack-dating is the sleuthing method. This method involves examining the crack and estimating an age based on what is in the crack. The sleuthing method is based on the theory of cross-cutting: If an object is crossed or cut by another or if it is filled by

another, it is older than that which cuts across or fills it. For example, paint on the inside edge of the crack indicates that the crack is at least as old as the last coat of paint. For exterior cracks, one can examine the microscopic debris in the crack, including dirt, anthropomorphic fibers, and biological matter. With this method, the examiner must be careful to perform the analysis as soon as possible after the initial observation to ensure that the evidence is not tainted by what could have accumulated between the discovery and the examination. Sleuthing only yields a relative age (i.e. the crack is older than a painting or patching and younger than another, i.e. patching).

The method explored herein permits crack-dating by measuring depth of carbonation in cementitious materials. Carbonation is a neutralizing reaction in cement paste that reduces the pH of the cement paste from above 12 to less than 9 (Parrott, 1987). In its simplest description, the method compares the depth of carbonation through the material face to that through the crack surface. If the carbonation through the crack surface is less than that through the material face, then the crack is younger than the material. This method, though applied in crack dating analyses, has limitations that are often overlooked. Simple comparison between the two carbonation depths does not consider that the exposure of the crack surface to circulating air is far less than the material face and as such the carbonation through the material face should always be greater than that through the crack surface. Second, surface texture plays a role in the carbonation rates through a surface. The local densities near the surfaces of the crack and material face are different due to finishing techniques applied to the material face. A more accurate method of crack-dating using carbonation involves comparing a crack of

known age with similar exposure and width to the crack of concern. This method allows a ratio comparison to determine the age since the cracks have similar characteristics and exposure.

Presentation of this thesis was divided into 6 chapters, including this introduction and a background chapter, which introduces basic information about the carbonation reaction, its measurement, and prediction of carbonation depth. The remaining 4 chapters, entitled Experiment, Results, Analysis, and Conclusions are summarized in the following paragraphs.

Specifically this thesis describes research undertaken to develop procedures to systematically measure carbonation rates under inexpensive, accelerated conditions for the purpose of crack dating. Acceleration is needed to compress the time span from "years" in the field to months in the laboratory, a time span easily managed by graduate students during their tenure. Rates of carbonation have been accelerated by employing a 100% CO_2 environment rather than at 0.03%, the concentration present in the atmosphere. To further accelerate the process, specimens were prepared with high contents of fly ash, which also quickens the rate of carbonation.

This accelerated procedure was employed to determine the effect of crack width on the penetration of carbonation through the crack surface. To measure this effect, mortar blocks were fractured and wired open at varying widths. The blocks were

incubated in a carbon dioxide chamber and allowed to carbonate. Cracks in the blocks were wetted with phenolphthalein solution to indicate carbonation penetration.

The "Results" and "Analysis" chapters present and compare carbonation penetration through the crack surface and carbonation depth from the material face to the crack width. The data determined that crack width does impact carbonation depth through a crack surface and that the relationship between crack width and carbonation penetration is linear. Trends identified in the data have at or near one standard deviation confidence about an overall average carbonation penetration line. Carbonation fronts with respect to depth into the crack also showed that a linear relationship is sufficient to describe the front after measurements that include carbonation through the material face were eliminated.

In conclusion, the research presented herein demonstrates that discrepancies from comparison of cracks of different widths could be compensated for by assuming a linear relationship between carbonation depth and crack width, which expands the application of the comparison technique by allowing comparison of cracks with more similar exposure that do not have the same crack width. The technique, however, still requires comparison to a crack of known age, which is not easily obtainable information. More research must be undertaken to be able to determine the age of a crack based solely on carbonation through its surface.

Chapter 2
Background

Carbonation is a reaction between hydroxides in cementitious paste and carbonic acid that form carbonates. Carbonic acid can be introduced in the pores by dissolution of gaseous CO_2 in pore water or by direct penetration of acidic rain water. Cementitious pastes are quite basic (pH as high as 14) and the reaction reduces the pH of the paste to less than 9 when fully carbonated. Carbonates formed in the carbonation reaction are larger molecules than the hydroxides, thereby increasing the density of the cement paste and, locally, the strength (Neville, 2003). Reduction of the cement paste pH is a concern for concrete reinforcing steel because it is more susceptible to corrosion at lower pH's. As a result, carbonation studies most often concern themselves with this potential corrosion and thus solely with depth of carbonation from the exposed material face.

Chemistry of Carbonation

Often the carbonation reaction is misrepresented in the literature (Hime, 2004). Many authors state carbonation as the reaction between carbon dioxide and calcium hydroxide that produces calcium carbonate. Some do state that water must be present and though this statement is true, it is not accurate. The actual chemistry involved is often overlooked. In order to reduce the pH of the cement, all the basic components in the cement paste must react, not just the calcium hydroxide. The most important alkali components that must react to reduce the pH are sodium and potassium hydroxide (Hime, 2004). Second, water is critical to the reaction since it is the carbonic acid produced from the combination of water and carbon dioxide that produces the reactant pathway with the alkalis. The carbonation reaction is most thoroughly described as carbonic acid formed from carbon dioxide in the air dissolved into water reacting with alkaline components of the concrete to neutralize them (Hime, 2004).

Cement chemistry is complicated and identifying the exact reactions is not always possible because of variability in the cement composition, as well as the composition of other components of the cement mix, for example addition of plasticizers or pozzolanic material. However, chemical hydration reactions of interest in carbonation are those which form calcium, potassium, and sodium hydroxides and include:

$$3CaO{\cdot}SiO_2 + 6\ H_2O \rightarrow 3CaO{\cdot}2SiO_2{\cdot}3H_2O + 3Ca(OH)_2$$

$$Na_2SO_4 + Ca(OH)_2 \rightarrow CaSO_4 + 2NaOH$$

$$K_2SO_4 + Ca(OH)_2 \rightarrow CaSO_4 + 2KOH$$

(Schiessl, 1988). These hydroxide molecules are those that react with the carbonic acid and produce carbonates. Pozzolanic materials, i.e. fly ash and slag, change the chemical reactions during hydration. Pozzolans react with the hydroxide components and reduce the amount of hydroxides present in the cement paste. The pozzolanic reaction with calcium hydroxide is:

$$3Ca(OH)_2 + 2SiO_2 \rightarrow 3CaO{\cdot}2SiO_2{\cdot}3H_2O$$

(Schiessl, 1988).

Measuring Carbonation

No standard method to measure carbonation exists, though several publications do discuss methods of analysis, e.g. Rilem Recommendation CPC 18, ASTM C 856, etc. (Neville, 2003). Several methods are available to measure carbonation, the most common method of which is spraying freshly broken surfaces with 1% or 2% phenolphthalein solution. The surface where the pH is greater than 9 turns magenta and a gradually lightening shades of pink for pH of 8-9. Figure 2.1 shows a concrete surface that has been sprayed with phenolphthalein solution. The location where the surface is colorless represents the depth to which full or nearly full carbonation has been achieved and the pH of the cement is at or below ~8. The phenolphthalein method is quick and economical, though it does not identify areas of partial carbonation. Rainbow indicators, which produce various colors for small ranges of pH, can be used in a similar method, but by observation the rainbow indicators require more subjective analysis in determining the location of the color changes and the colors are not as vivid as the phenolphthalein solution.

Figure 2.1. Photo of concrete surface sprayed with phenolphthalein. Magenta color indicates pH greater than 9, which colorless area indicates pH less that 9.

Phenolphthalein testing can be sufficient to determine the extent of carbonation, but it is critical to understand what is actually being measured. The test does not indicate the level of carbonation in the cement paste, but only the location where the pH is above or below 9. A pH of 9 or lower is generally accepted as 'fully carbonated' (Hime, 2004). A pH greater than 9, however, is not an indicator that no carbonation has occurred. In fact, as much as 90% of the cement paste can be carbonated and still have a pH greater than 9 (Hime, 2004).

Other methods of determining the extent or depth of carbonation are available. Measuring the pH of pore solutions, thin-section examination with petrographic microscope, x-ray diffraction, and infra-red absorption have been identified by Parrott

(1987); however, these methods require a significant amount of time and often expensive equipment. Campbell (1991) noted that when comparing results between pH-indicators and thin sections, the results are not significantly different. As such, pH-indicator tests are sufficient for crack-dating research.

Carbonation measurements are typically made perpendicular to the material face in order to observe the depth of carbonation. Carbonation measurements should be made on freshly broken surfaces. Broken surfaces are preferred over saw cuts because saw-cut surfaces can produce erroneous results. Saw cuts are often made with wet saws using water as a lubricant and the water used to make the cut can leach alkalis from both portions of the surface and inside the concrete that are not fully carbonated. This leaching is most evident in observing pink shades on aggregate surfaces exposed on the test surface. Surfaces should be freshly broken since new surfaces have little chance to react in their newly exposed state to the atmosphere.

Factors Affecting Carbonation of Cement Paste

Carbonation rates are greatly affected by both internal and external factors. Externally, the temperature, external relative humidity, carbon dioxide concentration, exposure, and material finishes are important. Internally, the relative humidity and cement paste composition are the most important factors. Optimal conditions for increased carbonation rates include temperatures near 20°C, relative humidity in the range of 50-70%, increased carbon dioxide volumes, water/cement or water/binder ratios at or above 0.6, and use of fly ash or slag as a cement replacement.

Internal factors tend to have the greatest impact on carbonation rates. The most important is the water/cement (w/c) or water/binder ratio of the concrete. Water/binder ratios are a more accurate description for mixes that replace cement with other cementitious materials, i.e. fly ash or slag; however, herein w/c will be used, as it is more commonly reported. Carbonation is often greatly reduced at w/c ratios below ~0.4 and a reduction in carbonation depth of approximately 50% is seen when the w/c ratio is reduced from 0.6 to 0.4 (Meyer, 1968; Parrott, 1987). Locally the w/c or water/binder ratio is not uniform. Local variations in w/c ratio cause local variation in carbonation rates, though they are difficult to quantify.

Other mix design factors that affect carbonation rates include replacement of cement with other binders, such as fly ash or slag. Addition of these pozzolanic materials tends to increase carbonation rates (Parrott, 1987), at least initially. In some instances, it is argued that addition of fly ash to concrete mixtures can increase resistance to carbonation over longer periods of time (Joshi and Lohtia, 1997). With the use of pozzolanic materials, hydroxide components in the cement paste are reduced. With this reduction, carbonation rates would ideally increase, as there is less material to react with, but pozzolans also have the effect of decreasing permeability of the cement paste. If the reduction in permeability overcomes the reduction in hydroxide components, then the overall carbonation is reduced.

Interior relative humidity of the samples can also impact carbonation rates. Carbonation rates are minimal at 100% relative humidity because CO_2 cannot easily

penetrate saturated pores. During curing, concrete releases water into the pore spaces and often in research settings, concrete is cured in a humidity room. As a result the interior relative humidity tends to be initially high, but decreases as the age of the concrete increases. The concrete tends to dry from the outside to the inside. Carbonation rates, therefore, are higher when the exterior portions of the concrete are reacting and they tend to decrease as depth into the sample increases. The decrease in carbonation rates is not only due to the increasing relative humidity, but also to the decreased diffusivity due to lower permeability of carbonated concrete and to the increased distance the diffused gas must travel to reach the reaction site.

External conditions that affect carbonation rates include environmental conditions and material conditions. Temperature and humidity, as mentioned above, for maximum carbonation range from 20-25°C and 50-70%, respectively. Carbonation rates decrease on either side of these rates. At or near 0% or 100% relative humidity carbonation rates are considered negligible. Indoor climate-controlled conditions tend to fall within these ideal ranges, allowing for optimal, more consistent carbonation rates. Variability of outdoor temperature and humidity can cause fluctuation in carbonation rates and therefore tend to decrease carbonation rates when compared to indoor rates. Another outdoor factor that affects carbonation rates is precipitation. If water, whether in the form of rain, ice, or snow, wets the cementitious material, the diffusion rate of carbon dioxide is reduced and carbonation rates are further reduced.

Another external factor affecting carbonation rates is treatment of the cement surface. Finishing cement surfaces, whether smoothing or texturizing, tends to locally densify the concrete at the surface. Increasing density decreases the permeability of the concrete, thereby decreasing carbonation rates. Other finishing techniques, including use of paints or sealants, also decreases carbonation rates by decreasing the ability of carbon dioxide to permeate the concrete. This variation in placement of cementitious materials is one of the most difficult factors to quantify when discussing carbonation rates.

Time-Rate Relationships

Relationships have been developed for estimating carbonation depth from a material face (Schiessl, 1988, Parrott 1987), but they: 1) can require too many factors to be practical, 2) are empirical or 3) do not consider all factors that can affect carbonation rates. Schiessl's equations require measurement of diffusion masses of CO_2, concentrations of CO_2 inside and outside the sample, and a diffusion constant that varies as relative humidity changes. The equations also are not dependent upon temperature, curing, and moisture and only consider mix design with respect to the diffusion constant. Often there is too little information to completely define all the required variables.

Equations presented by Parrott tend to follow the format $D = A*t^n$, where D is the depth of carbonation, t is the time of exposure and n is typically 0.5, but has been reported as 0.25 (Nagataki, 1986) and 0.35 (Nischer, 1984). The coefficient A is a function of curing, exposure, mixture design, etc. depending upon the specific experiments (Parrott, 1987; Nagataki, 1986; Nishi, 1962). In all cases, this coefficient

assumes entirely uniform conditions. Uniform conditions never occur in practice, but the formula may remain valid for slightly varying conditions (Hime, 2004). These formulas also tend not to consider temperature, CO_2 concentrations, moisture conditions, curing, density, or connectedness of pores. Some consider mix design with respect to w/c ratios, additives such as fly ash, surface finish, and type of exposure (internal or external), while others do not.

All relationships presented in Parrott consider freely exposed surfaces without cracks. Schiessl considers carbonation in a crack, but only the depth of carbonation as measured from the material face, since his research focused on the proximity of carbonation fronts to reinforcing steel for the purpose of corrosion analysis. Figure 2.2 shows Schiessl's consideration of carbonation through a crack surface.

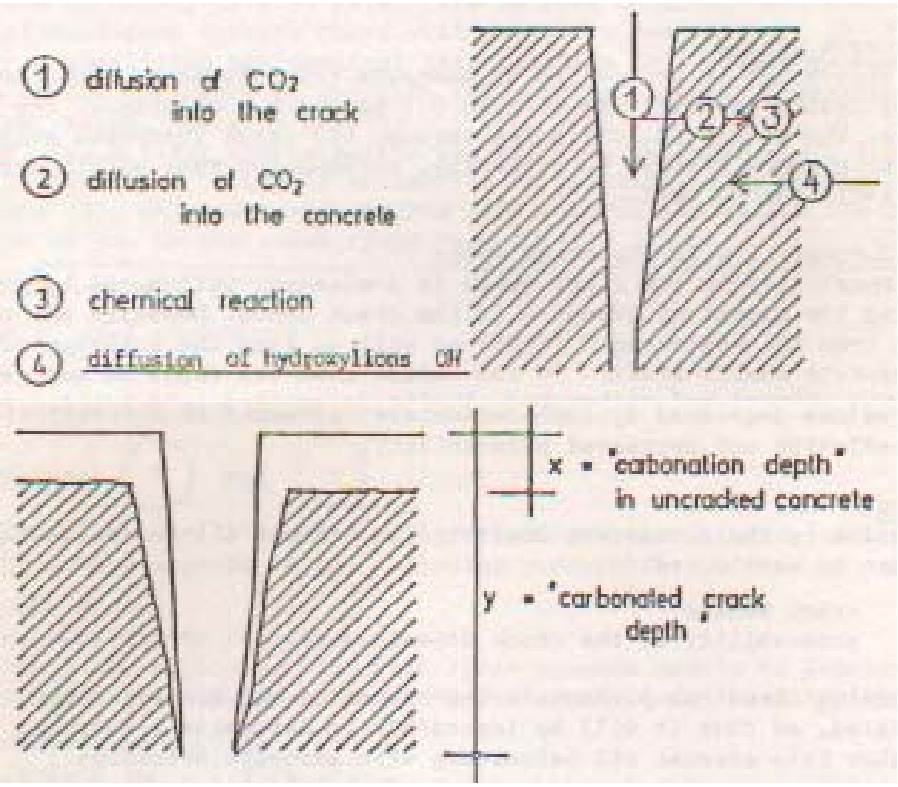

Figure 2.2. Schiessl's figures regarding carbonation due to a crack (Schiessl, 1988).

Chapter 3
Experiment

The goal of the experiment was to determine if a relationship exists between crack width and the rate of carbonation penetration through the crack face. The experimental parameters, such as cement mixes and CO_2 concentration, were selected to accelerate the carbonation process, since ordinarily the carbonation reaction is very slow in the natural environment; a few millimeters a year on average (Hobbs, 1993, Campbell, 1991). Two rounds of testing were performed, with a slightly different procedure for the second round as based on knowledge gained during the first round.

Laboratory Setup

A pure CO_2 environment was chosen to ensure that the reaction would not be limited by availability of the gas, to simplify maintenance of a constant concentration, and for economy. An atmosbag, a large plastic bag with gloves for working in the bag

and ports for tubing, was chosen to house the samples because of its economy and flexibility. As shown in Figure 3.1, the bag was set up on a laboratory counter and cardboard was placed on the bottom to protect the plastic from the concrete samples. Gas tanks of 100% carbon dioxide were located nearby and connected with flexible vinyl tubing. The gas flow was split to allow some of the flow to pass through a gas washing bottle. Gas pressure was controlled by a small needle valve, open at 1.5 mm. The amount of gas flow was just enough to maintain positive pressure in the bag to prevent air entry.

Figure 3.2 shows the sample layout in the bag for round 1. Samples were arranged around the exterior of the bag in a square pattern. They were situated such that the material face with the crack faced inward, toward the gas source in the center. A small fan was placed in the middle of the bag near the gas inlet to help circulate the fresh gas to prevent gas stagnation within the cracks. The fan location was changed every few days to more evenly distribute the flow in all directions.

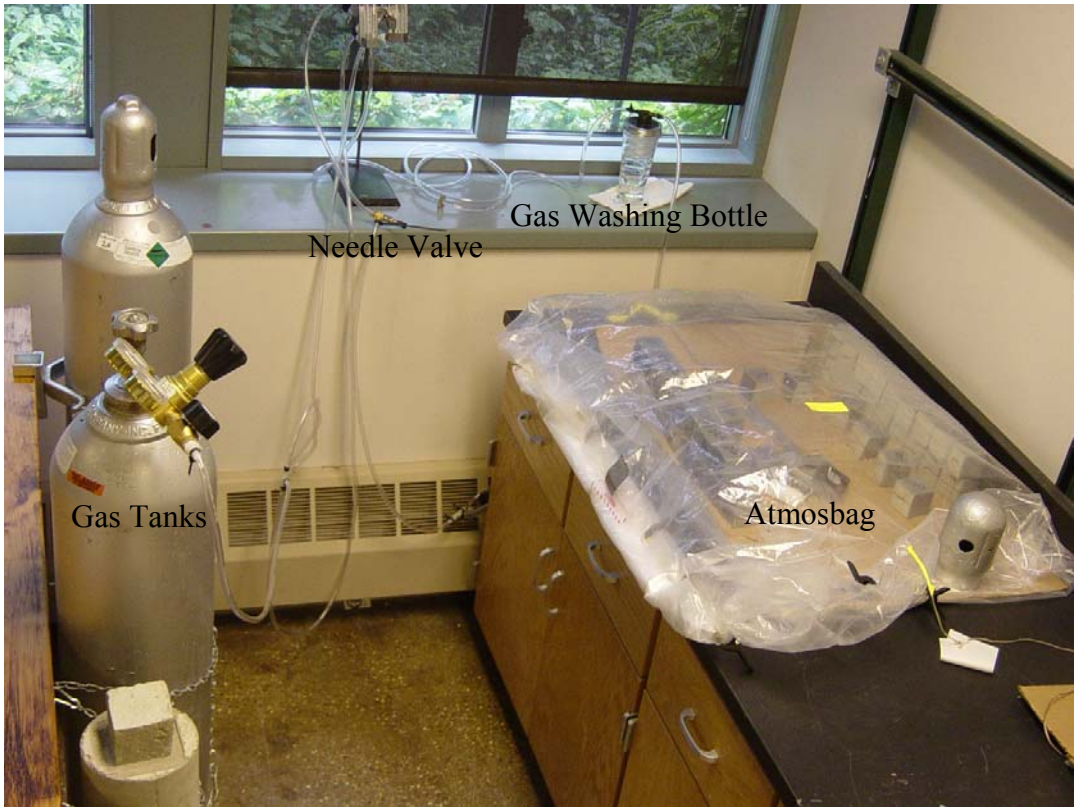

Figure 3.1. Photo of laboratory set up of the atmosbag and gas tanks.

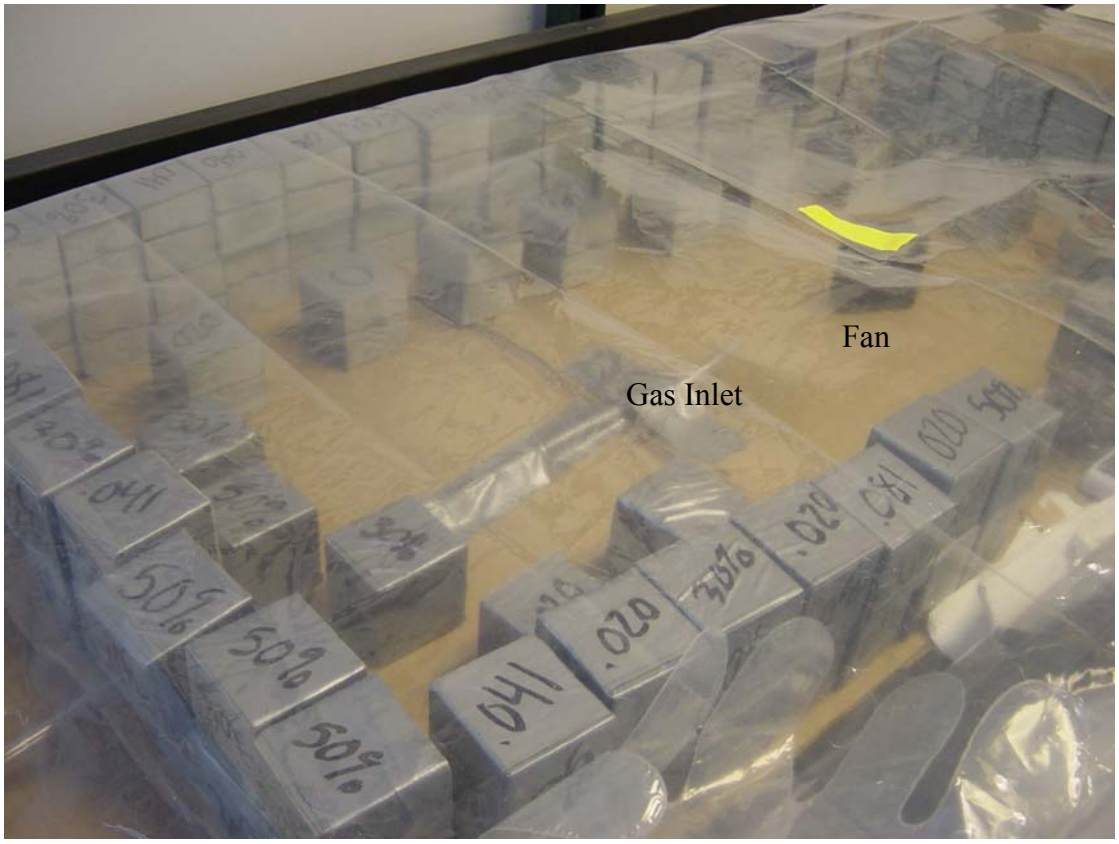

Figure 3.2. Photo of interior of the atmosbag for round 1.

Sample orientation in round 2 was modified to ensure that no samples were getting more CO_2 than other samples from the fan orientation. Samples were placed in the bag with the cracked face turned up, as seen in Figure 3.3. The fan was also directed upward so that it would not blow directly into any sample while gas was still distributed evenly around the bag as shown in Figure 3.4.

Figure 3.3. Photo of interior of the atmosbag for round 2.

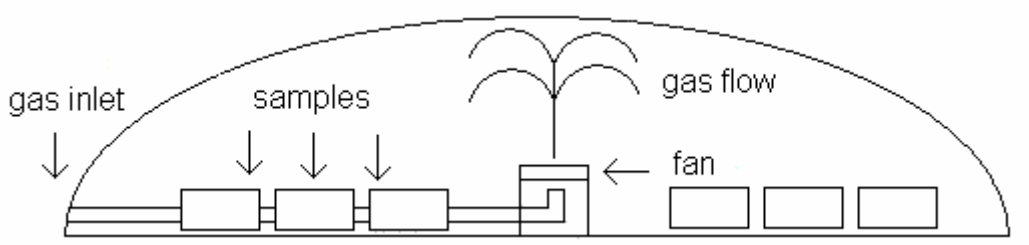

Figure 3.4. Schematic showing gas flow for round 2 testing. Fan is aimed at the top of the bag, preventing preferential flow at any given sample.

Initially it was believed that moisture would need to be added to the bag to maintain optimum relative humidity levels of 50-70%. A gas washing bottle, shown in Figure 3.1, was added to the tubing system, but the amount of water produced during the carbonation reaction and the continued curing of the samples kept the relative humidity

too high. During both incubation periods the relative humidity was above 50%, making it unnecessary to add additional moisture. Humidity was measured with a digital humidity meter with max/min memory capabilities. The humidity meter's range was 25% to 95% and had accuracy of +/- 5% in the range of 40 to 80% and +/- 7% outside that range.

Cement Mixes

High water/cement ratio mixes induce higher carbonation reaction rates. The mixes chosen were based on mixes described in "Microstructural Characterization of the Carbonation of Mortar Made with Fly Ash" (Goñi, 1997). Type I portland cement was used. The water/binder ratio was chosen to be 0.5 because it is on the high end for common mixes used in practice and is above the w/binder ratio of 0.4 at which the carbonation reaction rate declines significantly due to low permeability (Mindess, 1981; Meyer, 1968).

Fly ash was used to replace some of the portland cement to increase the reaction rate even more. Fly ash replaced 35% and 50% of the total cement weight for each mix. Pozzolanic materials, which include fly ash and slag, tend to densify concrete by reacting with the calcium, potassium, and sodium hydroxide components to form silica hydrates. The silica hydrates are larger molecules than the hydroxides, thereby reducing the amount of pore space in the cement matrix (Mindess, 1981). Because the density of the cement matrix is increased, adding fly ash would seem to reduce the carbonation reaction rate by decreasing permeability, but these pozzolanic reactions consume calcium, potassium, and sodium hydroxide components of the cement paste. With fewer

hydroxides that must be carbonated during the carbonation reaction, carbonation penetration rate is increased.

Cement was mixed following ASTM C 305 Standard Practice for Mechanical Mixing of Hydraulic Cement Pastes and Mortars of Plastic Consistency (ASTM, 2001). A mortar mix which omitted coarse aggregate was used because of the small sample size. In round one, two-inch (50 mm) cubes were poured and in round two 4"x 2"x 2" (100mm x 50mm x 50mm) prisms were poured. Both batches were allowed to cure in the mold in a laboratory setting for 24 hours. After they were demolded, they were then placed in a 100% humidity room for 27 days to continue curing. The high humidity in the room retarded the carbonation reaction during the curing process.

Sample Preparation

After curing, samples were notched down the center of the top face along the longest axis with a wet saw to help control the break location. Samples were cracked open with a chisel and a hammer to simulate a natural crack texture, as shown in Figures 3.5 and 3.6. For round 1, the samples were then taped back together with the top of the crack held open with wires of 0, 0.5, 1 and 2 mm, as shown in Figures 3.7 and 3.8. The entire sample was covered in duct tape in an attempt to prevent carbonation from occurring through faces other than the crack face and top face of the sample. Taping, which was conducted outside the curing room required several days and most likely allowed the samples' interior humidity to drop after the moist cure. This drying time was

important because with high interior humidity the carbonation reaction would not occur at a significant rate.

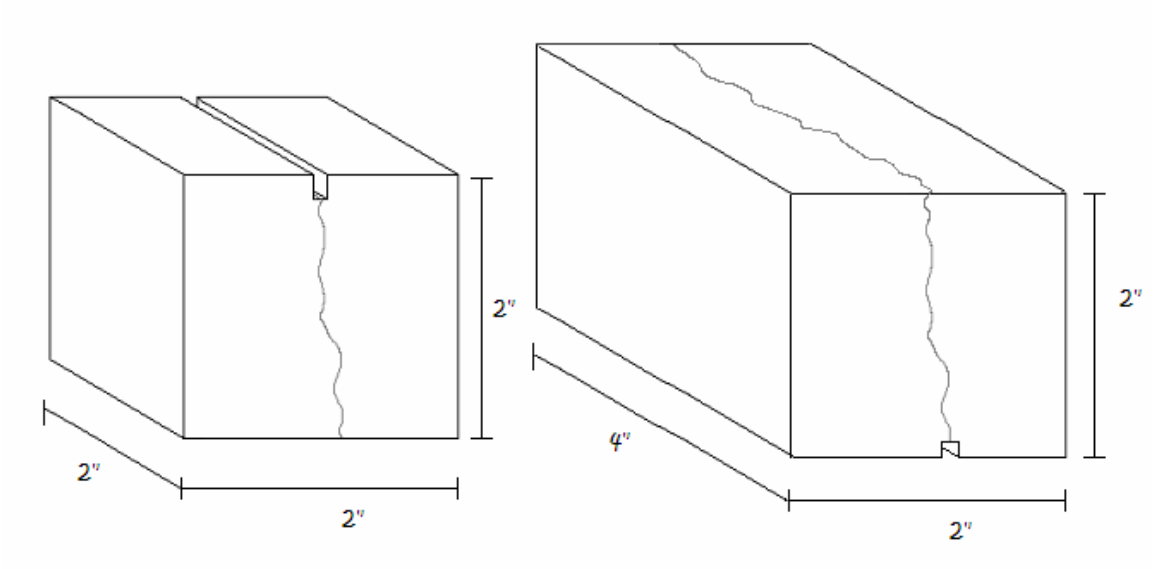

Figure 3.5. 3D view of cube showing saw cut and location of crack for both 2" and 4" cubes.

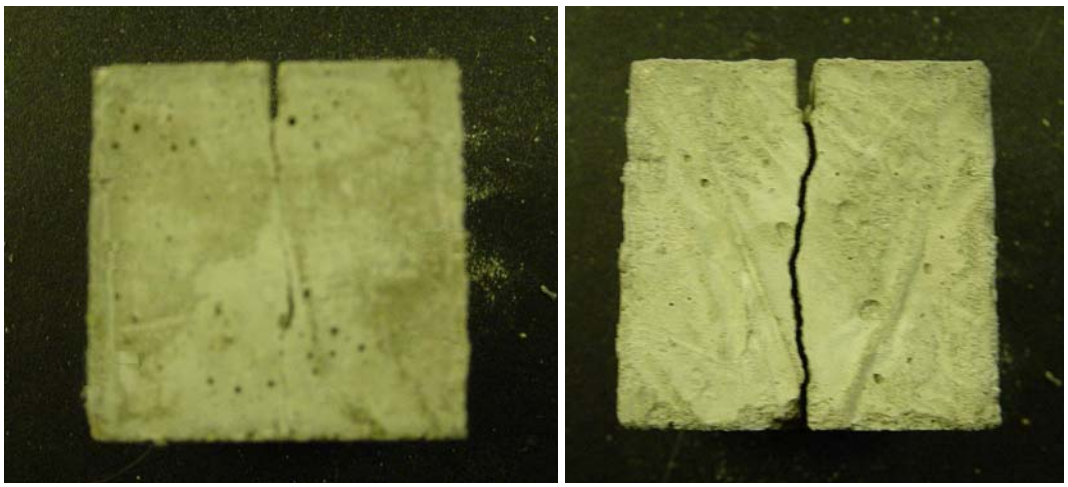

Figure 3.6. Side view of round 1 samples with saw-cut notch before and after cracking with a chisel and hammer.

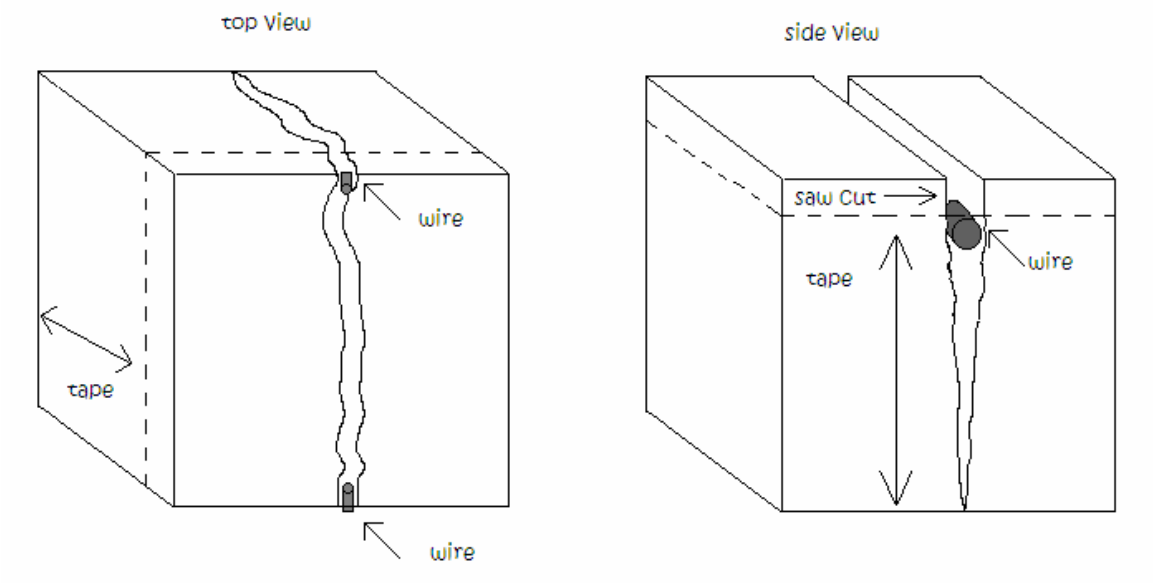

Figure 3.7. Figures showing location of wires on the samples.

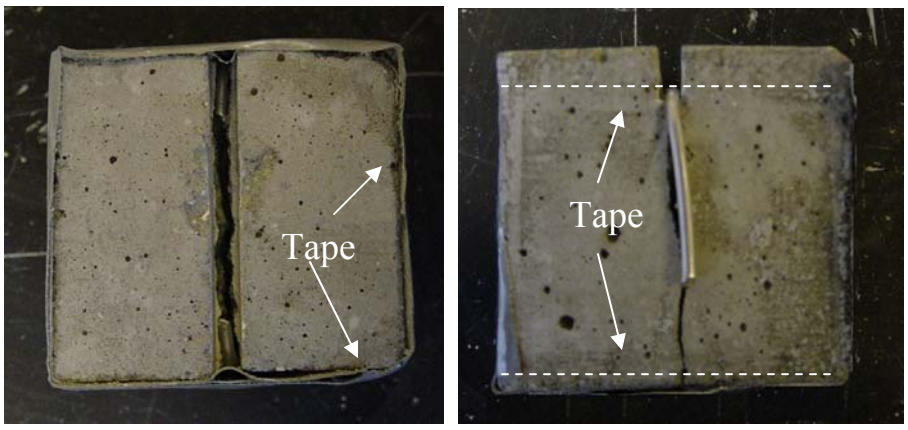

Figure3.8. Photos showing location of wires on the samples.

Round 2 samples were still wired open as shown in round 1 photographs, but they were not covered in tape. The wires were taped into place, but then the entire sample was covered in waterproofing epoxy in an attempt to prevent carbonation through faces other than the crack and sample top. Figure 3.9 shows the paint coverage on round 2 samples.

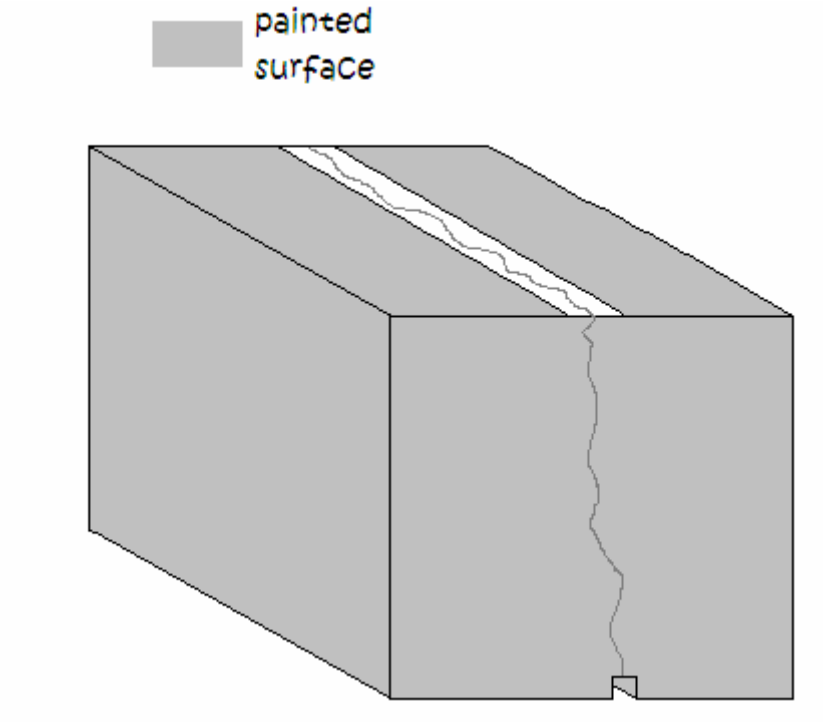

Figure 3.9. Paint coverage for round 2 samples.

Incubation Conditions

Once the round 1 samples were taped, they were placed in the atmosbag with the cracked face pointed towards the gas outlet, as seen in Figure 3.2. The bag was then inflated, purged, then inflated again to ensure that the primary gas in the bag was carbon dioxide. To check the concentration of CO_2 in the bag, gas chromatography was used. Gas is injected into the gas chromatograph and individual gases are detected at a particular time past the injection time. The output is a plot of concentration vs. time with a series of peaks whose area corresponds to that particular gas's concentration. A drawdown curve was created by injecting gas mixtures with various concentrations of CO_2 and air. The gas inside the bag was then tested and compared to the drawdown

curve. As can be seen in Figure 3.10, the tests show that there was approximately 100 % CO_2 in the bag, with no less than 90% being measured.

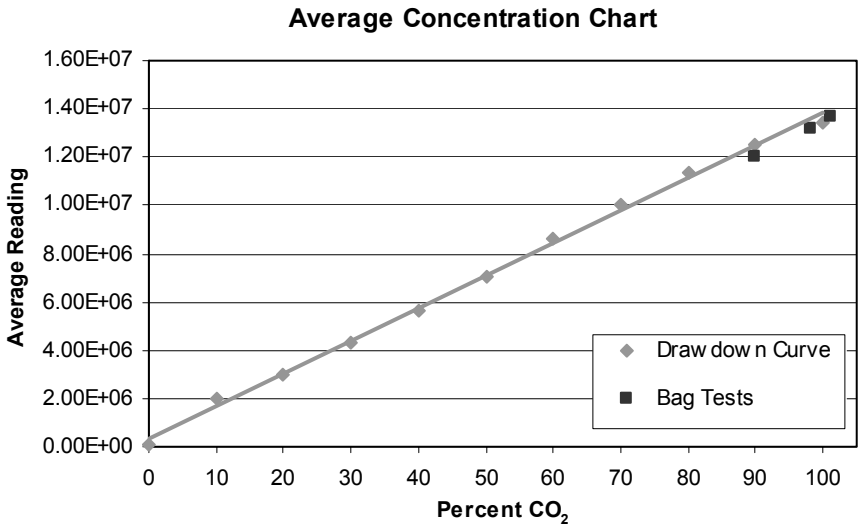

Figure 3.10. Drawdown Curve from gas chromatography showing CO_2 concentration from bag samples.

During incubation the temperature and relative humidity were checked regularly. The temperature ranged from 19° to 21°C for both incubation periods, near the optimum temperature of 20°C. The relative humidity fluctuated significantly during each incubation period. Figure 3.11 is a plot of relative humidity over time for the first round of testing. During the first incubation relative humidity ranged from 80% to 91% during the first two weeks of testing. Also during this period there were several issues with maintaining positive pressure in the bag. The regular fluctuation in gas type and pressure may have contributed to the initial fluctuations in relative humidity. Once control over the bag's gas pressure was achieved, the relative humidity steadied at 85% for the remainder of the test period.

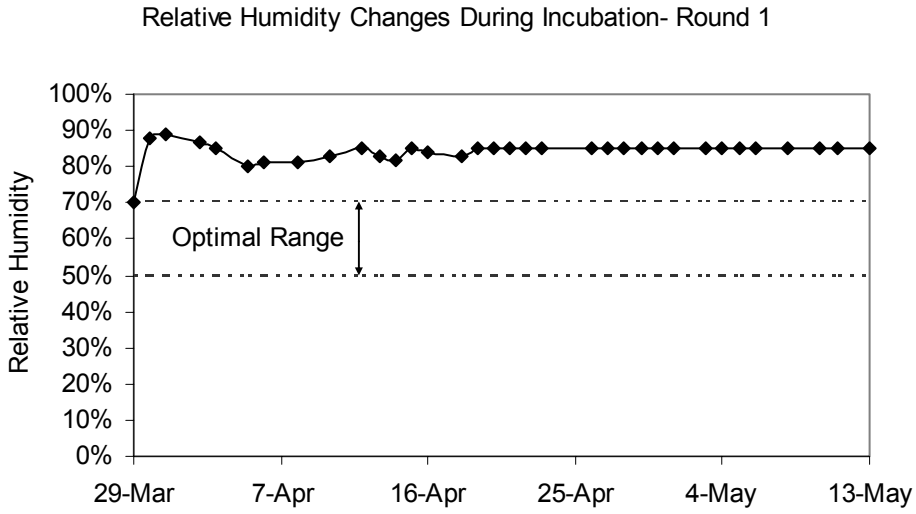

Figure 3.11. Curve showing general trends in the relative humidity during round one testing.

Daily fluctuations of relative humidity fluctuation data did not provide much information in round one, therefore only the trends were recorded during the second round. The trends of the relative humidity for the second test are shown in Figure 3.12. In the second round there was more cement in the bag due to the larger number and increased volume of the samples. More cement meant more water being expelled during post 28-day curing and during the carbonation reaction. In the first two weeks of testing the relative humidity fluctuated between 91% and 93%, which is too high to allow the reaction to occur. It was hoped that the relative humidity would gradually drop naturally to a level allowing the carbonation reaction to occur, but it did not. In order to decrease the moisture in the bag, desiccant was added on day 14. The relative humidity quickly dropped 20%, to near 70%, near the optimum range; however, once the absorption ability of the desiccant drastically declined, the humidity began to climb back towards 90%. On

day 28 more desiccant was placed in the bag to reduce the relative humidity, dropping again by 20%. The relative humidity stayed below 80% until half of the samples were removed on day 41. Once the volume of concrete in the bag was reduced the humidity dropped and remained within the optimum range of 50-70%.

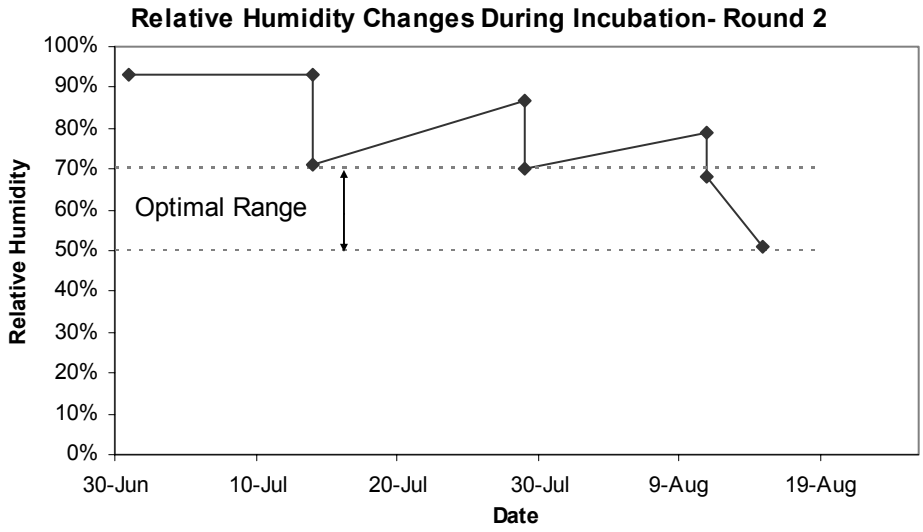

Figure 3.12. Relative humidity changes over time for round two testing.

Incubation times for round one were 45 days for both the 35% and 50% fly ash samples. Upon testing, it was discovered that 45 days was too long for the 50% samples because most of the samples had carbonated entirely. The 35% samples were significantly less carbonated and penetration measurements were obtained. The second round of testing incubated for 41 days for the 50% samples and 58 days for the 35% samples. Since the first 15 days produced little measurable carbonation due to the high humidity as discussed above, these carbonation durations were closer to 26 and 43 days respectively. In the second round the epoxy performed as hoped and stopped carbonation

penetration rates through all sample faces including the crack face. Data collected from the 50% fly ash samples produced results. The 35% fly ash samples in the second round were not carbonated enough to produce sufficient data for analysis. It is believed that the epoxy kept the water produced during continued hydration and the carbonation reaction inside the sample, keeping the humidity high and reducing the reaction rate.

Testing Procedure

After the samples were incubated, they were removed and prepared for application of phenolphthalein solution. Round 1 samples were cracked to constrain measurement of carbonation penetration at specific distances into the crack; since the carbonation front tends to decrease with increasing depth into the crack, as shown in Figure 3.13, samples were fractured at 10 mm, 20 mm, and 35 mm below the exposed material face. Fracturing samples in this manner allowed examination of the carbonation front along the entire length of the crack. Their fractures were produced from saw-cut notches shown in Figure 3.14. Samples were then broken at the notch with a chisel and hammer and a phenolphthalein solution was applied to the freshly broken surfaces. Figure 3.15 shows the broken surface orientation. The carbonation front was identified as the location of the colorless front on the concrete surface, as shown in Figure 3.16. The maximum, minimum, and average depths of the colorless front were measured and a digital photo was taken of each test surface. Figure 3.17 shows the regression of the carbonation front as the depth into the crack increases. The digital photos were used to measure the total area of the test surface and the total carbonated area on the test surface. Figure 3.18 shows the area calculation for a sample.

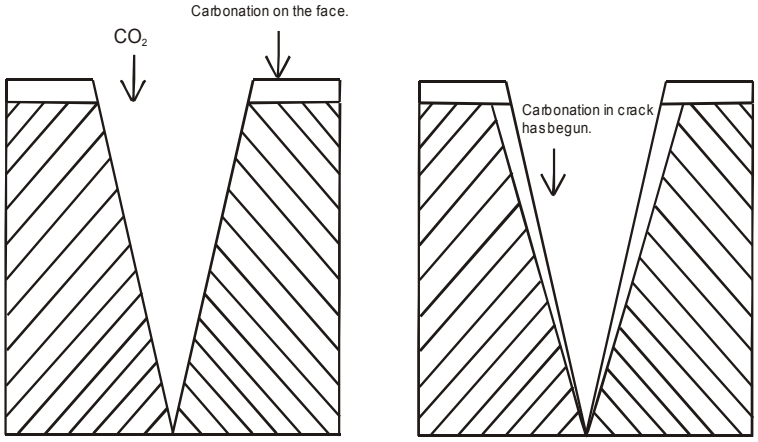

Figure 3.13. Variation in carbonation penetration with depth into the crack.

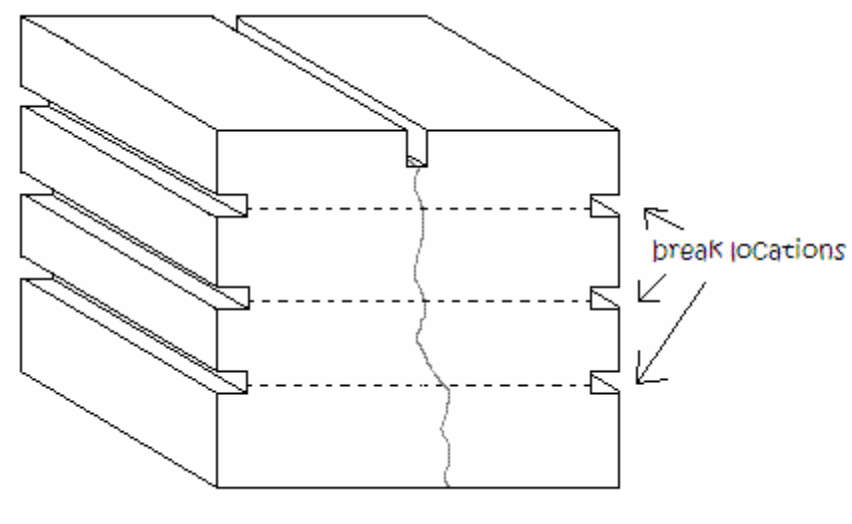

Figure 3.14. Schematic showing break locations used during round 1 for phenolphthalein testing and a sample waiting to be broken for testing.

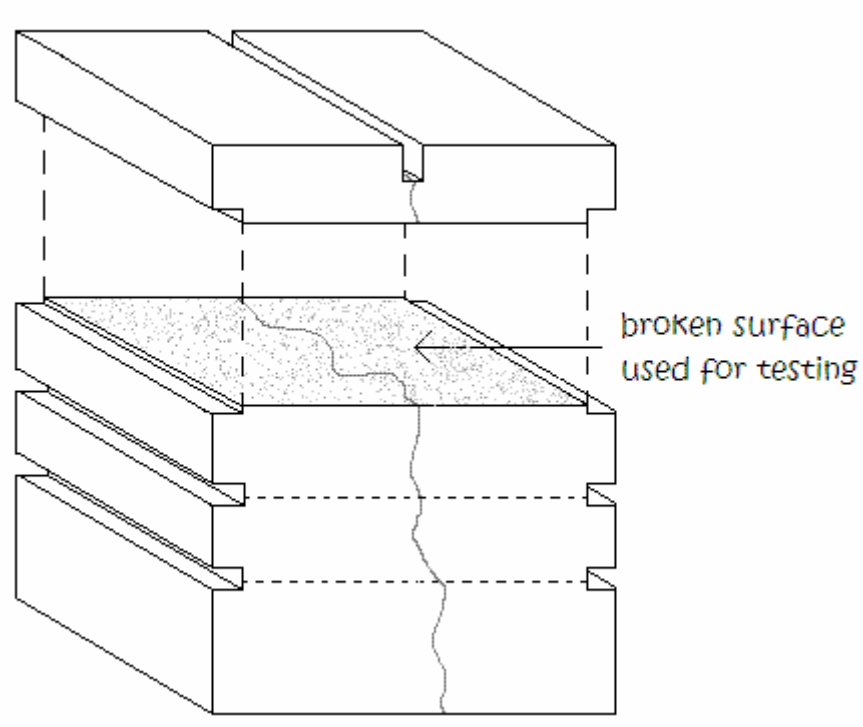

Figure 3.15. Break-away drawing showing broken surface used for testing.

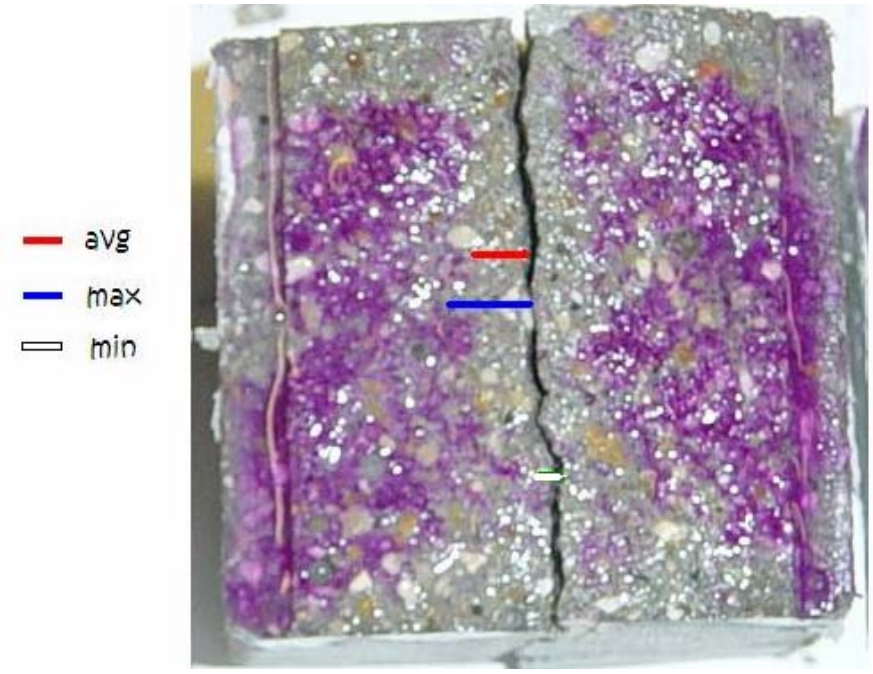

Figure 3.16. Photo showing maximum, minimum and average readings taken during round 1 testing.

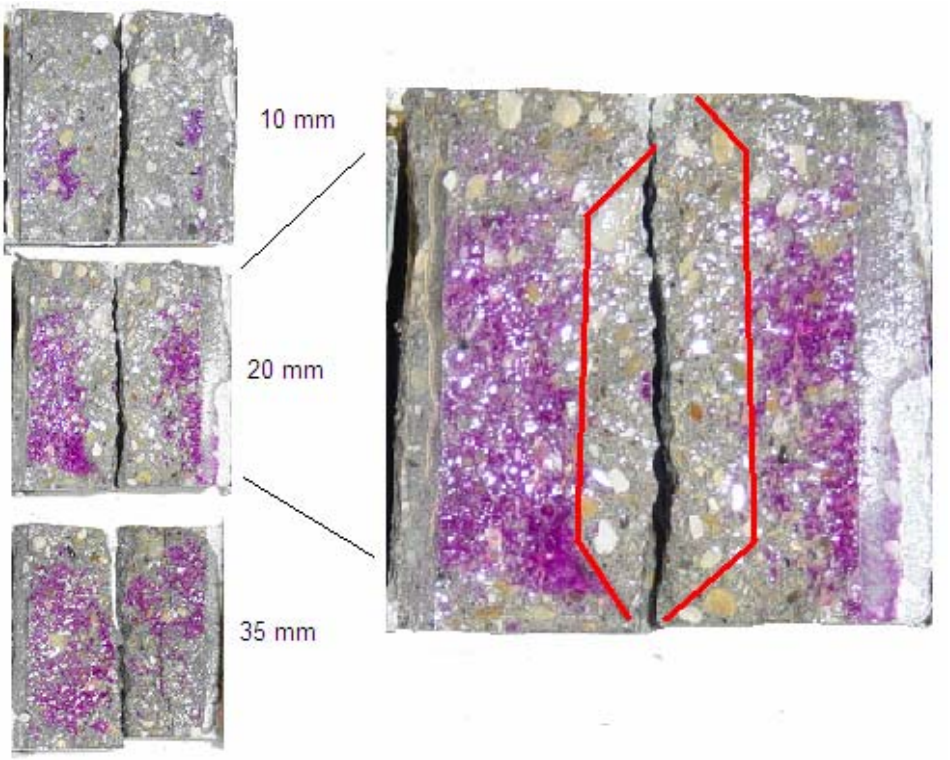

Figure 3.17. Sample from round 1 showing regressing carbonation front as the depth into the crack increases and the parabolic shape of the carbonation front.

Figure 3.18. Digital photo of sample with area calculations shown.

Round 2 samples were broken with a vertical test surface, as opposed to a horizontal test surface used in round 1. Figure 3.19 shows the orientation of the test surfaces and a sample waiting to be broken for testing. Figure 3.20 shows a break-away section showing the testing surface. This test surface orientation allows for a continuous reading of the carbonation front with respect to depth into the crack. After the samples were broken, phenolphthalein was applied and penetration measurements were taken at 0mm, 3mm, 5mm, 10mm, 20mm, and 25mm below the material face. Figure 3.21 shows the reading locations and how the measurements were taken.

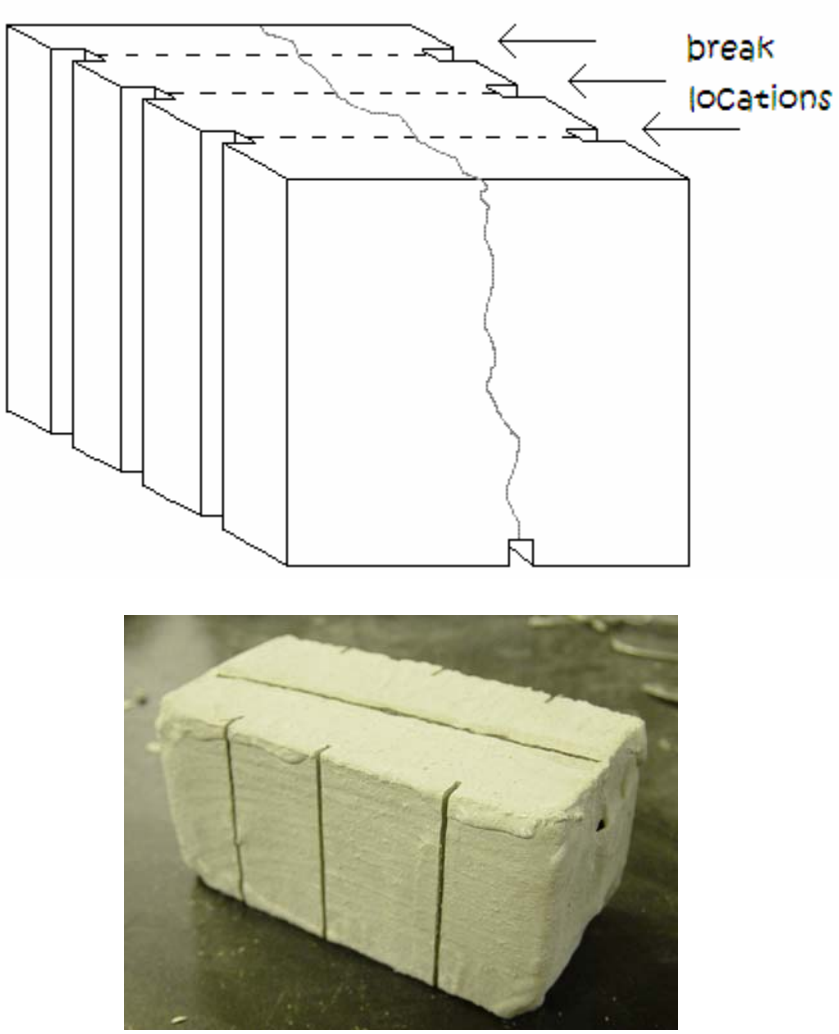

Figure 3.19. Break locations for round 2 testing and a sample waiting to be broken for testing.

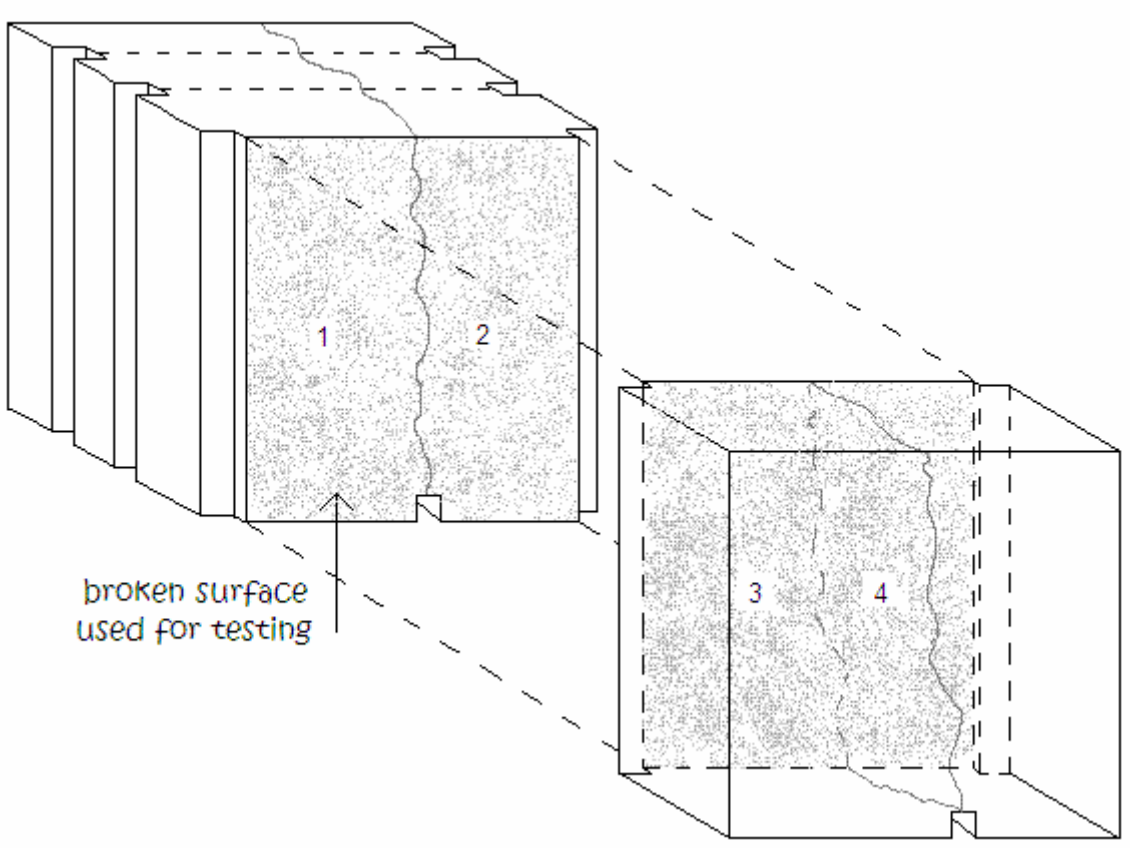

Figure 3.20. Drawing showing location of testing surface in round 2 samples and numbering the 4 surfaces tested at each break location.

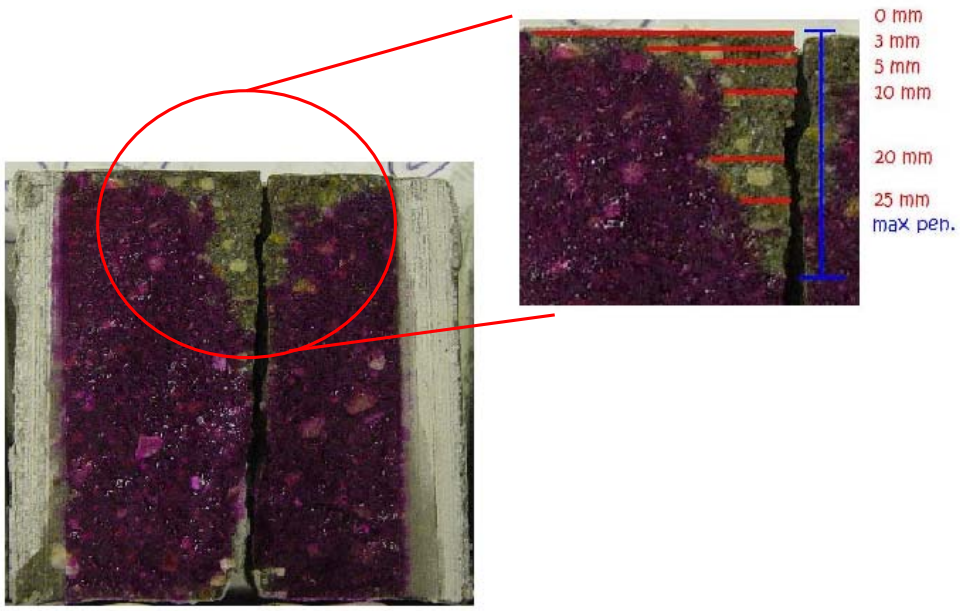

Figure 3.21. Photo showing broken surface of a round 2 sample and penetration measurements recorded.

Carbonation fronts for round 2 tended to have two patterns: one with an inward curve whose legs paralleled both the material face and the crack face and one with an outward curve that tended to be rectangular in shape. Figure 3.22 shows an example of the inward curve front while Figure 3.23 shows an example of the outward curve. The inward curve seems to be a result of carbonation occurring simultaneously through the material face and the crack face. The carbonation fronts for the material face and the crack surface converge at the corner, making the front curved. The carbonation through the material face extended up to 5 mm in this experiment. The outward curve seems to indicate that carbonation through the material face was slowed significantly or stopped by the paint. Gas penetrated the sample only through the crack face and the small area around the crack on the material face not covered by the paint. The front tends to be

parallel to the crack front until close to the maximum penetration depth where the front tapers off to zero. A small area of carbonation reached under the paint behind the 'rectangle' of carbonation. This carbonation 'tail' is considerably shorter and tapers off quicker than the carbonation in the same area on the inward curve samples.

Figure 3.22. Round 2 sample showing inward curve carbonation front. Arrows indicate the direction of the gas penetration and subsequent carbonation front progression.

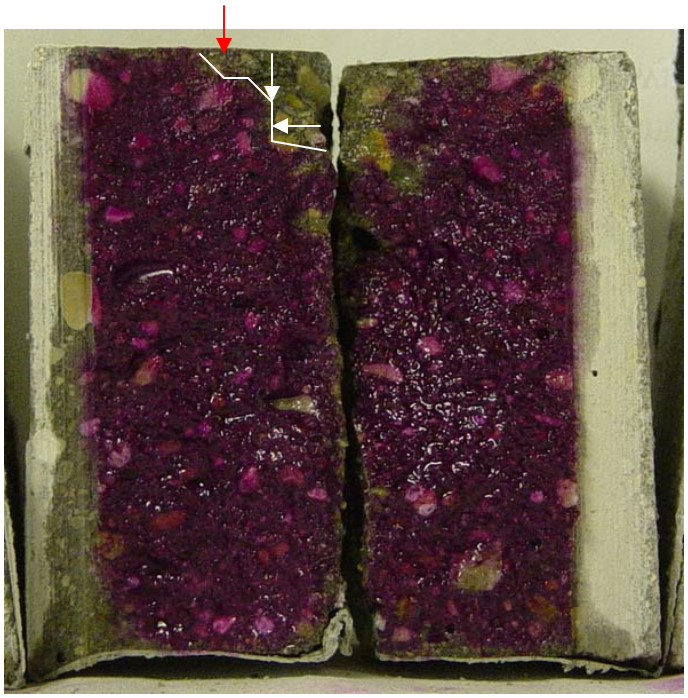

Figure 3.23. Round 2 sample showing outward curve carbonation front. White arrows indicate the direction of gas penetration and the subsequent carbonation front progression. Red arrow identifies carbonation 'tail' as described above.

Experimental Improvements

While examining the carbonation fronts in the round 1 samples, several procedural errors were identified. It was originally believed that the several layers of duct tape would be sufficient to prevent carbonation from occurring though sides other than the material face and crack face. Carbonation however was found around the edges that had a consistent penetration throughout the depth of the sample. This can be seen in Figure 3.17 at both the top and bottom of the photos at each depth. It is believed that this carbonation occurred both during the wiring process, at which time the cubes were exposed to the natural environment for over 1 week, and through the tape during the incubation time. Carbonation that could be positively identified as originating from these

faces was omitted from the data used to determine the penetration rate through the crack face.

A second observation during the phenolphthalein testing in round 1 was that the carbonation fronts tended to have curved shapes. The front tended to have sloping sides for several millimeters along the length of the crack and then flattened out until the other side slope was reached. The photo at 20 mm in Figure 3.17 shows the parabolic shape. This parabolic front is believed to have been caused by the air currents being disturbed by the wires protruding into the crack. Even though they only protruded a few millimeters into the crack, they may have affected the flow of air into the crack, and therefore the fresh gas supply.

Another issue that became apparent was controlling the break location during round 1 testing. Carbonation penetration changes with depth into the crack. Thus forcing the break to be horizontal, as is drawn in Figure 3.14 was very difficult. The broken surface varied as much as ±3 mm from the horizontal, as shown in Figure 3.24. Carbonation penetration varies over distance as depth into the crack increases. Figure 3.25 shows variation of carbonation penetration with depth into the crack. The small variations in the carbonation depth measurements as a result of the break location may have affected the results.

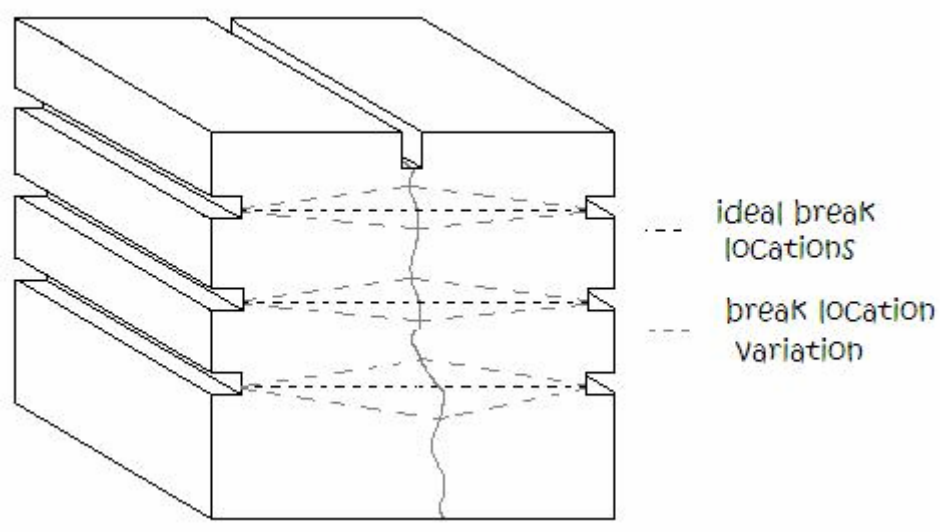

Figure 3.24. Sample from round 1 showing variation in break locations associated with lack of control in the breaking method.

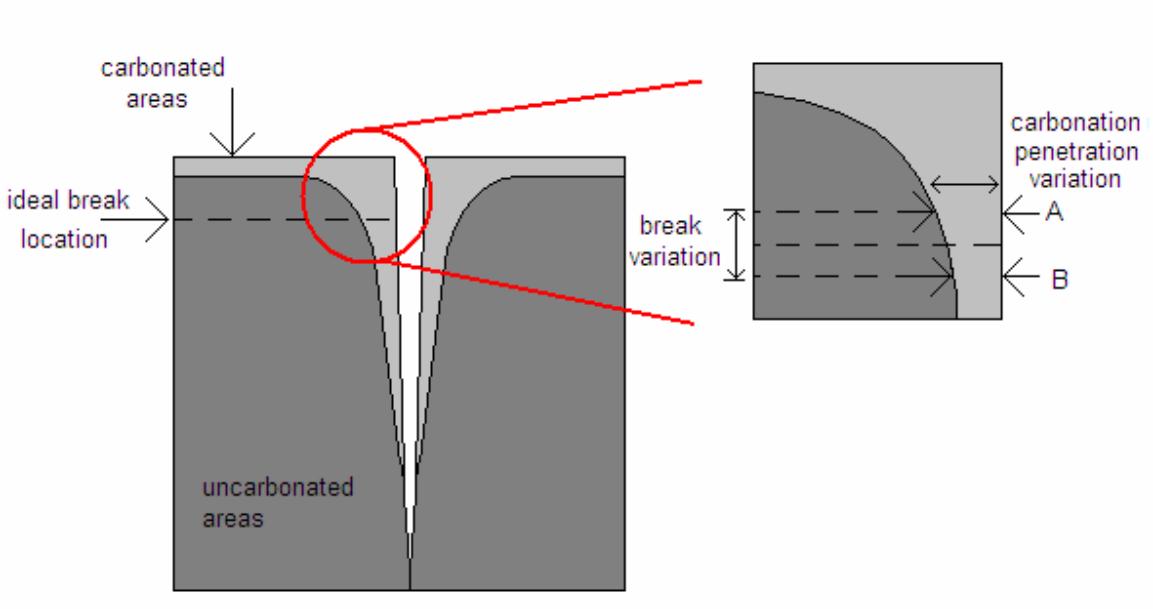

Figure 3.25. Drawing showing variation in carbonation penetration as depth into the crack varies.

Carbonation was also discovered to have been occurring more rapidly through the face of the cube that was not touching the mold during the curing process. It is believed that this face had a different density because it was not cured against the smooth surface of the mold. Carbonation data related to this face was not used. Molds also may have had another impact, though this one was not as easily identified in all the samples. Two different molds were used for the cube samples, one made of plastic and one of MDO (Medium-Density Overlay) plywood, plywood overlain by a poly veneer. These two materials produced different textures on the faces they touched; which may have changed the carbonation rates though these faces. This carbonation rate difference was only identified in a few samples that could conclusively be identified as coming from one mold set over another. Also associated with the faces that touched the molds is the impact of the oil used to lubricate the molds on the surface texture and chemical makeup of the cement immediately adjacent to the mold. These surface affects were not evaluated.

Another area of concern that arose during the first round of testing involved the inaccuracy of the crack location with respect to the face of the material. Cracks are most often flush with the material in which they occur. In these samples, the natural crack did not begin for 5-7 mm below the face of the cube, changing the exposure of the natural crack to the gas. This change in exposure may have impacted the variation of carbonation penetration with respect to depth into the crack. Again, the impact of this exposure variation was not entirely evaluated in this experiment, but is noted as an

inaccuracy. To more accurately reflect natural conditions, the crack should be flush to the face of the material.

Several major changes in procedure were introduced during the second round, as based upon the above observations. First, the issues with sample preparation were addressed. The sizes of the samples were modified to 4" x 2" x 2" prisms in order to increase the length of the readable carbonation front, i.e. that which is not affected by the wires at the crack ends or any potential carbonation that could occur through faces other than the crack face. Special molds were made to make samples this size and all were made of MDO so that all samples have similar surface texture on the faces that touched the mold. Also, to reduce the parabolic shape of the carbonation front, the wires were trimmed and placed such that they penetrated the crack as little as possible to minimize gas flow impedance.

Second, the observation crack orientation was modified and the method of protecting carbonation from faces other than the crack was changed. The access crack was made flush with the material face by wiring the side opposite the saw cut. Figure 3.26 shows the wire orientation with respect to the saw cut. After taping the wires in place, the entire sample, except a small strip around the crack itself was covered with 3 coats of waterproofing epoxy that is labeled to reduce gas transmission. Figure 3.26 also shows the areas of the specimen with epoxy cover. The epoxy was believed to be more impermeable than the original duct tape and thus should greatly reduce, if not prevent, carbonation through faces other than the crack. The top of the sample with respect to the

mold was made the bottom of the sample so that any change in properties due to it not touching the mold would not impact the carbonation front.

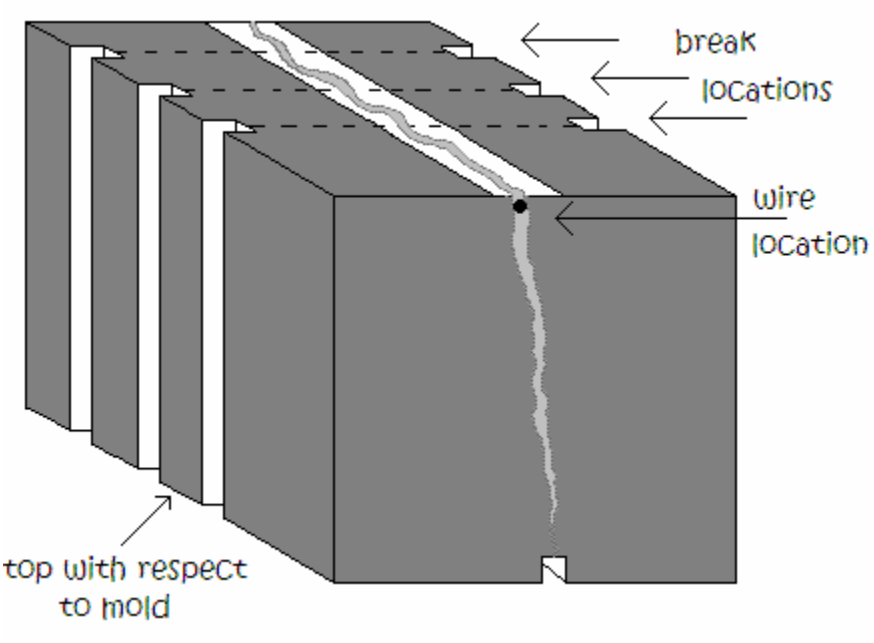

Figure 3.26. Schematic showing paint cover, break locations and saw cut location for the 4”x2”x2” cubes used in the second round.

Third, the sample orientation in the atmosbag was changed. The samples were placed in the bag with the crack facing upward, instead of into the center of the bag, and the fan was placed facing upward, too. Orientation was changed so that the fan did not directly force air into any of the cracks, as it did during the first round of testing. Thus all samples should be subjected to the same air flow pattern and thereby reducing potential variation in the samples. (See Figures 3.3 and 3.4 for the round 2 orientation in the atmosbag.)

Finally, the orientation of the phenolphthalein testing surface was changed from horizontal to vertical, as shown in Figures 3.15 and 3.20. Changing the orientation allows for continuous measurement of the carbonation front as depth into the crack increases, Figure 3.21. This change allows for more precise data collection because measurements can be taken at exact distances from the top of the crack and are not dependent on how well the break was made (see Figure 3.24 above). With this type of measurement the test surface orientation does not have to be controlled quite as strictly since the break surface does not have to be at an exact location. As long as measurements are performed from a 90° angle to the prism faces, the data can be more accurately compared.

Error Analysis- Round 2

Second round errors were reduced by making the changes described above, but several new issues arose with the changes. First, although the epoxy did help prevent carbonation through faces other than the crack face and the small portion of the material face that was exposed, it also prevented water escape from the sample. Water was produced from the continued hydration of the cement paste as well as from the carbonation reaction itself. Preventing this water from escaping the samples kept the interior humidity high. It is believed the high humidity is the reason that the 35% fly ash samples were not sufficiently carbonated to allow measurement and why the carbonation fronts in the 50% fly ash samples did not progress as quickly as they did during the first round of testing. This situation, though not ideal for laboratory conditions, is comparable

to field conditions where the water produced in the hydration and carbonation reactions is only able to escape through the material face and cracks.

A second issue with the epoxy was the uniformity of coverage and ease of application. The epoxy was thick and difficult to work with. Its texture was such that it did not smooth out well and tended to slide down the vertical faces. Bubbles were often observed in the wet paint, which may have affected the paint's impermeability. Since the paint was of similar color to the concrete, ensuring even coverage was difficult. Several coats of paint were applied to ensure sufficient coverage to prevent gas penetration.

Using a larger sample also caused several issues. Larger sample size, though good for reducing the air current disturbance from the wires, made breaking samples more difficult. The chisel used did not span the entire length of the sample and as a result the crack did not break perpendicular to the material face. The cracks tended to be angled with respect to both the depth of the sample and the length of the sample. Figure 3.27 shows typical break conditions for the large samples with θ being the angle the break makes with the vertical axis and ϕ being the angle between the break and the longitudinal horizontal axis.

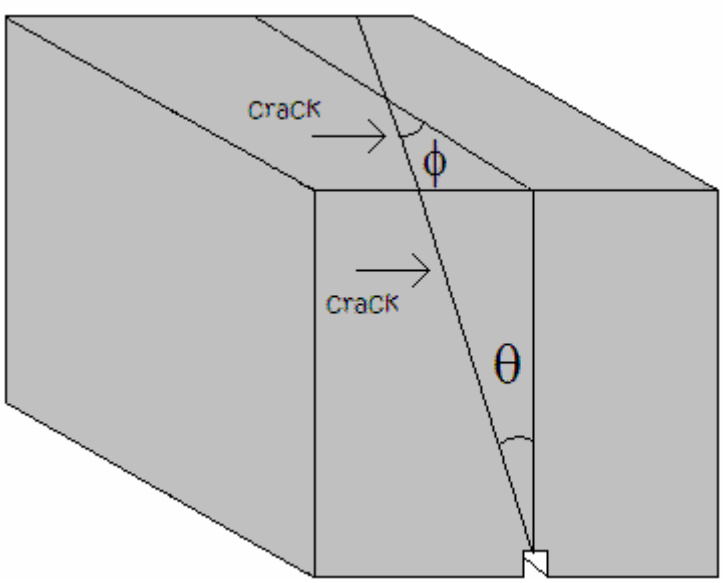

Figure 3.27. Break variation for large samples used in round 2.

Chapter 4
Results

Despite the experimental challenges outlined above, usable data was obtained in both rounds. Data from both rounds supports the hypothesis that the carbonation penetration is proportional to the width of the crack and that at small crack widths the relationship between crack width and carbonation penetration is linear. The primary difference between rounds 1 and 2 was the reduction of carbonation through the faces by painting the samples. Furthermore carbonation determined to have occurred through faces other than the crack face on round 1 was omitted from measurements.

Round 1- Taped, Test Surface Parallel to Material Face

Round 1 data for the 35% fly ash samples is presented in Figures 4.1 – 4.12. Figures 4.1- 4.4 present the average penetration readings. The maximum penetration data are presented in Figures 4.5-4.8, while the minimum penetration data are presented in

Figures 4.9 and 4.10. Figure 4.11 presents carbonation area data and Figure 4.12 presents carbonation profiles with respect to crack depth. Refer to Figure 3.16 to see the measurement locations for Figures 4.1- 4.10 and to Figure 3.18 for Figure 4.11.

Figure 4.1 contains all the average penetration readings, as defined in the previous chapter, at 10 mm below the material surface and Figure 4.2 contains the same data with the high and low points for each crack width removed. Figure 4.1 shows that most points were within a reasonable range relative to each other, with the exception of one 18 mm reading at the 2 mm crack width. This point varied significantly from the other points and affected the best fit line and more significantly the standard deviation. Overall, the plot shows that there is a linearly increasing carbonation penetration as the crack width increases, as was hypothesized. Average carbonation depth at each crack width was calculated and a best-fit linear trend line was fitted through the points. The overall average was also calculated and plotted to determine if the variation over the crack width range had any statistical significance.

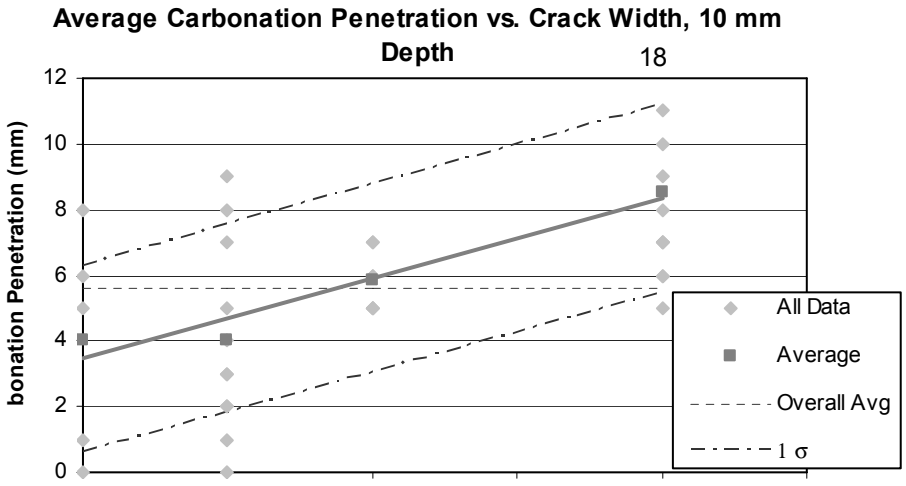

Figure 4.1. Round 1 data of average carbonation penetration readings 10 mm below the material face for the 35% fly ash mixture.

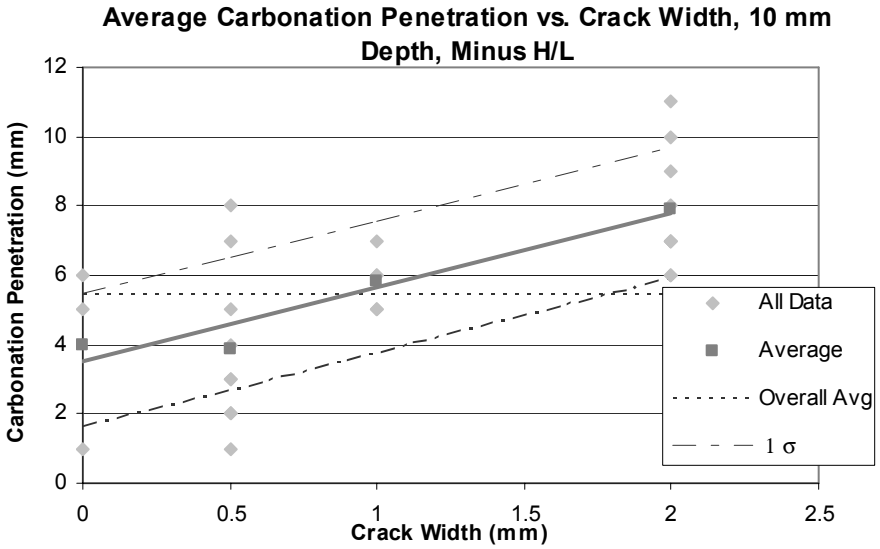

Figure 4.2. Round 1 data of average carbonation penetration readings 10 mm below the material face minus the extreme points for 35% fly ash mixture.

Standard Deviation was calculated based on all data points with respect to the best fit line and lines of ± 1 σ were plotted. With 67% confidence the data shows that there will be more carbonation than the overall average if the crack is 2 mm or wider and that there will be less carbonation than the overall average if the crack is present, but closed (0 mm). Also noticeable on the plot is the wide range of readings for each crack width: 8-9 mm. For the 1 mm crack samples the range of only 2 mm is artificially small due to unfavorable breaking conditions that reduced the number of samples in the data set. The wide range is likely due to local variations in w/c ratio, interior humidity, aggregate placement with respect to the crack face, etc. Because these conditions are difficult to control a significant reduction in the range is not likely. Some reduction in the range may be achievable by better controlling carbonation through surfaces other than the crack face and ensuring similar gas exposure to all areas inside the crack.

The data were then manipulated by removing the high and low points for each crack width. Figure 4.2 shows the data minus the high/low values. This data manipulation reduced the effect of the extreme points, especially the 18 mm reading. Averages were slightly changed by the reductions for the 0, 0.5, and 1 mm crack widths. The most significant change occurred in the 2-mm crack set. Removing the single reading of 18 mm significantly reduced the average. As a result, the averaged data has a better linear fit and the standard deviation was greatly reduced, from a value of 2.9 mm to 1.9 mm, a 34% reduction. This plot again confirms that there is a linear trend of increasing carbonation penetration as the crack width is increased and that within one standard deviation there is a trend about an overall average line.

Figures 4.3 and 4.4 show the average carbonation penetration for a depth 20 mm below the material face. These plots show an even stronger linear correlation between carbonation penetration and crack width than do the 10 mm plots. The least-square best-fit lines for the data gave intercepts slightly less than zero and this does not comply physically with the samples; therefore, in these plots the linear best fit lines were manipulated for an intercept of 0 at 0 mm crack width. Figure 4.3 shows a linear trend with one standard deviation confidence without removing the extreme points, despite the large discrepancy in the 12 mm reading at the 2-mm crack width. When the extreme values for each crack width are removed, an even stronger correlation is achieved. By removing the extreme values, the standard deviation decreases from 2.0 mm to 1.2 mm, a 40% reduction.

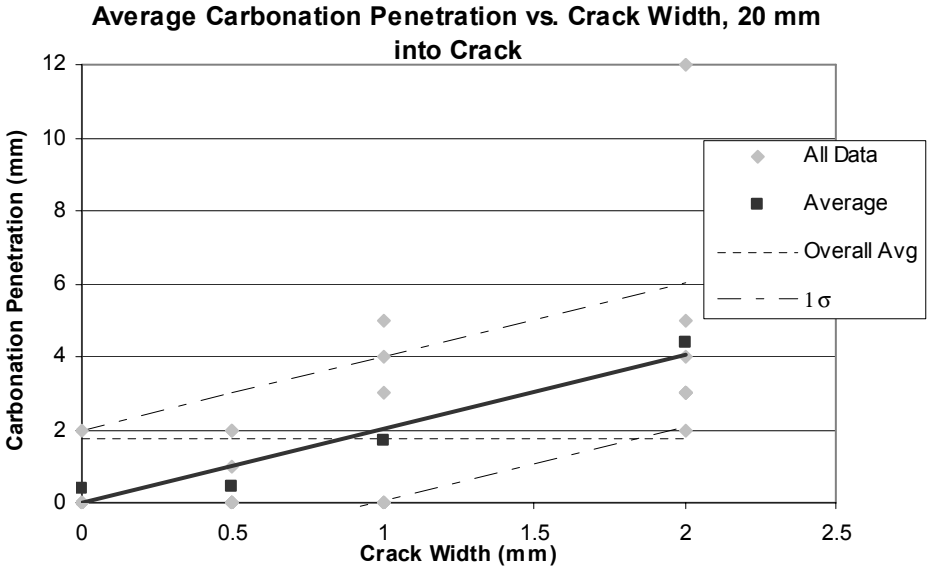

Figure 4.3. Round 1 data of average carbonation penetration readings 20 mm below the material face for the 35% fly ash mixture.

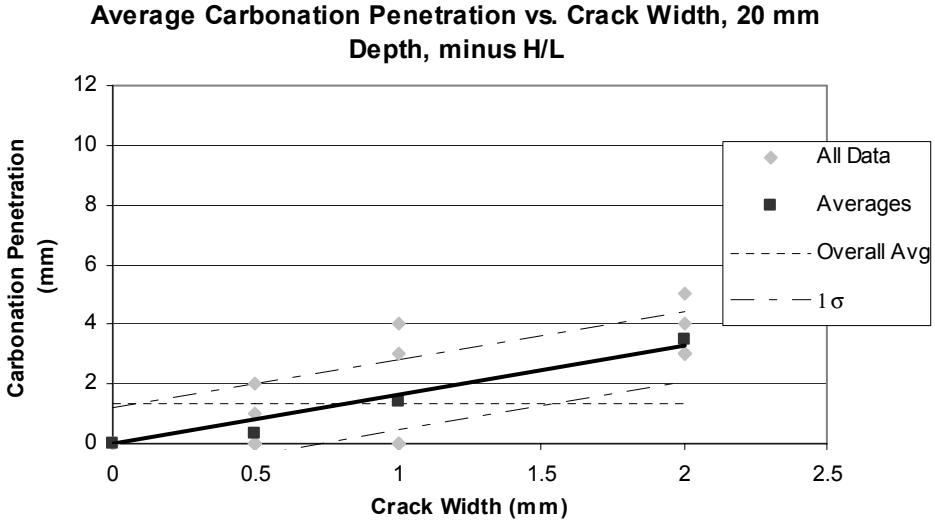

Figure 4.4. Round 1 data of average carbonation penetration readings 20 mm below the material face minus the extreme points for the 35% fly ash mixture.

Figures 4.5 and 4.6 show the maximum carbonation penetration plots at 10 mm below the material surface with respect to crack width. Figure 4.5 represents all data collected while Figure 4.6 has the data minus the high and low points. Readings that indicated total carbonation were eliminated from the data if evidence of carbonation occurring through the edge parallel to the crack face was present. Eliminating these points produced a trend in the data; however, there is still not a statistical significance. The standard deviation lines in Figure 4.5 indicate that there is a good deal less than 67% confidence in the trend. Removing the extreme points in the data set, the high and low points for each crack width, improves the statistical significance of the best-fit line to within one standard deviation. The standard deviation for all data was calculated to be 5.6 mm, but when the extreme points are removed, this value drops to 3.7 mm, a 34% reduction. Figures 4.7 and 4.8 present the maximum carbonation penetration versus crack width at 20 mm into the crack. Figure 4.7, showing all data, is close to showing one standard deviation confidence, but when the extreme points are removed, the upward linear trend about the overall average line attains 67% confidence. Removing the extreme points, as shown in Figure 4.8, reduces the standard deviation from 5.4 to 3.9, a 27% reduction.

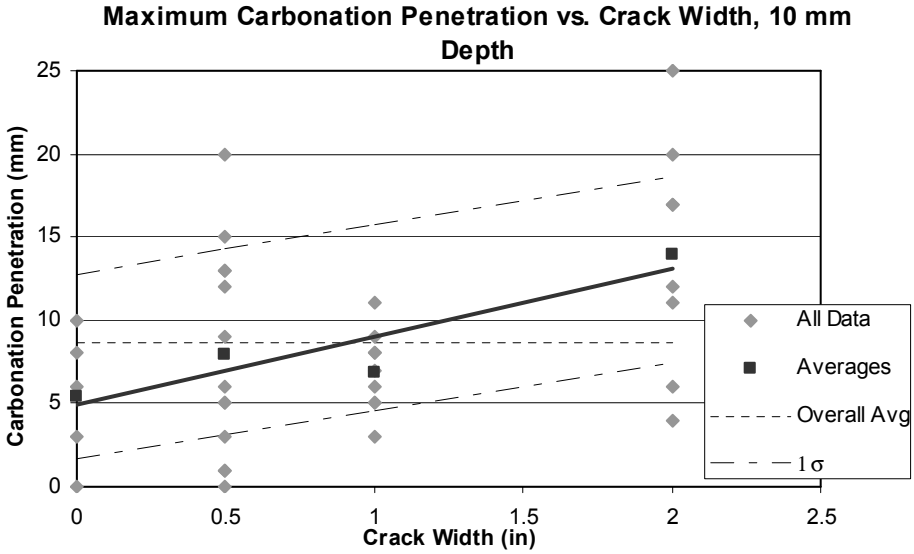

Figure 4.5. Round 1 data showing maximum penetration readings at 10 mm below the material face.

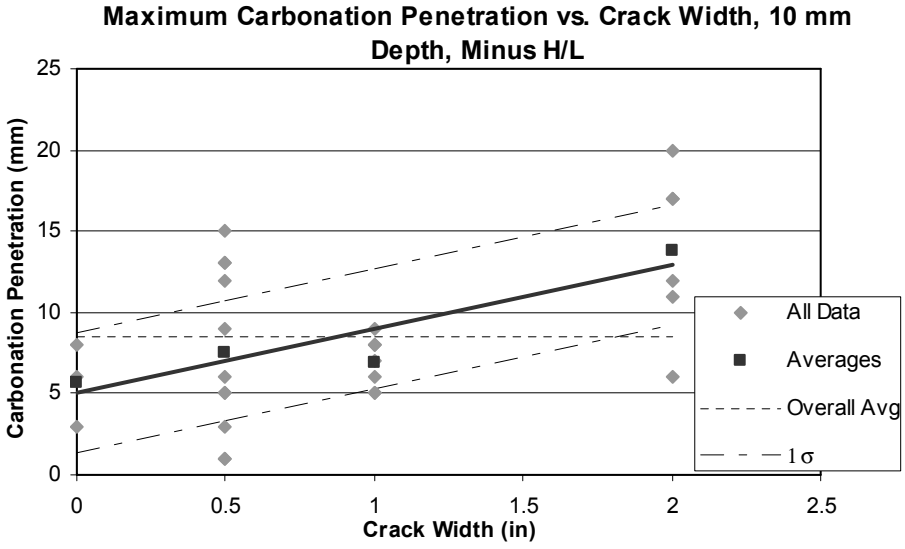

Figure 4.6. Round 1 data showing maximum penetration readings minus the high and low points at 10 mm below the material face.

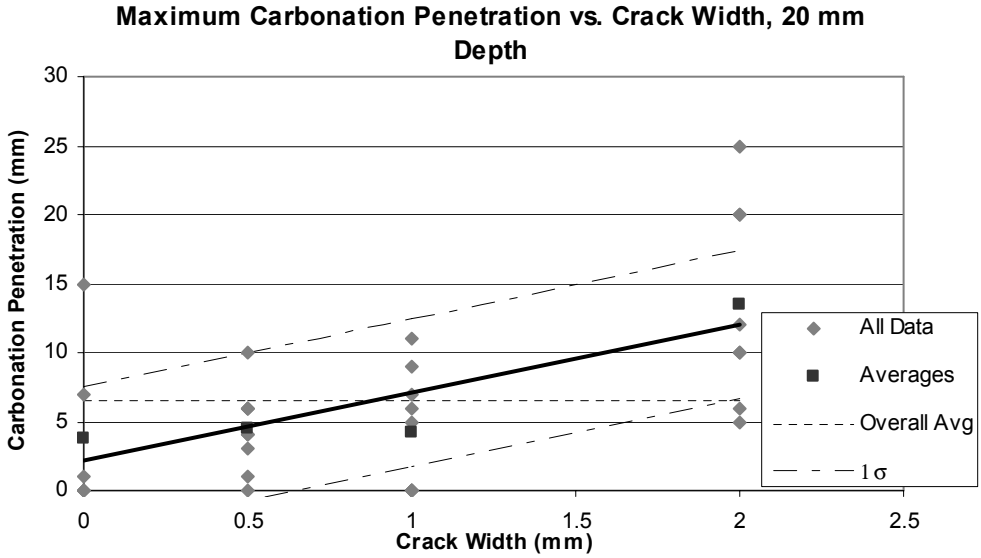

Figure 4.7. Round 1 data showing maximum penetration readings at 20 mm below the material face.

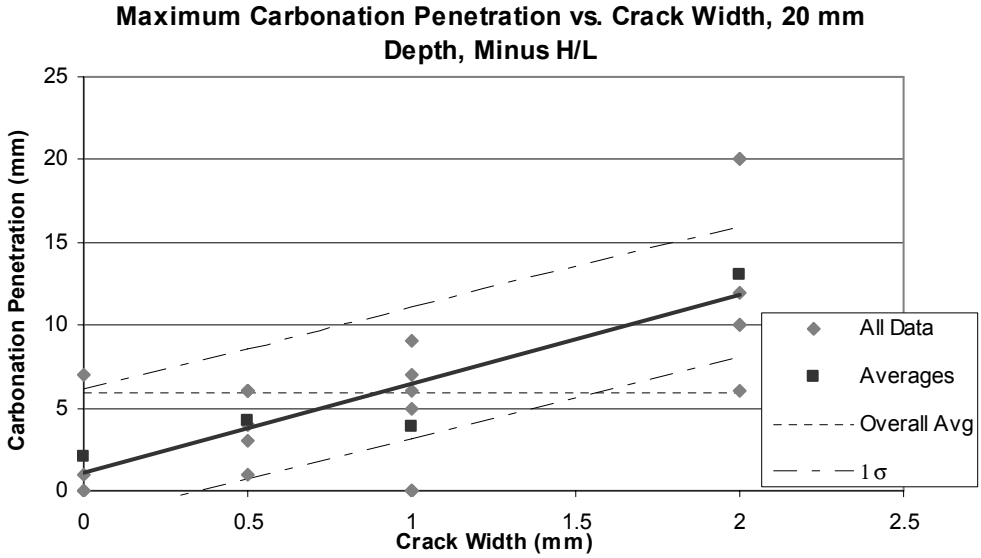

Figure 4.8. Round 1 data showing maximum penetration readings minus the high and low points at 20 mm below the material face.

Minimum measurements were taken in the center portion of the samples, avoiding the curved ends of the carbonation front. Figure 4.9 shows that the minimum readings at 10 mm below the material face again reasonably follow the linear trend, but there is no statistical significance around the overall average line. Data for the minimum readings at 20 mm below the material face were not plotted since many readings were zero. Possible reasons for the high standard deviation include local variations that cause the carbonation reaction to vary, inability to reduce all error out of the data set, and judgment on where to begin the minimum reading with respect to the curved front, etc. Removing the extreme points for each crack width significantly improves the standard deviation for the minimum readings. Figure 4.10 shows the minimum carbonation penetration depth minus the high and low points for each crack width. By removing the extreme points, the standard deviation lines follow the upward linear trend around the overall average line and reduces the standard deviation from 3.1 to 2.4, a 23% reduction.

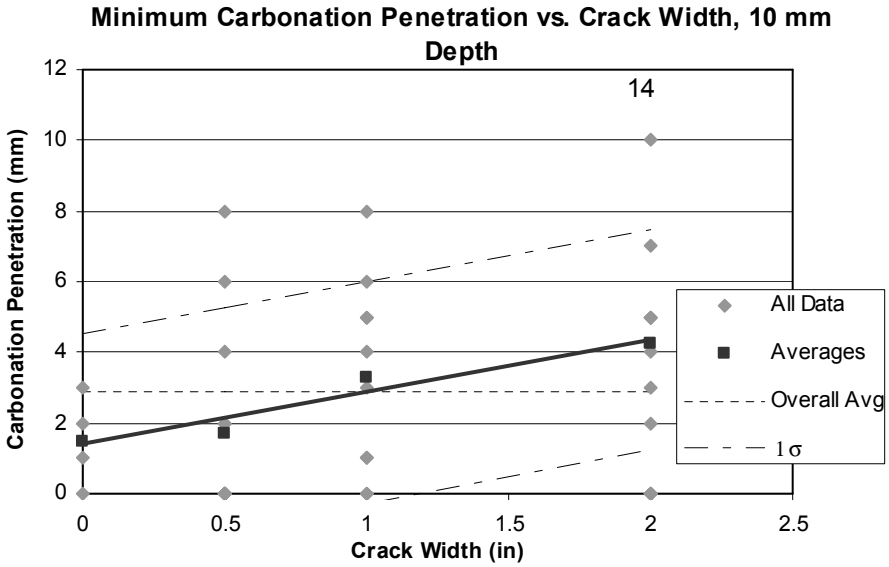

Figure 4.9. Minimum carbonation penetration depth for round 1, 35% fly ash mix.

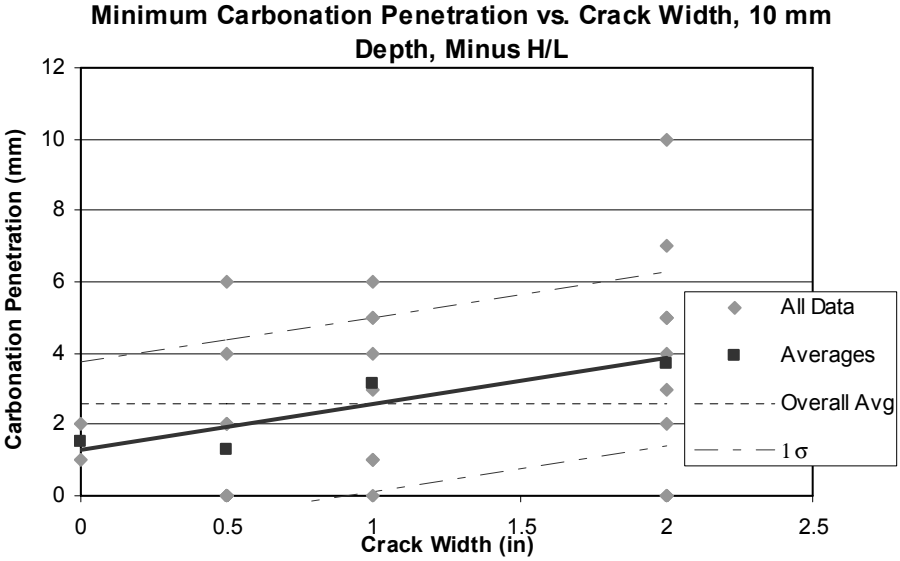

Figure 4.10. Minimum carbonation penetration depth vs. crack width minus the extreme points for round 1, 35 % fly ash mix.

Measurements of the maximum and minimum carbonation penetration were not as useful for this type of analysis for several reasons. Extremes are largely affected by local variations in the cement paste. For example, the minimum carbonation penetration reading may have resulted from a large piece of aggregate at that location that prevented the carbonation from occurring beyond it, or that area may have had saturated pores that kept the local humidity too high to allow the reaction to occur at a measurable rate, or wires impeded air flow and slowed nearby carbonation rates. Maximum penetration readings were most largely affected by carbonation through the sample face running parallel to the crack. At times carbonation fronts from the crack surface and the side face parallel to the crack surface converged and made evaluation of carbonation through the crack face impossible.

In addition to the maximum, minimum and average readings of the carbonation front, digital photos of each test surface were taken and the total carbonated area was calculated using AutoCAD. Areas, shown as percentage of total area of the sample, are plotted with respect to crack width in Figure 4.11. Area calculations show the linear trend, but with very little confidence. The data collected for the 0 mm crack width did not fit the trend at all and a best-fit line through the remaining averages did not show one standard deviation confidence around the overall average line.

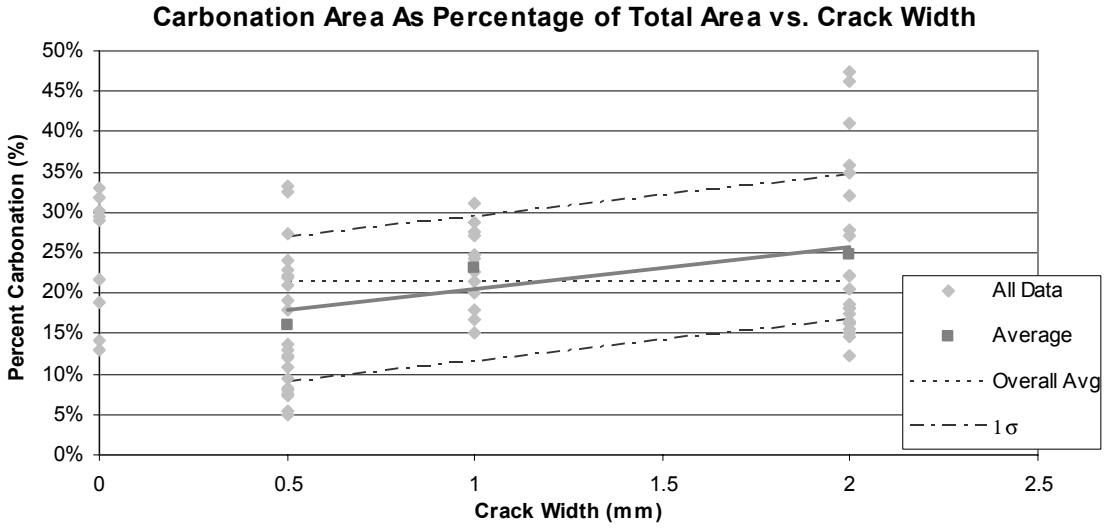

Figure 4.11. Round 1 data of total carbonated area as percentage of total area for 35% fly ash mixture.

These poorer results can be attributed to several issues with the procedure and sample makeup. First, the accuracy of the area measurements depends on the resolution and color sensitivity of the camera. These factors affect the ability to clearly identify the carbonation front on the photo. Minute color changes were not as visible on the photos as they were to the eye due to the color sensitivity and to the inability to view the sample at varying angles as is possible when measuring the actual sample. Second, all carbonation was included in the measurements. As described above, carbonation was occurring through faces other than the crack face; this carbonation was not as easily removed from the area calculation as it was from the maximum, minimum, and average front readings.

Carbonation Penetration and Crack Depth

Carbonation penetration can be compared to the depth into the crack, as shown in Figure 4.12. Data are plotted at 10 mm, 20 mm and 35 mm below the material surface. From the plots one can see that the curves are not well defined since measurements were made at only three depths and there were many zero readings in the smaller crack widths' data sets. Also, the data begins at a depth 10 mm below the material face. Important data are present above this depth, but due to the method of breaking, data were not attainable above 10 mm. A general trend is noticed in the data that supports the observation that there is a decrease in carbonation penetration as depth into the crack increases. In comparing the average fronts of the data, one can again see that at 0 mm and 0.5 mm crack widths trends are similar, as is the case in many of the previous figures. As the crack width increases beyond 0.5 mm, the averaged fronts tend to increase in magnitude and become flatter in nature, indicating that a potential linear relationship exists. Readings at more depths than those in this round of testing would help verify the linearity of this relationship.

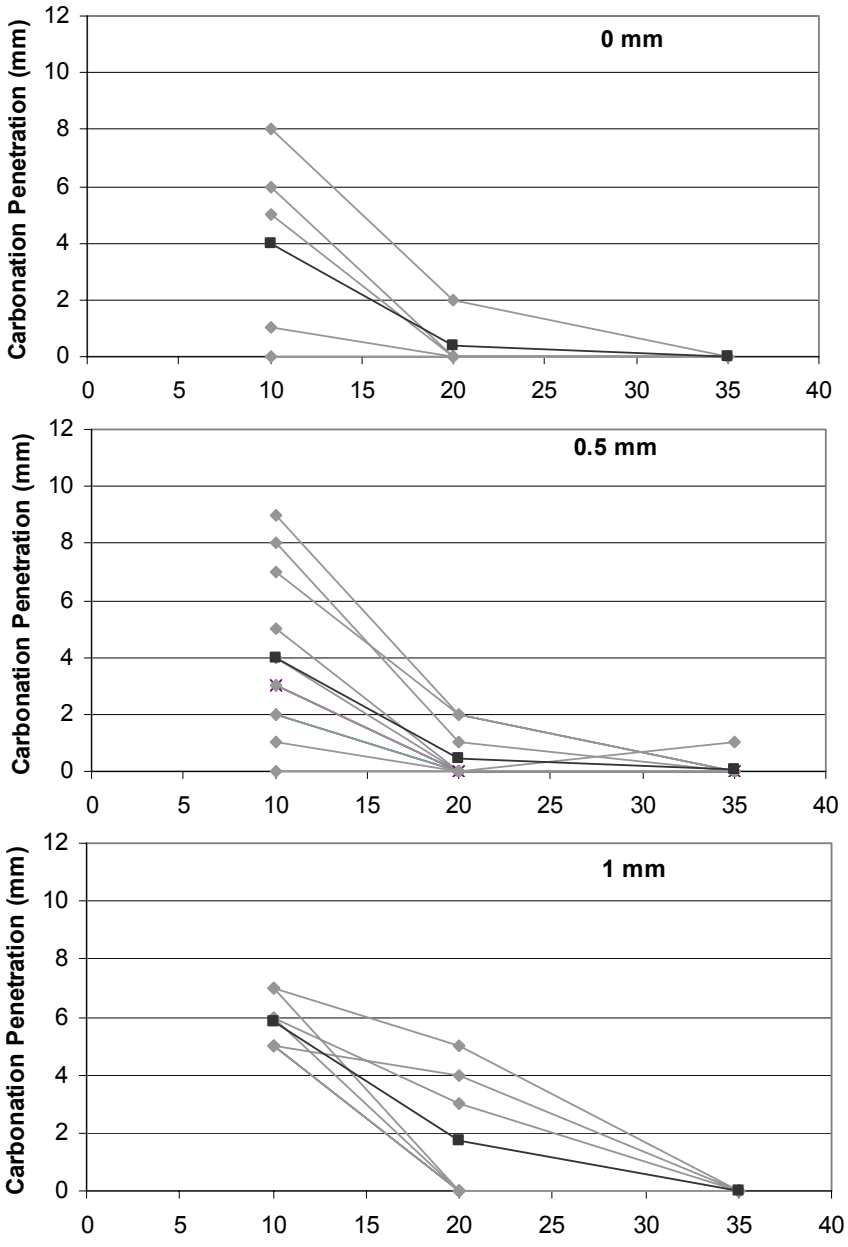
0 mm
0.5 mm
1 mm
Carbonation Penetration (mm)
0
2
4
6
8
10
12
0
5
10
15
20
25
30
35
40

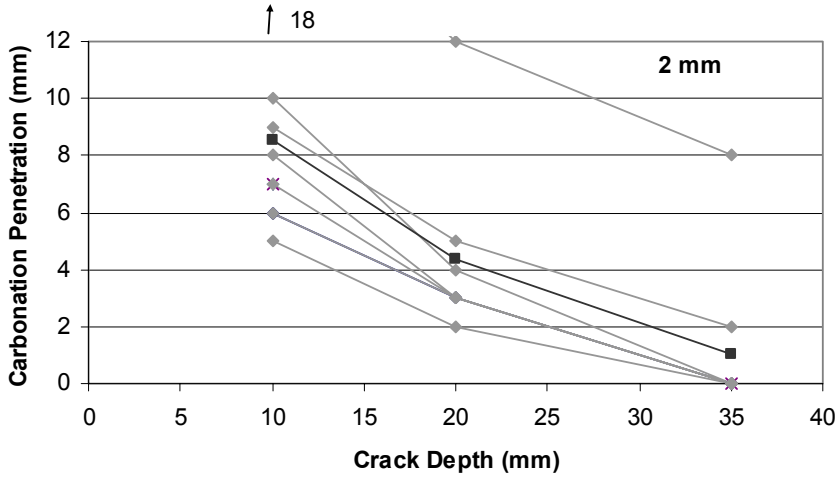

Figure 4.12. Carbonation front progression with respect to depth into the crack for all crack widths.

Round 2- l

Round 2 data from the 50% fly ash samples is presented in Figures 4.13 - 4.21. As stated in the experiment chapter, penetration readings were taken at 0 mm, 3 mm, 5 mm, 10 mm, 20 mm, and 25 mm from the top of the sample (the material face) and the maximum depth into the crack where carbonation occurred was also recorded. After readings were taken at 3 locations in the sample (see Figure 3.19 for test surface locations), the 12 data points at each depth were averaged. Averaging was done to attempt to better quantify the data since many readings were near the measurement precision of 1 mm. The average carbonation penetration for each sample was then plotted versus crack width.

Figures 4.13 and 4.14 show the averaged data at 0 and 3 mm crack penetrations. These plots do not follow the upward linear trend established in the first round of testing. Their average lines are almost horizontal, indicating that the crack width has no impact on the results. It is believed that these readings are affected by carbonation through the top face of the material, despite the coating of impermeable paint on the top surface. Carbonation occurring at the surface of a sample is independent of the crack width. The

slight downward trend in Figure 4.13 and the slight upward trend in Figure 4.14 are not significant since the change is less than 1mm, which was the precision to which the readings were taken. These results do stress the importance of taking crack penetration readings beyond the depth where surface carbonation has occurred.

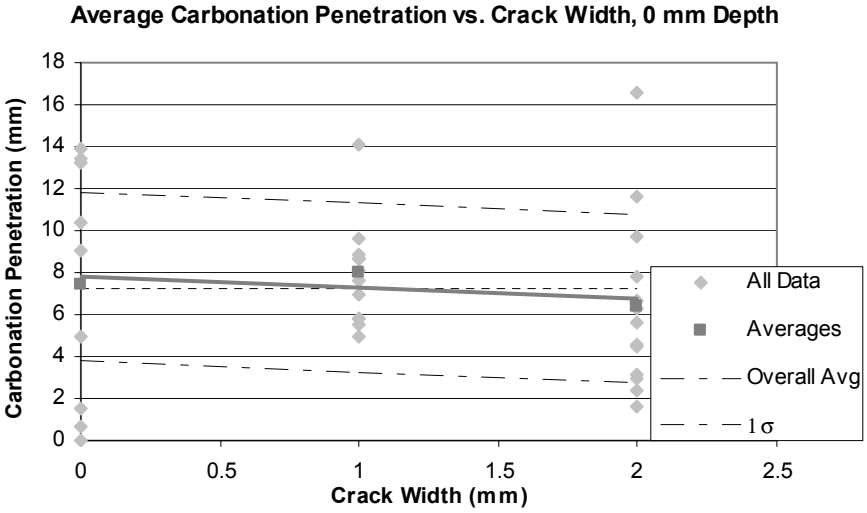

Figure 4.13. Round 2 data for 50% fly ash samples at 0 mm into the crack.

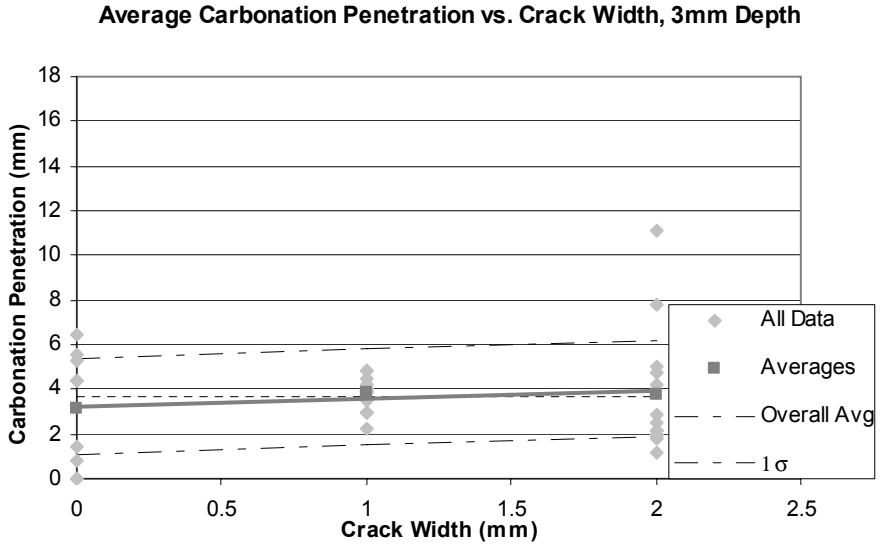

Figure 4.14. Round 2 data for 50% fly ash samples at 3 mm into the crack.

Carbonation penetration at 5 mm into the crack began to be affected by crack width as can be seen in Figure 4.15. The results are not as statistically significant as the results obtained in round 1. First, the standard deviation is near the precision to which the readings were taken, 1 mm. This poorer fit can be attributed several sources of error. First, some of the readings may have been slightly impacted by surface carbonation, as described above for the 0 mm and 3 mm plots and shown in Figures 4.13 and 4.14. Second, the carbonation rates were significantly slowed due to the inability to remove excess water inside the samples. The slower reaction rate reduced the penetration, therefore making the readings closer to the precision value. Measurement precision would have to be increased to collect more accurate information given the same experimental protocol.

When extreme points are removed from the 5 mm deep data set the overall average or the standard deviation were not notably changed. Figure 4.16 shows the 5 mm depth data minus the high and low points. The standard deviation was reduced from 1.1 mm to 1 mm, only a 9% reduction. The range was already rather confined for this data set, so removing data points only reduced the data set. A more confined range for this data set may indicate that the experiment was better controlled than in round 1, i.e. a smaller number of readings were impacted by significant errors associated with the first round of testing. See Chapter 3, "Experiment", for details.

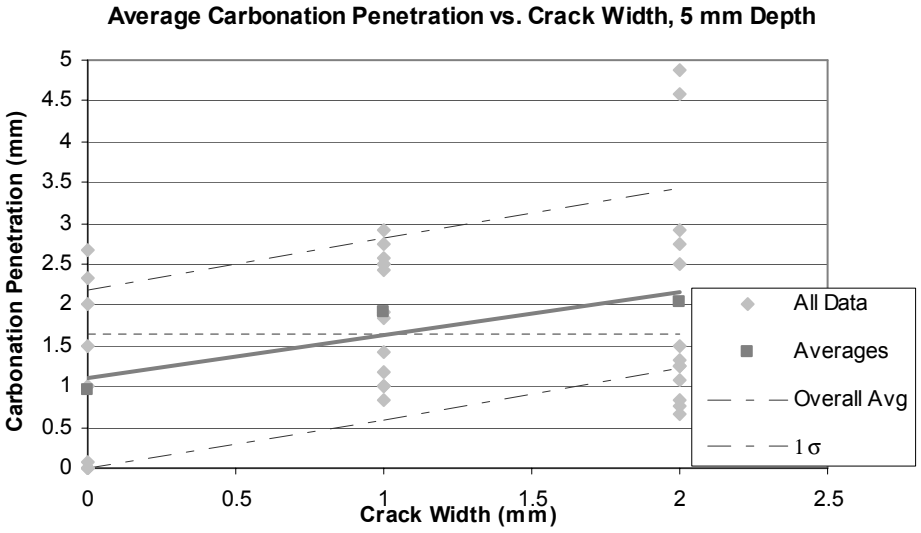

Figure 4.15. Round 2 data for 50% fly ash samples at 5 mm into the crack.

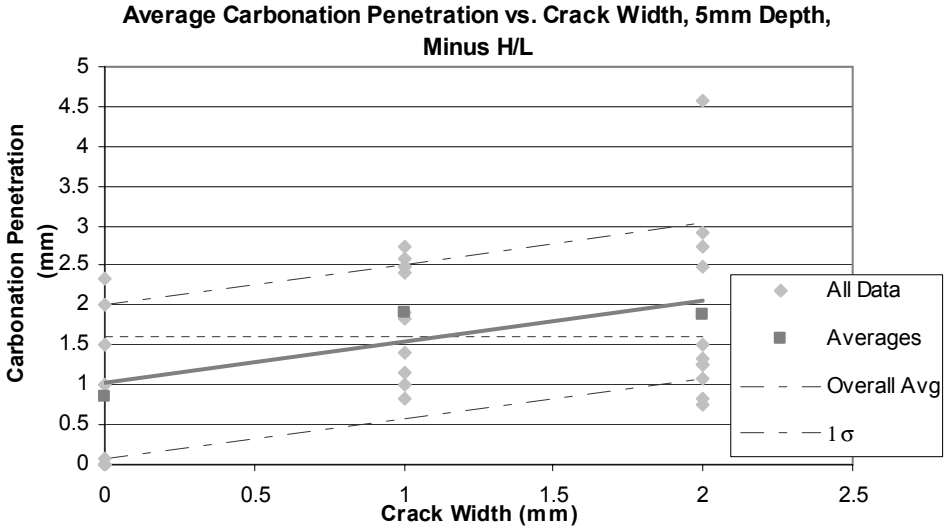

Figure 4.16. Round 2 data for 50% fly ash samples at 5 mm into the crack minus extreme points at each crack width.

Readings taken at 10 mm distance into the crack again showed a linear trend, indicating that there was no effect of carbonation through the material face. Figures 4.17 and 4.18 show the carbonation penetration vs. crack width with all data and excluding the high and low points, respectively. In both figures there is high agreement between the best-fit line and the average points for each crack width. The standard deviation is reduced significantly by removing the high and low points from each crack width data set. Removing the unusually high reading of 4.5 mm at the 2 mm crack width had the most effect in reducing the standard deviation from 0.8 to 0.5, a 37% reduction. This data set, though, because of the small values measured, had a significant number of zero readings, indicating that no carbonation took place on many samples and as a result, the averages for each sample tended to be less than the measurement precision of 1 mm.

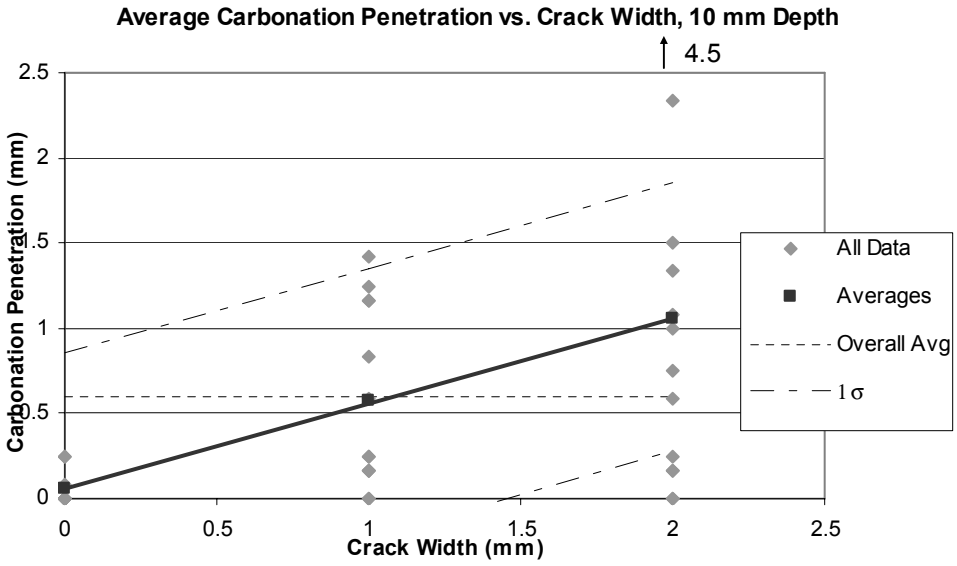

Figure 4.17. Round 2 data for 50% fly ash samples at 10 mm into the crack.

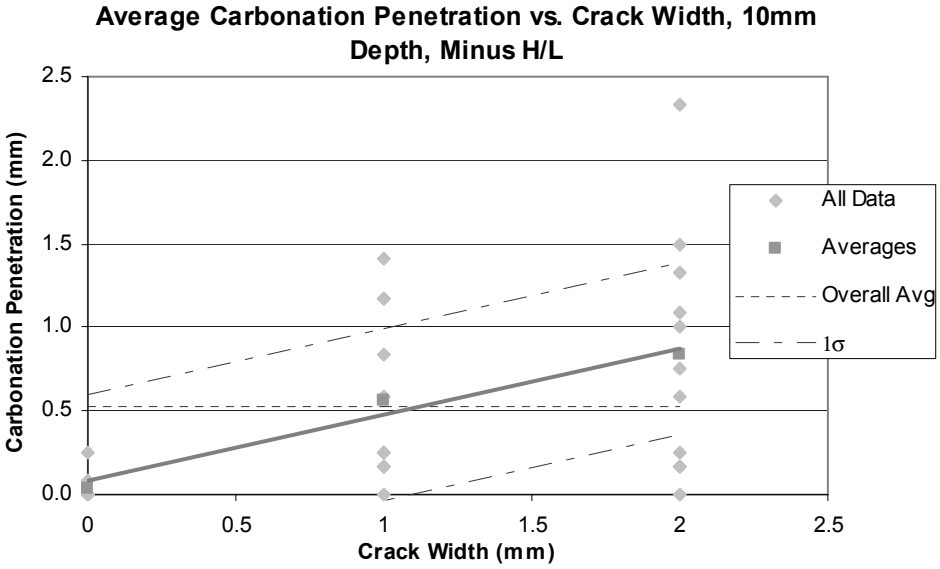

Figure 4.18. Round 2 data for 50% fly ash samples at 10 mm into the crack minus extreme points at each crack width.

The maximum depth to which carbonation penetrated the crack was recorded to determine if a linear relationship could be obtained for such readings, as well. Figure 4.19 shows the crack width versus the maximum penetration of the carbonation into the crack. A linear trend is seen and a comparison of the standard deviation indicates there is approximately 67% confidence in the trend. Schiessl (1988) theorizes that there is a square root relationship between the depth the carbonation front will reach into the crack and the crack width. The relationship is complex and requires detailed analysis of diffusion rates of CO_2 into the cement paste and differences between CO_2 concentrations in the air and at the carbonation front. Iyoda and Uomoto (1998) tested concrete for maximum carbonation depth in a crack and stated crack width had little effect on maximum carbonation depth into the crack. Not enough data were collected to test the validity of Schiessl's square root relationship as affected by crack width and the data

presented disagrees with Iyoda and Uomoto's observations. It appears that as a first order approximation a linear relationship may be employed with 67% confidence for cracks of 0 to 2 mm width.

Removing the high and low values for each crack width improves the fit of the data, though not significantly. By reducing the data set the statistical significance improves to within one standard deviation for the maximum crack penetration. Figure 4.20 presents the maximum crack penetration data minus the extreme points. The standard deviation reduces 19%, from 3.2 mm to 2.6 mm, when the extreme points were removed.

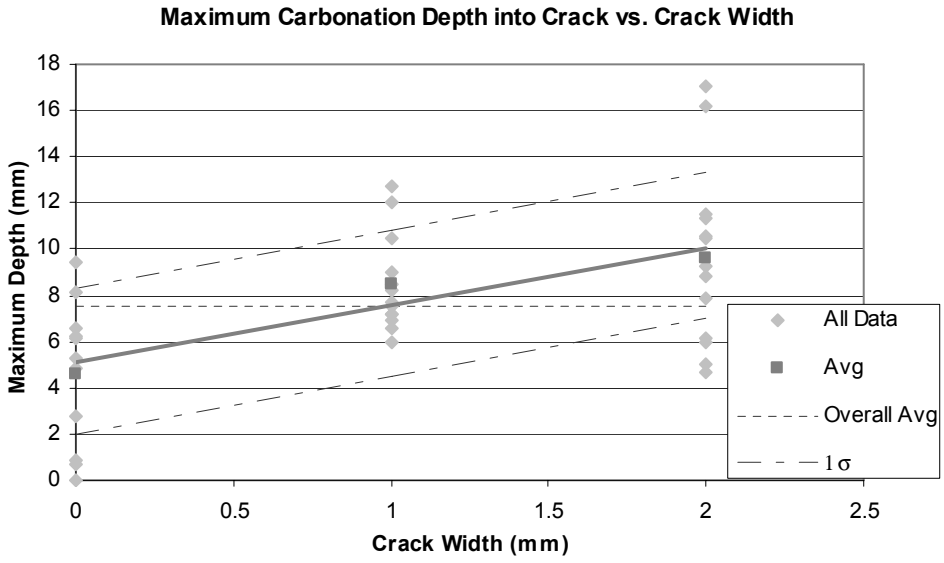

Figure 4.19. Maximum depth carbonation reached into the crack for Round 2 data, 50% fly ash samples.

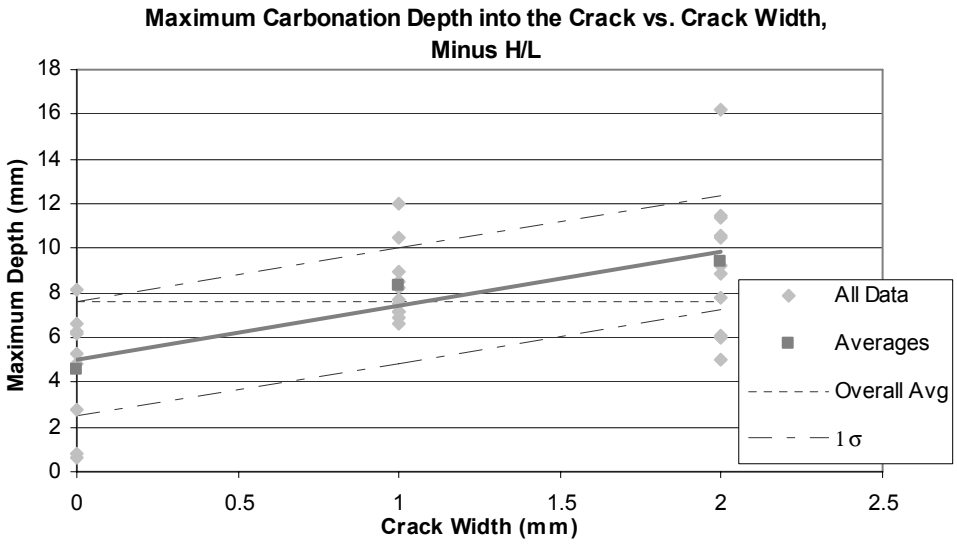

Figure 4.20. Maximum depth carbonation reached into the crack for Round 2 data minus the high and low points, 50% fly ash samples.

Analysis of Continuous Carbonation Fronts

Due to the method of breaking the samples perpendicular to both the material face and the crack surface, the entire carbonation front was examined on the round 2 specimen. With this data the linearity of the carbonation front with respect to crack depth can be evaluated. Data is only plotted to a depth of 10 mm since little carbonation occurred beyond that value. Figure 4.21 shows the carbonation front progression with respect to depth into the crack for each crack width. On each plot there are two best fit lines, one fitted through all 4 average points and a second one fitted through the average points deeper than 3 mm. As can be seen in all three plots the average carbonation depth at 0 mm into the crack is around 7-8 mm, indicating something other than crack width is controlling the carbonation penetration at that point. In this case, carbonation through the

material face is governing the data. By fitting the best fit line through only three points there is a much higher agreement at the 10 mm depth into the crack since the high values at 0 mm depth are not forcing the line to have a steeper slope.

Upon examination of the two best fit lines on each plot, a trend is identified. As the crack width increases, the two best fit lines become more similar in slope. At 2 mm crack width the two lines are almost indistinguishable. This behavior can likely be attributed to the fact that as the crack width increases, the carbonation penetration value increases, thereby approaching the value that is attributed to carbonation through the material face.

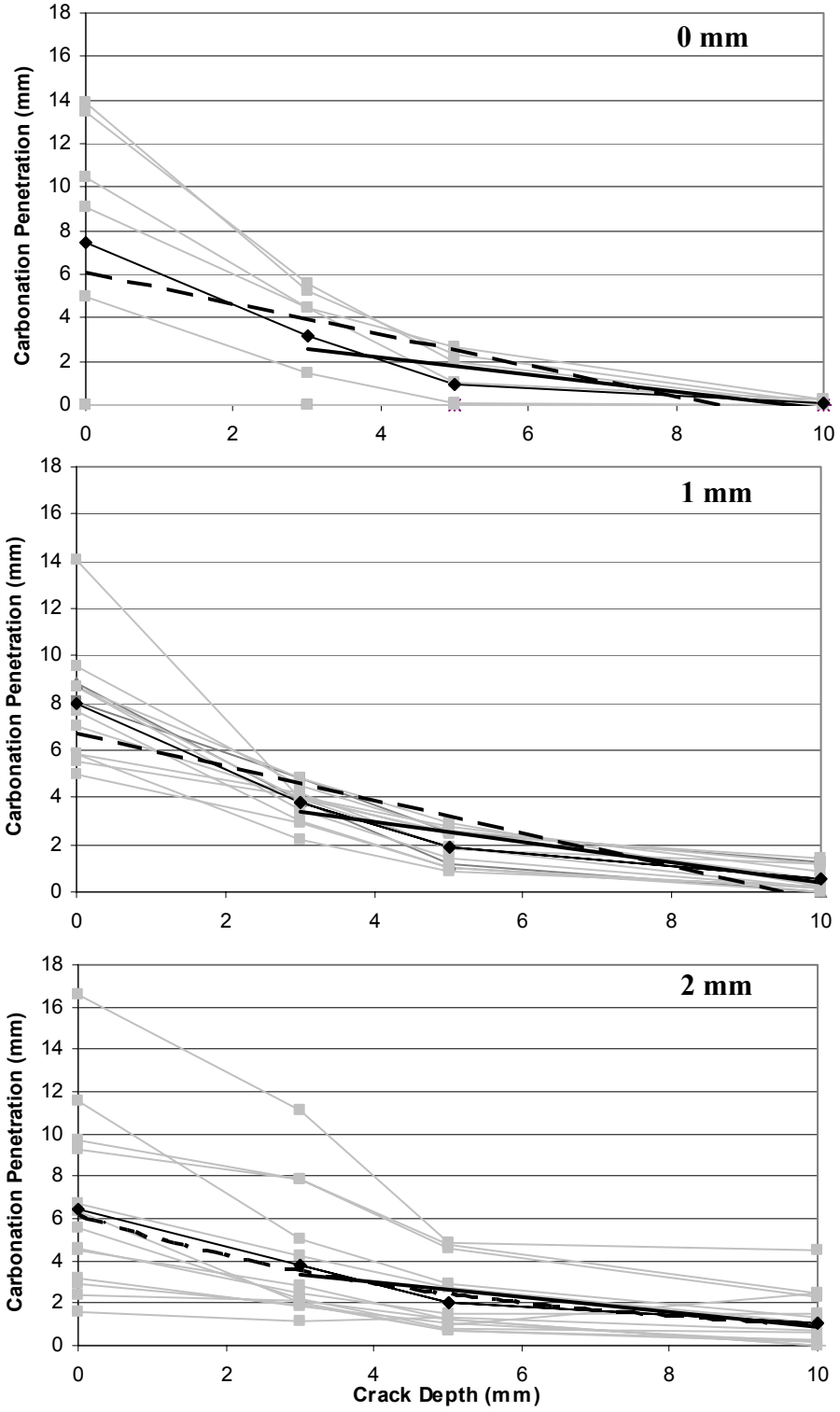

Figure 4.21. Carbonation front progression with respect to depth into the crack for samples with 0, 1, and 2 mm crack widths. Best fit lines are linear.

Another trend that is apparent when studying the carbonation front progression is the shape of the curves for the 2 mm crack width. As was described in Chapter 3, there were two trends in the shape of the carbonation fronts, a concave inward curve and a rectangular curve. Graphs for the 0 and 1 mm crack widths tend to have the concave inward curve while the 2 mm crack width curves can have either the concave inward curve or the rectangular curve. This is likely a result of the changes in the exposure of the crack face due to the wider crack width. The wider crack width allows more of the crack surface to be exposed to open gas currents, as opposed to the confined gas currents in the crack. There seems to be a tendency for the 2 mm curves to be concave inward. The cause for the change from the concave inward curve to the rectangular curve is unknown.

Chapter 5
Analysis

Overall Observations

Overall, these observations confirm the hypothesis that penetration of carbonation into the crack surface increases linearly with crack width. The linear trend is seen in most of the data collected with a confidence of 67% as calculated by comparison with the standard deviation of the data about the best fit line. Breaking samples perpendicular to both the material face and crack surface to expose a continuous carbonation front with depth into the crack allows continuous observation of the phenomenon. Round 1 samples tend to have larger carbonation penetrations (because the carbonation progression was not hindered by high interior relative humidity) than the samples in round 2; However, the statistical significance about the overall average line remained similar for both experiments. Measuring the carbonated area from photographs is not recommended because of the difficultly of photographically capturing minute color changes that are visible by eye on a fresh sample through rotation of the sample.

Statistical Significance of Observations

All of the trends of the rates of carbonation penetration with crack width have a statistical significance of 67%, or one standard deviation, σ. As shown by the comparison in Figure 5.1 the confidence exceeds 1σ upon removal of the high and low values. Thus it is hypothesized that increasing the size of the data set would improve the statistical significance by reducing the effect extreme values have on the averaged data.

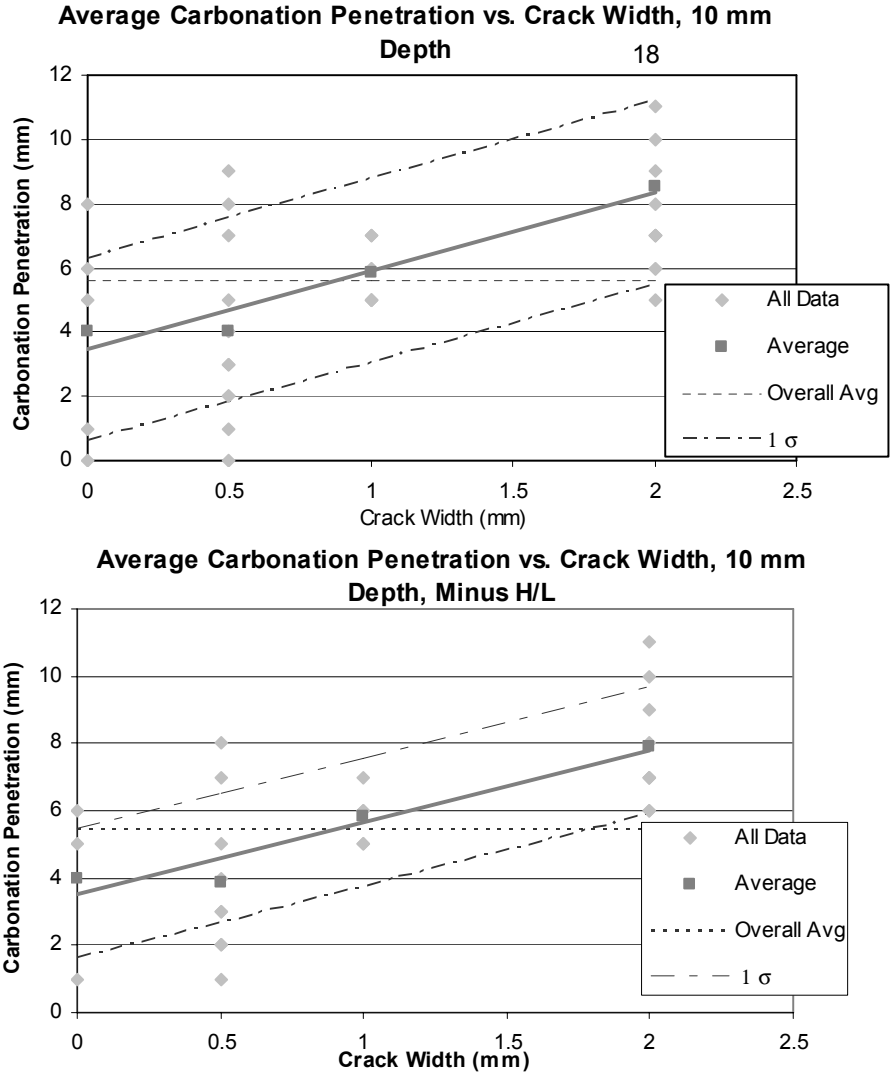

Figure 5.1. Comparison of trends of increasing carbonation penetration with crack width with and without extreme values.

Testing procedures and the measurement process can be improved but are likely to improve the fit of the data only slightly because of non-systematic factors such as local variations in the cement paste, i.e. humidity, temperature, water/cement ratio and aggregate location. These slight fluctuations can cause variation in the carbonation reaction. Slight improvement can be achieved by increasing measurement precision and improving breaking conditions.

It is hypothesized that variation could be reduced significantly by reducing the interior humidity of the samples. This reduction could be achieved by dry curing the samples in an environment free from CO_2 for longer than a typical 28 day cure time. Dry curing samples would allow the moisture from hydration to evaporate which would tend to decrease the interior humidity of the samples. Also, longer curing times would reduce the amount of hydration occurring during the carbonation experiment. If these steps are taken, the primary moisture source during the carbonation experiment would be only the carbonation reaction itself.

Trends in Carbonation Penetration with Depth

When plotting carbonation penetration fronts with respect to crack depth, as shown in Figures 4.12 and 4.21, only one observation can readily be made: carbonation penetration decreases as depth into the crack increases; however, if the average lines from those plots are placed on one graph, three observations can be made. Figure 5.2 presentes the average carbonation penetration lines from the series of plots in the above mentioned figures. From these plots, three observations can be made. First, as was stated above,

carbonation penetration decreases as depth into the crack increases. The data from both rounds show this trend with values tapering off at 35 mm in round 1 data and at 20 mm in round 2 data.

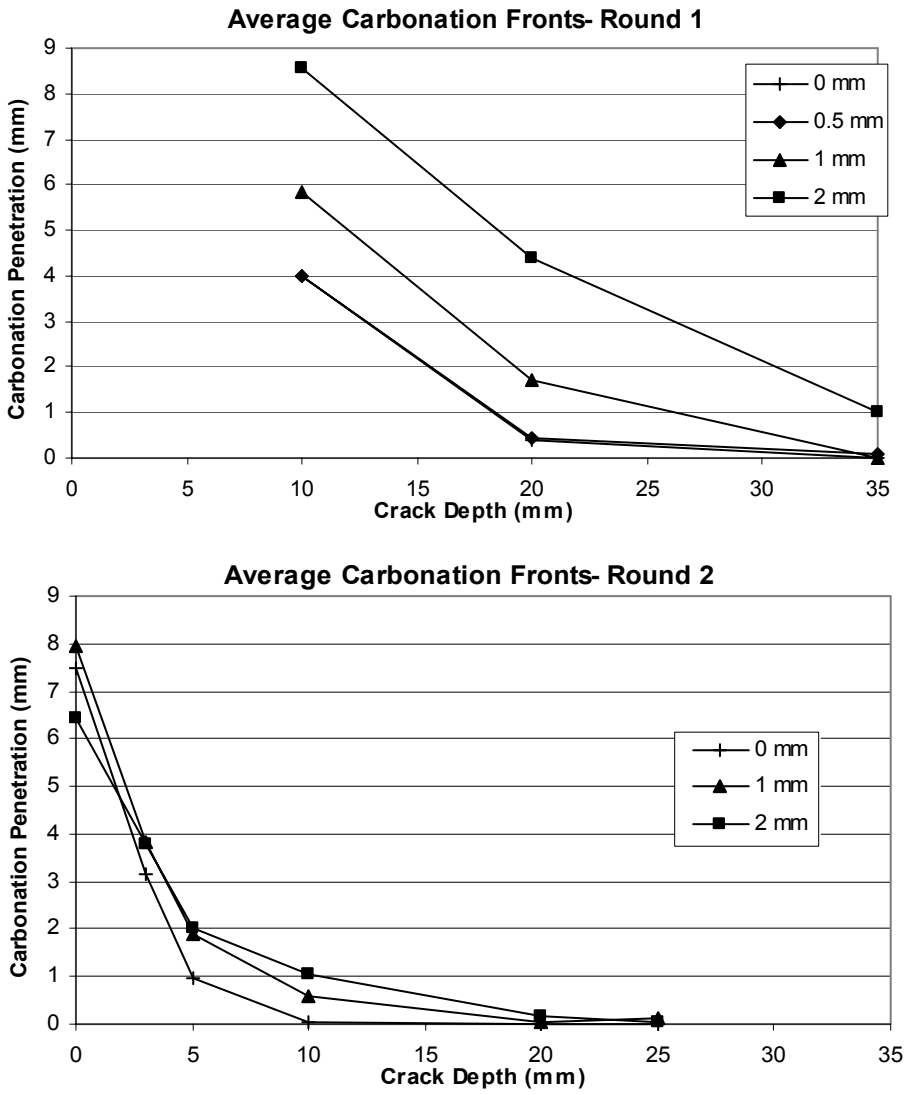

Figure 5.2. Average carbonation fronts showing trends of decreasing carbonation penetration with increasing crack depth and increasing carbonation penetration with increasing crack width.

The second trend identifiable in Figure 5.2 is the increase in carbonation as the crack width increases for the round 1 plot. The carbonation front lines plot progressively higher as the crack width increases, affirming the relationship of increased carbonation penetration with increasing crack width. The exception of this relationship is with the 0 and 0.5 mm crack widths in round 1. These lines plot on top of each other. It is assumed that at these low crack widths, the crack width may not necessarily be the only factor governing carbonation penetration. In the plot for round 2, the lines for the three different crack width plot within a small range. This observation indicates that in this case, the crack width was not the controlling factor in the amount of carbonation that occurred.

The third observation from Figure 5.3 is that there is significantly less carbonation in round 2 when compared to round 1. The carbonation fronts from round 1 plot higher than those in round 2 and the carbonation fronts penetrate deeper into the crack in round 1. These trends indicate that some factor or combination of factors retarded the carbonation penetration in round 2. This factor is discussed in further detail in later sections of this chapter.

Trends are most easily identified and supported in round 2, shown in Figure 4.21, as there were more observations. More observations were available because the samples were broken perpendicular to both the material face and the crack surface and a continuous carbonation front could be observed. If the effect of material face carbonation is filtered by omitting the 0 mm depth readings from the trend line, a linear trend line fits

the data well. Carbonation penetration versus crack depth from round 1, shown in Figure 4.12, shows the same trend as round 2; however, because of the smaller number of observations, no attempt was made to fit trend lines.

The carbonation penetration vs. crack depth relationships in round 2 were fit with both linear and exponential best-fit lines. Figure 5.3 shows the carbonation front plots with both linear and exponential best-fit lines. Standard deviations were calculated for both lines and are compared in Table 5.1. As can be seen in the table, modifying the best-fit line to exponential form improves the fit to the average line of the data, but not significantly. At best, the improvement was only 13%. Also, improvements in the fit are on the order of 10^{-2} mm, which is insignificant considering measurement precision was to the nearest millimeter. Improvement of the fit is only 10% of the measurement precision.

	Standard Deviation			
Crack Width	Linear	Exponential	Difference	% Diff
0	1.6	1.4	0.2	12.50%
1	0.8	0.7	0.1	12.50%
2	1.20	1.10	0.1	8.33%

Table 5.1. Variation in standard deviation with respect to the linear and exponential best fit lines for the carbonation penetration with respect to crack depth.

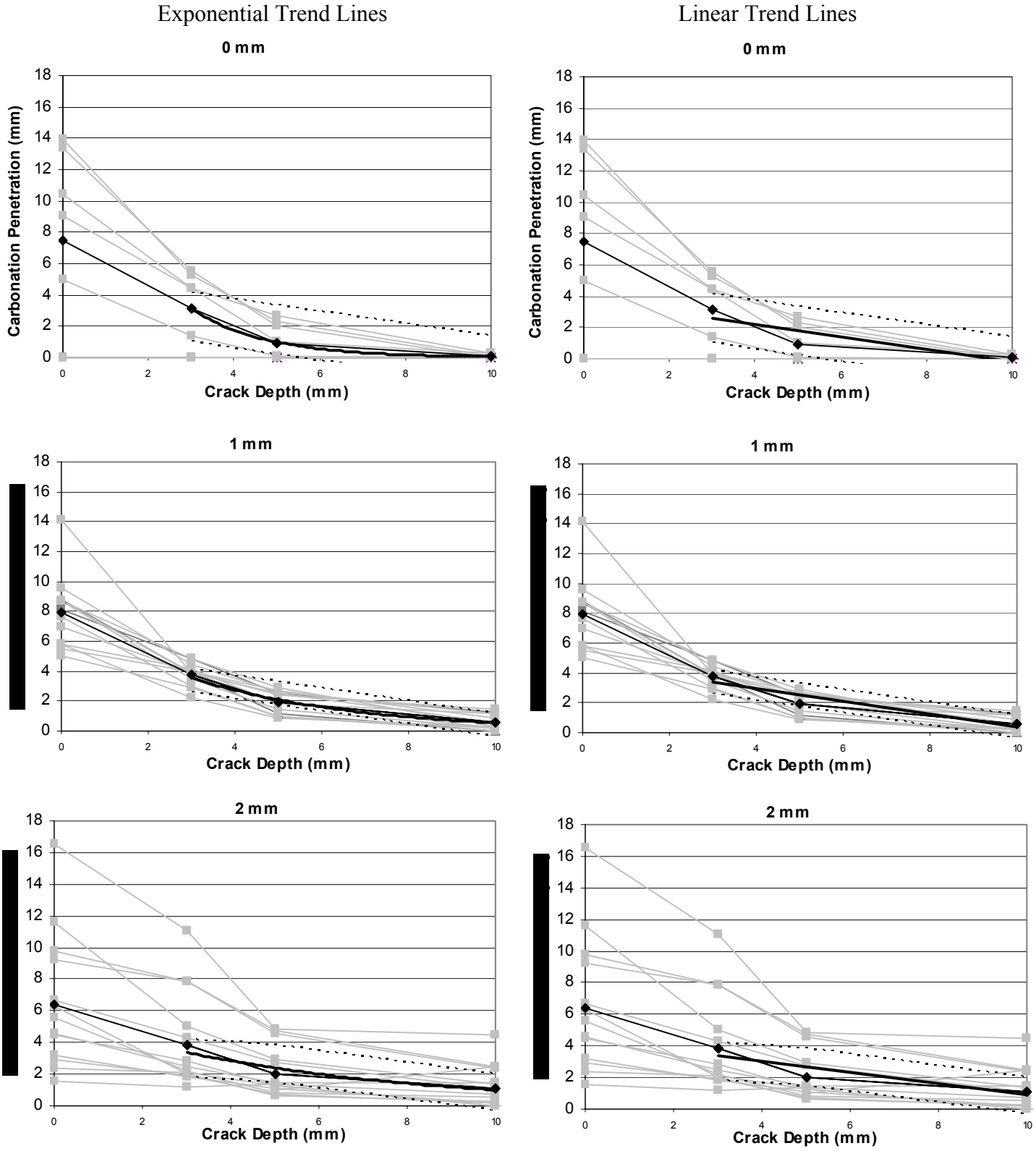

Figure 5.3. Carbonation fronts with exponential and linear best fit lines.

Variation in the carbonation front shape, as discussed in Chapter 3, Experiment, are evident in the 2 mm plots of Figure 5.3. Figure 5.4 shows the 2 mm carbonation front plot. These fronts with the rectangular shape show significantly more carbonation than do those with the curved shape. The greatest variation occurs right below the material face, above the 5 mm measurement. At 0 mm, carbonation is due to exposure of the material face. The 3 mm data are also affected by this material face carbonation. The 3 mm depth is where the rectangular fronts show the most variation from the curved fronts. It is believed that the 3 mm data are influenced by the exposure of the top corner to more freely flowing gas, which then produces the rectangular-shaped fronts, as described in the experiment chapter. If the few samples with shallow rectangular carbonation fronts are removed from the data set, the variation as expressed by the standard deviation is reduced, from 1.9 mm to 1 mm, a 53% reduction, as shown in Figure 5.4.

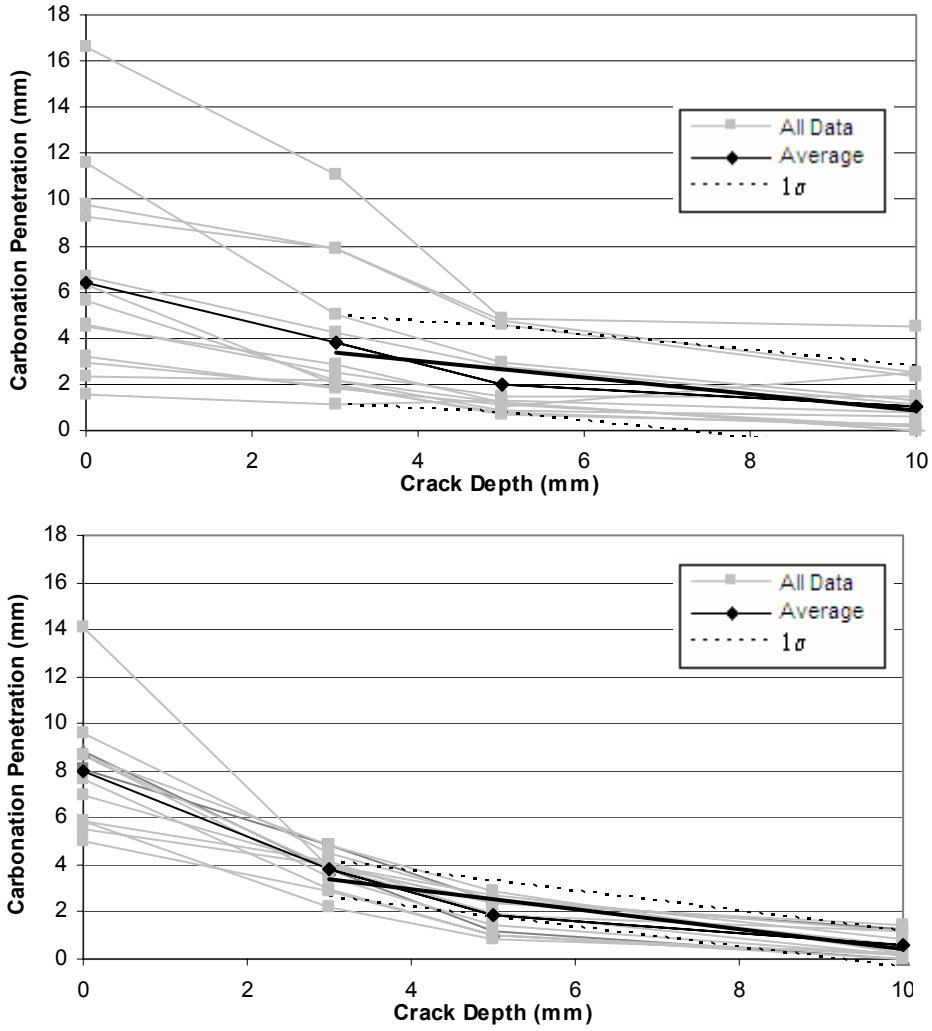

Figure 5.4. Reduction of standard deviation for the 2 mm crack width in round 2 data when rectangular-shaped fronts are eliminated.

As shown in Figure 5.5, sawing the access face in round 1 produced an additional 1.2 mm width of access to a depth of 5 mm. To account for the different exposures, it is assumed that the saw cut allows for full exposure of the top of the crack; therefore, data at 10 mm below the material face in round one is compared to data at 5 mm below the

material face in round 2 in Figure 5.6. The disparity in the overall amount of carbonation is evident.

Carbonation penetrations shown in Figures 4.12 and 4.21 are compared in Table 5.2. As the crack width increases, the range and average penetration increase. This increase could be attributed to the higher variability in air currents in the wider cracks, as well as the increased exposure of the top portion of the crack surface due to the wider crack width, shown in Figure 5.5. The exception to the increasing range with increasing crack width is the 1 mm crack width in both the 35% and 50% fly ash samples. For the 50% fly ash sample, the difference between the 0 mm range and the 1 mm range is less than the measurement precision; therefore the trend cannot be substantiated. The smaller range for the 1 mm crack width in the first round is artificially small because of a smaller sample set, as stated previously.

	35% Fly Ash Samples				50% Fly Ash Samples			
Width	Minimum	Average	Maximum	Range	Minimum	Average	Maximum	Range
0	0	4	8	8	0	0.1	2.7	2.7
0.5	0	4	9	9	--	--	--	--
1	3	5.9	7	4*	0.8	0.6	2.9	2.1
2	7	8.5	18	11	0.7	1.1	4.9	4.2
σ	--	--	--	2.84	--	--	--	0.78

Table 5.2. Ranges of penetration at 10 mm below the material surface for both sample sets. * Artificially small due to sample set size.

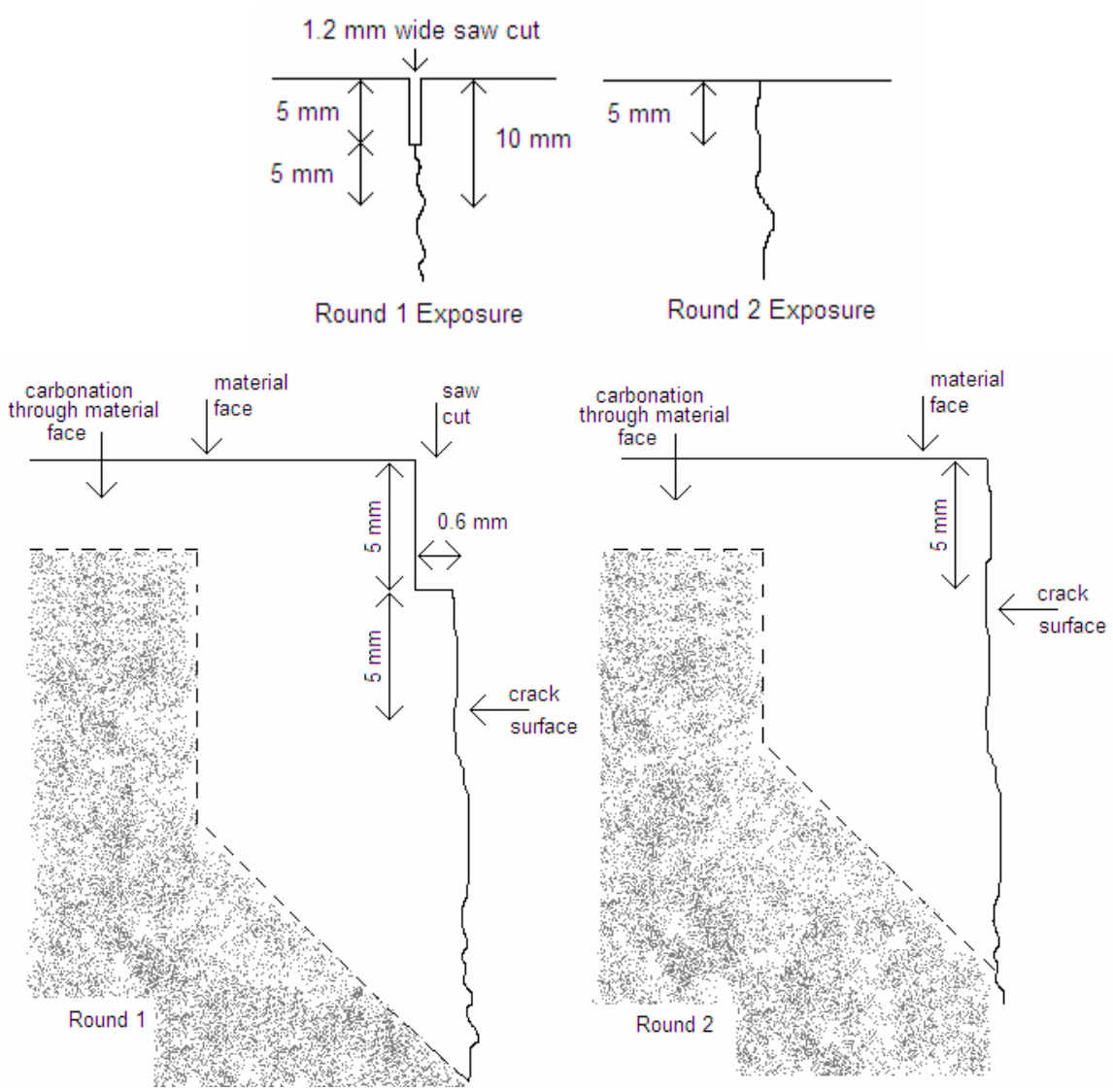

Figure 5.5. Figure showing the difference in exposure of the top of the crack from round 1 and round 2.

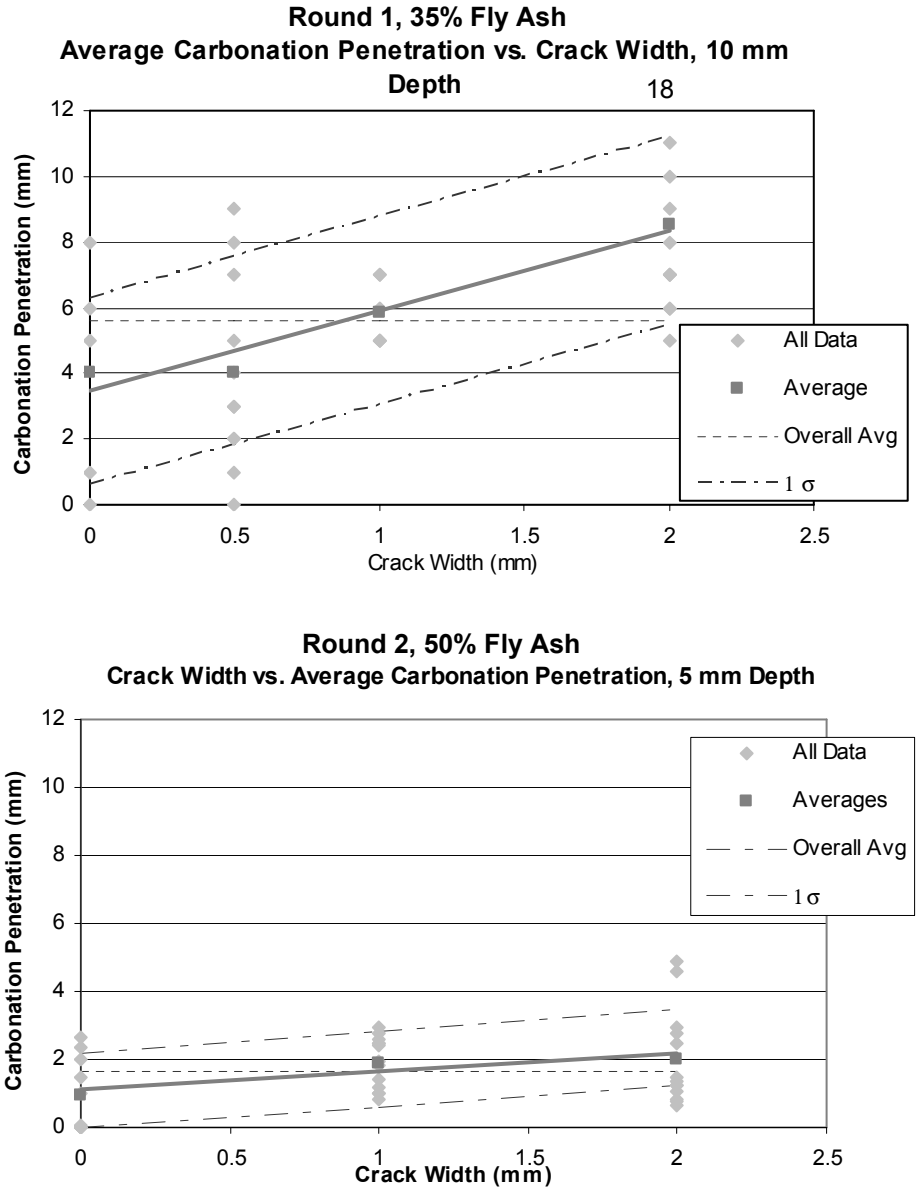

Figure 5.6. Plots of carbonation penetration vs. crack width for both the 35% and 50% fly ash samples, respectively.

It is also apparent that there is a large difference in the ranges between the two sample sets, with the maximum range of 11 mm in the round 1, 35% fly ash samples and only 4.2 mm range for the round 2, 50% samples. The same is true for the standard deviation. Figure 5.7 shows a scaled drawing for ranges in carbonation penetration for the 0 and 2 mm crack width. The figure highlights the difference in the amount of carbonation between each round and between each crack width. This large difference is a result of many differences in the two testing procedures. First, the variation in fly ash content would have a significant effect, but it is expected that the higher fly ash content would result in greater carbonation penetration. This is not seen in these data sets; therefore another factor must be causing large difference. The 50% samples' carbonation penetration was likely reduced by the high interior humidity of the samples caused by the epoxy. Another reason for the large difference is that the round 1, 35% fly ash samples had a significant amount of carbonation through the side faces of the samples and it is uncertain that all the carbonation that can be attributed to those side faces was removed from the data set. As a result the penetration may be slightly greater than if this overall sample carbonation was controlled, as it was in the second round when epoxy was used to cover the samples.

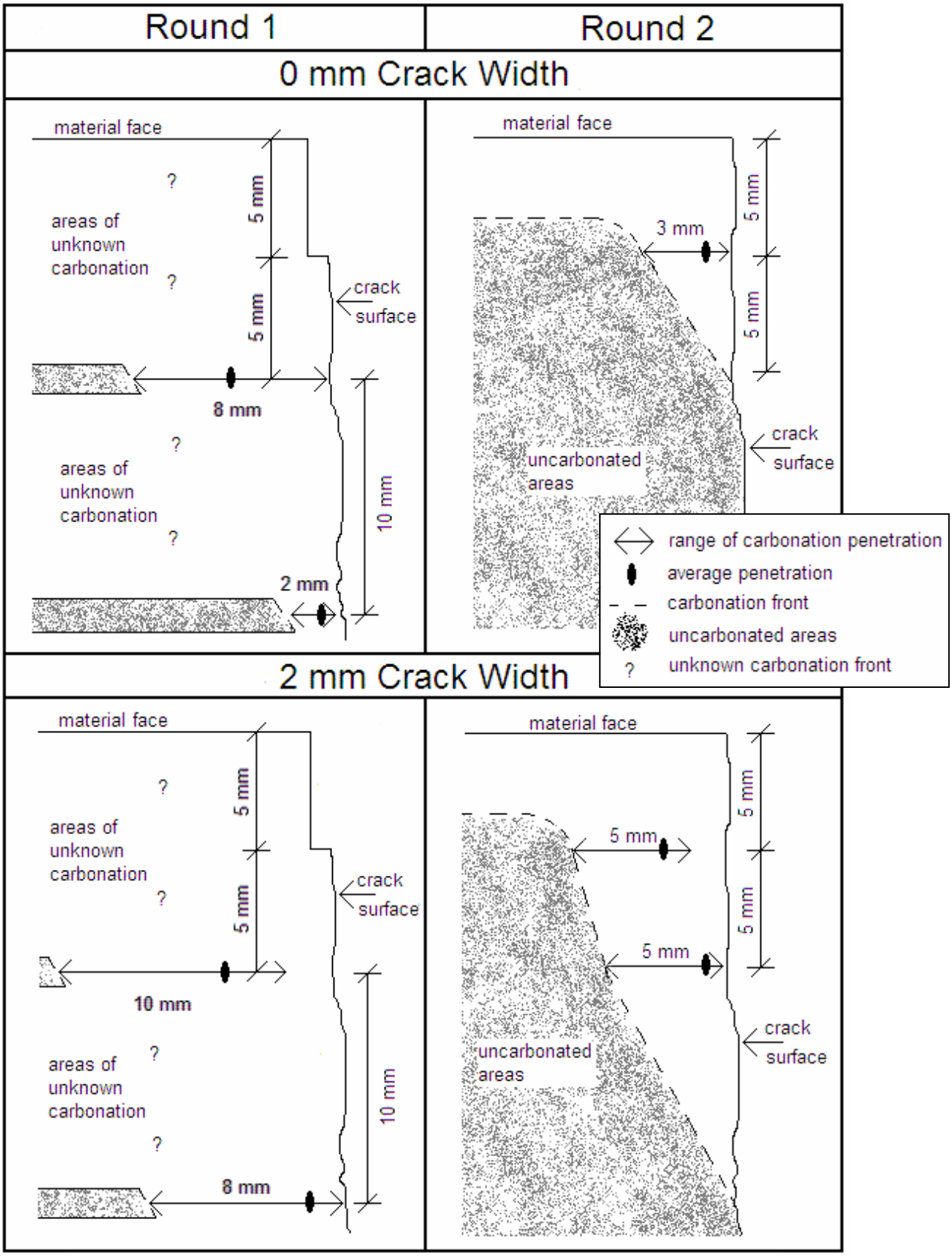

Figure 5.7. Comparison of carbonation penetration in Round 1 and Round 2. Stippled areas differ due to different test surface orientations (refer to Figures 3.15 and 3.20 for test surface orientations.)

Round 2 data, shown in Figure 4.21, are the most consistent because of the procedural changes, discussed earlier in Chapter 3, Experiment. As shown in Table 5.3 for all crack widths, the average and range of carbonation penetration decreases as the depth into the crack increases. However, for any single crack depth, trends in the average and range of penetration with crack width are not evident. Only at the 10 mm depth do average and range of penetration increase with increasing crack width. For the 0 mm and 3 mm crack depths differences between the averages of penetration for each crack width are not greater than the precision of measurement. As identified in Chapter 4, Results, these reactions were influenced by carbonation through the material face, rather than through the crack surface. All samples, independent of crack width, experienced the same exposure on the material face. The average penetrations for the 5 mm crack depth and the 10 mm crack depth increase with crack width and support the hypothesis of increasing average carbonation penetration with increasing crack width.

	0 mm Crack Depth				3 mm Crack Depth				5 mm Crack Depth				10 mm Crack Depth			
Width	Min	Max	Range	Avg	Min	Max	Range	Avg	Min	Max	Range	Avg	Min	Max	Range	Avg
0	0	13.9	13.9	7.5	0	5.6	5.6	3.2	0	2.7	2.7	1	0	0.25	0.25	0.1
1	5	14.1	9.1	8	2.3	4.8	2.5	3.8	0.8	2.9	2.1	1.9	0	1.4	1.4	0.6
2	1.6	16.6	15	6.4	1.2	11.1	9.9	3.8	0.7	4.9	4.2	2	0	4.5	4.5	1.1

Table 5.3. Ranges of carbonation penetration with respect to crack depth for all crack widths.

Precision of Data

The precision of the information presented must be addressed to appreciate the statistical significance of the trends identified throughout. Precision is first dependent upon the measurement technique. All measurements were made to the nearest 1 mm.

This limitation occurred for several reasons. Since the exact location of the colorless front is highly subjective, more precision simply placed more dependency on the subjectivity of the measurement. Also, in many instances it was difficult to place the scale immediately adjacent to the surface and therefore difficult to precisely measure the carbonation penetration due to the rough texture and uneven breaking of the surfaces to be measured.

Precision is also controlled by the degree to which calculation are carried out. All calculations were computed to the nearest 4 decimal place and then rounded to the nearest one decimal place. Values were only rounded once, at the end of the calculation, to ensure as little precision as possible is lost.

The number of observations differed significantly between rounds 1 and 2. Round 2 data were presented as the average of the carbonation penetration for the 12 surfaces that were measured for each sample, whereas each data point for round 1 represented only 1 observation. Thus there were 492 separate observations in round 2 and only 42 separate observations in round 1. See Figure 3.20 for the 12 surface locations in round 2 samples.

Relationship between Laboratory and Field Conditions

Laboratory conditions are not comparable to the conditions in the natural environment. For this type of research, accelerating the carbonation process is important in order to observe reactions within the tenure of a graduate student. As was stated in the

experiment chapter, cement mix and CO_2 levels were chosen to facilitate carbonation reactions in a relatively short period of time. Environmental conditions, i.e. temperature and humidity, were also manipulated to accelerate the process.

When selecting a mix design, several factors were considered. First, a mix that would facilitate the carbonation reaction was the primary concern. Goni (1997) showed measurable results in a similar time frame for mixes with w/c ratios of 0.5 and replacement of cement with fly ash at 30% and 50% by weight. Typically in practice w/c ratios are lower than 0.5, but it has been argued that carbonation does not occur significantly in mixes with w/c ratios less than 0.4 (Hime, 2004; Meyer, 1968). In an attempt to maintain mix proportions as similar as possible to those used in practice, a value of 0.5 was chosen. In typical mixes ratios of fly ash replacement is often in the range of 15% -30%. A replacement percentage of 35% was chosen to be at the highest end of generally accepted values to attempt to use a mix that had potential field use while still having the potential to produce significant carbonation during the testing procedure. The 50% replacement percentage was chosen to counteract the potential negative affects the relatively low w/c ratio may have on carbonation rates. Other potential additions to the mix design, such as plasticizers and other pozzolanic materials were omitted to prevent any unknown affects on the carbonation reaction.

The most significant laboratory factor manipulated to accelerate the testing procedure was the 100% CO_2 environment. Carbon dioxide concentrations in the atmosphere are typically around 0.036% (U.S.EPA, 2002), but this concentration varies

seasonally and locally. The CO_2 concentration is highest in the winter months and in urban areas where transportation emissions can accumulate and have been measured as high as 0.06% (Idso, 1998). Carbonation tests performed in natural conditions have taken as long as 20 years to obtain an average of 5-15 mm carbonation penetrations (Campbell, 1991). Most research facilities are unable to sustain activities this long. Future work in carbonation research should include identifying relationships between carbonation penetration rates and CO_2 concentration. Such relationships would enable comparison between carbonation penetration rates obtained during accelerated testing and those collected under natural conditions.

Temperature and humidity were chosen to accelerate response. The temperature was maintained around 20°C, which maximizes the rate of carbonation and represents a reasonable value for both indoor and outdoor temperatures (Neville, 2003). Maintaining a constant temperature accurately represents indoor conditions. Most exterior climates experience wide temperature variation over the year and hence the rate of carbonation would vary with the varying temperature.

Humidity levels were relatively high in the atmosbag for the first experiment and fluctuated in a 70-90% range. A typical humidity level indoors ranges from around 40-50%, while outdoors the range can be from near zero in an arid climate to 100% during a precipitation event. Originally, it was thought that the humidity inside the bag would be manipulatable, but it was discovered early on that the amount of water produced during continued hydration and during the carbonation reaction itself was enough to keep the

humidity above the desired range. Attempting to control the humidity with a desiccant was difficult, since the absorptive properties declined over short periods of time. As a result the humidity fluctuated within a 20% range. Arguably this fluctuation could be comparable to those in a natural environment and as such the laboratory test was successful in mimicking somewhat natural conditions.

Linearity of Relationships

Relationships developed herein have been assumed to be linear, which may not be applicable in practice for all situations. It is possible that the relations are 'S' shaped curves, as shown in Figure 5.8. As seen in Figures 4.1 and 4.2, there is little difference between the data collected for the 0 mm crack width and the 0.5 mm crack width. This may be indicative that there is little change in carbonation rates when the crack width variation is small. A threshold value may exist where the crack width is the primary factor controlling the carbonation rate. At crack widths below this threshold value carbonation rate is not related to crack width as penetration is more a function of material surface reactions. Carbonation rates in this range could be represented by a constant value related only to the carbonation rates of the material, independent of the crack width.

In situations where the samples are infinite or can be assumed to be infinite, i.e. a large slab, the assumption that the carbonation rate is constant over long periods of time is inappropriate. As the concrete is carbonated the permeability decreases, as the products of carbonation, carbonates, are larger molecules than the initial hydroxide molecules. A decreased permeability means that the rate of CO_2 carbon dioxide

penetration is slowed, thereby slowing the carbonation rate. The carbonation front may reach a point where the CO_2 penetration is so slow that the carbonation rate becomes negligible. Another result of decreased permeability is the interior relative humidity is not dissipated as easily. The relative humidity inside a large sample may never be significantly below 100%, indicating the carbonation rate at that location would be zero or negligible (Hime, 2004). If a carbonation front reaches such areas inside a large concrete sample, carbonation appears to stop suddenly. In this case the crack width is no longer the primary factor controlling the carbonation penetration rates. Figures 5.8 and 5.9 demonstrate these effects. The required amount of time for carbonation fronts to reach such areas varies with mix design, pouring conditions, curing conditions, etc. but this phenomenon must be acknowledged when using this type of analysis in determining crack age.

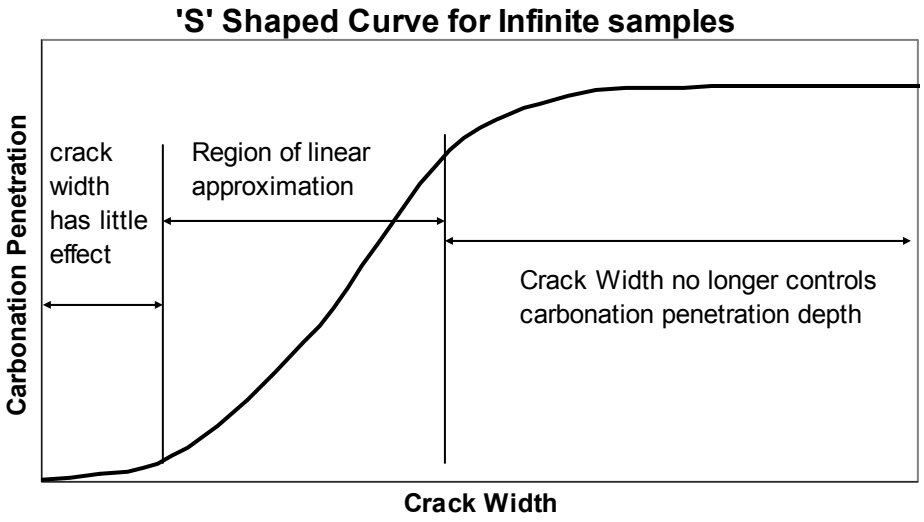

Figure 5.8. Graph identifying the thresholds where crack width controls carbonation penetration rates.

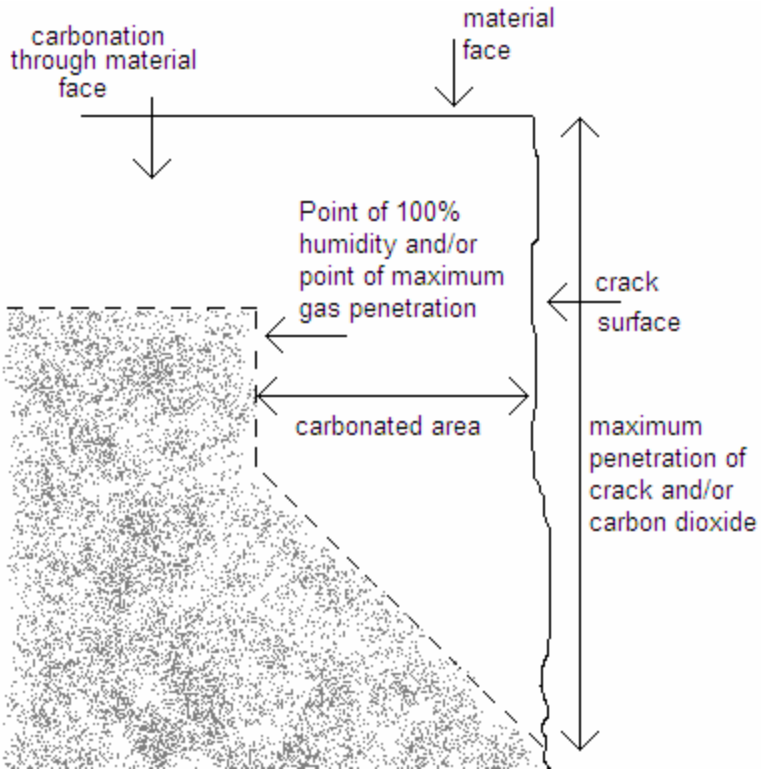

Figure 5.9. Schematic showing carbonation front shape when carbonation rates reach near zero.

Finally, cracks created in the field are often non-uniform in both shape and direction. They are often partially covered with paint or patching materials and may only be quasi-perpendicular to the material face. Even though cracks produced in the laboratory by the chisel and hammer method are planar and relatively perpendicular to the material face, they are rough like real cracks. As was discussed in Chapter 3 'Errors-Round 2' the larger samples did not break as perpendicular to the material face as did the smaller samples. Also, cracks in the field may vary in width along their length, depending on their propagation and direction. In the lab, the cracks are held open at a constant width along the entire length of the crack. These artificial laboratory uniformities may have a significant affect on carbonation, namely with respect to air flow. Round 1 samples tended to have parabolic carbonation fronts along their length that tapered off near the ends of the crack. These tapering fronts were attributed to the protruding wires that impeded free air flow to the entire length of the crack. Potential impedances in the field, like paint spanning the crack, can have similar effects on air flow and cause more fluctuation in carbonation reaction by reducing available CO_2. Another factor that may help replicate field conditions in the laboratory would be to first paint the samples, then crack them, allowing for the paint to overlay the crack, as it would on a naturally cracking material.

Chapter 6
Conclusions

Results of the two experiments to determine the effect of crack width on carbonation rates help clarify issues related to the use of carbonation in crack-age determination. The accelerated response procedure with 100% CO_2 and high fly ash content proved economical and rapid and is acceptable as long as time-independent relationships are tested. Future work is necessary to establish time-dependent relationships between CO_2 concentration and carbonation rates. Accelerated testing allows relatively rapid evaluation of several time-independent factors such as effects of water/cement ratio, fly ash content, humidity, temperature, etc. In addition, the several month reaction times are compatible with typical time scales of laboratory evaluations and thus do not create exceptional demands on laboratory resources.

Experimental Technique: Effect of Humidity

Control of humidity, both the interior sample humidity and that within the atmosbag, was a primary factor that affected results. Water produced by continued curing and the carbonation reaction itself produced humidities above optimum levels. Humidity should ideally be within 50-70% to produce the most efficient carbonation rates. Measured humidities in the atmosbag during testing were all above 70% and in some cases, above 90%, which significantly reduced carbonation rates. Humidity was reduced in the atmosbag with a desiccant, but their batch application caused fluctuations as high as 20% in the humidity levels. Interior sample humidity has an even greater impact on carbonation rates than does the exterior humidity and is not easily controlled. Carbonation rates are negligible at 100% humidity because the carbon dioxide cannot easily penetrate saturated pores. Reducing interior humidity while still preventing carbonation through faces other than the crack surface and/or the exposed material face is virtually impossible. It is theorized that epoxy used to prevent carbon dioxide from penetrating the sides of the sample also trapped water vapor produced during the continued curing of the concrete and during the carbonation reaction itself. Samples in future experiments may need to be aged in a dry, CO_2-free environment to allow for sufficient drying, while also preventing carbonation. It is recommended that this curing take place in a carbon dioxide-free environment, for instance inside the atmosbag with nitrogen or nitrogen-oxygen mixtures.

Wider Cracks Facilitate Carbonation Penetration

Measurements show carbonation penetration through a crack surface to be linearly proportional to the width of the crack. The observations have at or near one standard deviation confidence about an overall average. Carbonation profiles are also linear with respect to depth into the crack; however, carbonation through the material face must be removed from the profile to accurately apply the linearity to the carbonation front. Maximum carbonation depth in the crack from the material face appears to have a relationship with the crack width and it can be approximated with a linear relationship for small crack widths. Linear relationships are sufficiently simple to apply while still adequately describing the phenomena. These observations are based on moderately sized sample sets and as a result extreme measurements had a significant impact on the standard deviation. Larger sample sets can improve the statistical significance by reducing the impact of single extreme values on the standard deviation.

Applicability of Carbonation as an Age Dating Technique

Measurement of carbonation of concrete can be a useful tool in investigating the age of a crack in cementicious materials. Its usefulness, however, is limited to relative age and not the more desirable absolute age. Too many factors are as yet unquantified, namely the influence of environmental variation and mix design, to determine the absolute age of a single crack based on the amount of carbonation. Presently the most accurate method for applying carbonation in absolute age dating involves comparing the crack of unknown age to one of known age with similar width and exposure and determining the age based on the ratio of carbonation on each crack. The research

presented herein shows that differences from comparison of cracks of different widths could be compensated for by assuming a linear relationship between carbonation depth and crack width, which expands the application of the comparison technique by allowing comparison of cracks with more similar exposure that do not have the same crack width. The technique, however, still requires comparison to a crack of known age, which is not easily obtainable information. More research is needed to determine the age of a single crack solely based on carbonation through its surface.

Future Work

Carbonation as a means of determining crack age is a largely unresearched field. Little has been written on the subject of carbonation in cracked concrete, and those articles that have been written are generally associated with determining the depth that carbonation reaches into the crack from the material face, not carbonation penetration perpendicular to the crack surface. Literature that has mentioned carbonation as a crack-aging tool is not detailed in the application of such a method in the field nor are methods suggested in the limited applications of the method.

Additional research is needed to improve measurement of carbonation for crack dating. Determination of relationships between carbonation rates and concentration of carbon dioxide would provide the basis for extrapolation of carbonation rates measured at elevated concentrations to standard low concentrations. Additional research into crack width relationships would be helpful for present crack comparison analysis, but more effort should be made to move towards single crack analysis. Quantification of the

relative effect of variables affecting carbonation can facilitate prediction of carbonation rates for various cement mixes and different environmental conditions. Already there exists a relationship between w/c ratio and depth of carbonation as a percentage with respect to a reference w/c ratio. Similar relationships between carbonation penetration and factors such as admixtures, fly ash content, temperature, humidity, etc. will enable prediction of carbonation penetration for many different situations.

References

ASTM (1999) *Book of Standards*. C 305 -99 Standard Practice for Mechanical Mixing of Hydraulic Cement Pastes and Mortars of Plastic Consistency, American Society of Testing and Materials, Philadelphia, PA

Aurelius, Earl, ed. (1994) *The January 17, 1994 Northridge, CA Earthquake: An EQE Summary Report.* March 1994. http://www.eqe.com/publications/northridge/northridge.html

Campbell, D.H. et al. (1991) "Detecting Carbonation", *Concrete Technology Today*, Vol. 12, No. I.

Goni, S. (1997) "Microstructural Characterization of the Carbonation of Mortar made with Fly Ashes", *Performance and Curability of Cementitious Materials*, Vol. 4.

Hime, W.G. (2004) Personal Communication.

Hobbs, D.W. (1993) "Carbonation of Concrete Containing PFA", *Concrete Research*, Vol. 46, No. 166.

Idso, C.D., Idso, S.B. and Balling, R.C., Jr. (1998) "The urban CO_2 dome of Phoenix, Arizona", *Physical Geography* **19**: 95-108

Iyoda, T. and Uomoto, T. (1998) "Effect of Existence of Cracks in Concrete on Depth of Carbonation", Translated from Japanese.

Joshi and Lohtia (1997)

Meyer, A. (1968) "Investigations on the Carbonation of Concrete", Proceedings Chemistry of Cement, Tokyo, Vol. 3.

Mindess, S. and Young, J.F. (1981) *Concrete,* Prentice Hall, Inc., Englewood Cliffs, N.J.

Nagataki, S., Ogha H. and Kim, E. (1986) "Effect of Curing Conditions on Carbonation and Corrosion in Fly Ash Concrete", ACI SP-91, Madrid Proceedings, Vol. 1.

Neville, A. (2003) "Can We Determine the Age of Cracks by Measuring Carbonation? Part 1", *Concrete International*, December 2003.

Neville, A. (2004) "Can We Determine the Age of Cracks by Measuring Carbonation? Part 2", *Concrete International*, January 2004.

Nischer, P. (1984) "Effect of Environment and Concrete Quality on Carbonation", Betonwerk und Fertigteil-Tec

Nishi, T. (1962) “Outline of the Studies in Japan regarding the Carbonation of Concrete”, Proceedings RILEM Symposium 1962, Testing of Concrete.

Parrott, L.J. (1987) *A Review of Carbonation in Reinforced Concrete*, Cement and Concrete Association, London.

Patty, T. and Jackson, D.J. (2002) “Use of Carbonation to Date Cracks in Concrete” *Proceedings- Texas Section American Society of Civil Engineers* March 27-30, 2002

Schiessl, P. ed. (1988) *Corrosion of Steel in Concrete,* Report of the Technical Committee 60-CSC RILEM, Chapman and Hall, London.

U.S. EPA (2002) *Inventory of U.S. Greenhouse Gas Emissions and Sinks: 1990 – 2000*, U.S. Environmental Protection Agency, Office of Atmospheric Programs, EPA 430-R-02-003, April 2002. www.epa.gov/globalwarming/publications/emissions

Appendices

a. Round 1 Data 102

b. Round 2 Data 110

c. Relative Humidity Data 116

d. Gas Chromatography Data 118

e. Concrete Strength Data 119

a. Round 1 Data

10 mm Depth- Average Carbonation Penetration

Crack Width	Reading	Linear Best Fit	Variance
0	6	3.4623	0.19515
0	1	3.4623	0.18372
0	5	3.4623	0.07165
0	0	3.4623	0.36326
0	8	3.4623	0.62396
0.5	0	4.6842	0.6649
0.5	8	4.6842	0.33317
0.5	5	4.6842	0.00302
0.5	4	4.6842	0.01419
0.5	3	4.6842	0.08596
0.5	3	4.6842	0.08596
0.5	2	4.6842	0.21833
0.5	7	4.6842	0.16251
0.5	9	4.6842	0.56443
0.5	2	4.6842	0.21833
0.5	1	4.6842	0.41131
1	5	5.9061	0.02488
1	5	5.9061	0.02488
1	6	5.9061	0.00027
1	7	5.9061	0.03626
1	7	5.9061	0.03626
1	5	5.9061	0.02488
1	6	5.9061	0.00027
2	6	8.3499	0.16733
2	5	8.3499	0.34006
2	9	8.3499	0.01281
2	10	8.3499	0.08251
2	7	8.3499	0.05522
2	11	8.3499	0.21282
2	7	8.3499	0.05522
2	8	8.3499	0.00371
2	6	8.3499	0.16733
2	7	8.3499	0.05522
2	18	8.3499	2.73895
		sum	8.23873
		STD	2.87032

n = 34

Averages	
0	4
0.5	4
1	5.857143
2	8.545455
Overall	5.600649

Width	Linear	STD	σ_1	σ_1	Average
0	3.4623	2.870318	6.3	0.591982	5.6
0.5	4.6842	2.870318	7.6	1.813882	5.6
1	5.9061	2.870318	8.8	3.035782	5.6
2	8.3499	2.870318	11	5.479582	5.6

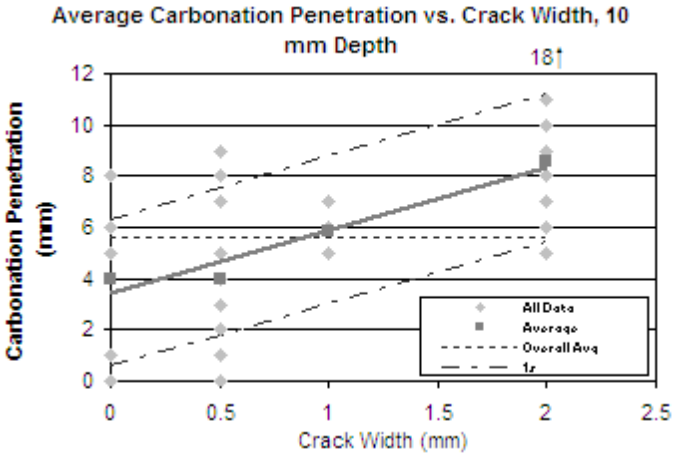

10 mm Depth- Maximum Carbonation Penetration

Crack Width	Reading	Linear Best Fit	Variance
0	8	7.2092	0.01839
0	3	7.2092	0.5211
0	6	7.2092	0.043
0	0	7.2092	1.5286
0	10	7.2092	0.22908
0.5	13	8.6787	0.54924
0.5	1	8.6787	1.73417
0.5	0	8.6787	2.21526
0.5	5	8.6787	0.39801
0.5	5	8.6787	0.39801
0.5	12	8.6787	0.32445
0.5	6	8.6787	0.21103
0.5	1	8.6787	1.73417
0.5	9	8.6787	0.00304
0.5	13	8.6787	0.54924
0.5	3	8.6787	0.94844
0.5	15	8.6787	1.17528
0.5	20	8.6787	3.76979
1	5	10.148	0.7795
1	5	10.148	0.7795
1	7	10.148	0.29149
1	9	10.148	0.03877
1	8	10.148	0.13572
1	11	10.148	0.02135
1	3	10.148	1.5028
1	8	10.148	0.13572
1	6	10.148	0.50608
2	11	13.087	0.1281
2	12	13.087	0.03475
2	25	13.087	4.1741
2	17	13.087	0.45034
2	17	13.087	0.45034
2	4	13.087	2.42863
2	6	13.087	1.47722
2	20	13.087	1.40558
		sum	31.0903
		std	5.57587

n = 35

Averages	
0	5.4
0.5	7.923
1	6.889
2	14
Overall	8.686

Width	linear	σ1	σ1	Overall Avg.
0	7.209	12.785	1.633	8.685714
0.5	8.679	14.255	3.103	8.685714
1	10.15	15.724	4.572	8.685714
2	13.09	18.663	7.511	8.685714

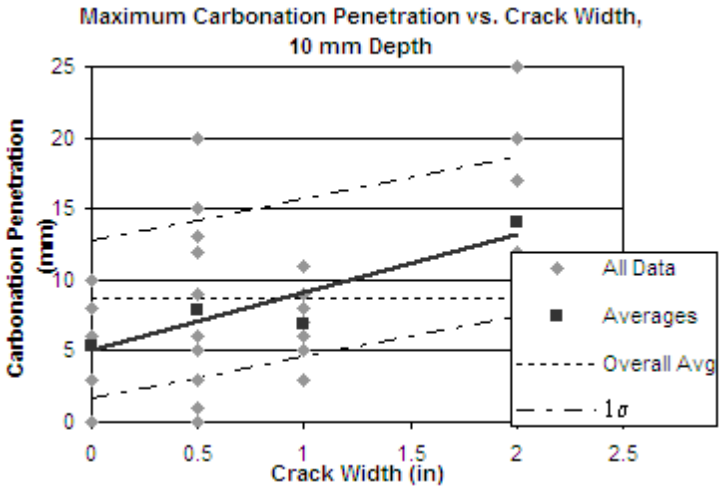

10 mm Depth- Minimum Carbonation Penetration

Crack width	Reading	Linear Best Fit	Variance
0	3	1.3908	0.0664
0	1	1.3908	0.00392
0	2	1.3908	0.00952
0	0	1.3908	0.0496
0.5	0	2.12795	0.11611
0.5	0	2.12795	0.11611
0.5	0	2.12795	0.11611
0.5	2	2.12795	0.00042
0.5	0	2.12795	0.11611
0.5	8	2.12795	0.88413
0.5	0	2.12795	0.11611
0.5	0	2.12795	0.11611
0.5	4	2.12795	0.08986
0.5	6	2.12795	0.38443
0.5	0	2.12795	0.11611
0.5	0	2.12795	0.11611
0.5	2	2.12795	0.00042
1	4	2.8651	0.03303
1	5	2.8651	0.11687
1	5	2.8651	0.11687
1	3	2.8651	0.00047
1	1	2.8651	0.08919
1	1	2.8651	0.08919
1	8	2.8651	0.67608
1	0	2.8651	0.21048
1	0	2.8651	0.21048
1	6	2.8651	0.25199
2	5	4.3394	0.01119
2	2	4.3394	0.14033
2	0	4.3394	0.48283
2	5	4.3394	0.01119
2	10	4.3394	0.8216
2	5	4.3394	0.01119
2	7	4.3394	0.18151
2	4	4.3394	0.00295
2	3	4.3394	0.046
2	0	4.3394	0.48283
2	0	4.3394	0.48283
2	0	4.3394	0.48283
2	14	4.3394	2.393
		sum	9.76248
		std	3.1245

n = 40

Averages

0	1.5
0.5	1.6923
1	3.3
2	4.2308
overall	2.9

Width	linear	avg.	1 s	1 s	
0	1.3908	2.9	4.5153	-1.734	-1.7337
0.5	2.128	2.9	5.2524	-0.997	-0.9965
1	2.8651	2.9	5.9896	-0.259	-0.2594
2	4.3394	2.9	7.4639	1.2149	1.25

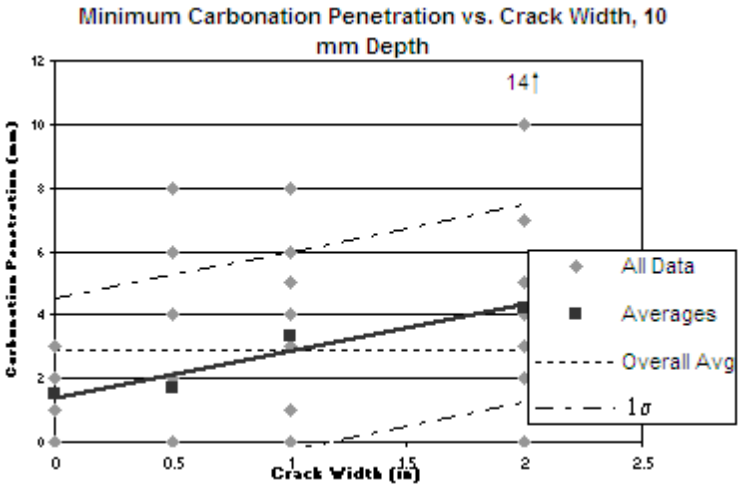

20 mm Depth- Average Carbonation Penetration

Crack Width	Reading	Linear Best Fit	Variance			Overall Avg.	Linear	1 s	
0	0	0.000	0.000	Width	average				
0	0	0.000	0.000	0	0.40	1.74	0.00	1.975	-1.975
0	0	0.000	0.000	0.5	0.45	1.74	1.02	2.993	-0.956
0	0	0.000	0.000	1	1.71	1.74	2.04	4.011	0.062
0	2	0.000	0.133	2	4.38	1.74	4.07	6.048	2.098
0.5	0	1.018	0.035						
0.5	1	1.018	0.000						
0.5	0	1.018	0.035						
0.5	0	1.018	0.035						
0.5	0	1.018	0.035						
0.5	0	1.018	0.035						
0.5	0	1.018	0.035						
0.5	2	1.018	0.032						
0.5	2	1.018	0.032						
0.5	0	1.018	0.035						
0.5	0	1.018	0.035						
1	4	2.037	0.129						
1	0	2.037	0.138						
1	3	2.037	0.031						
1	5	2.037	0.293						
1	0	2.037	0.138						
1	0	2.037	0.138						
1	0	2.037	0.138						
2	3	4.073	0.038						
2	2	4.073	0.143						
2	5	4.073	0.029						
2	4	4.073	0.000						
2	3	4.073	0.038						
2	3	4.073	0.038						
2	3	4.073	0.038						
2	12	4.073	2.095						
		sum	3.899						
		std	1.975						
n =	31								

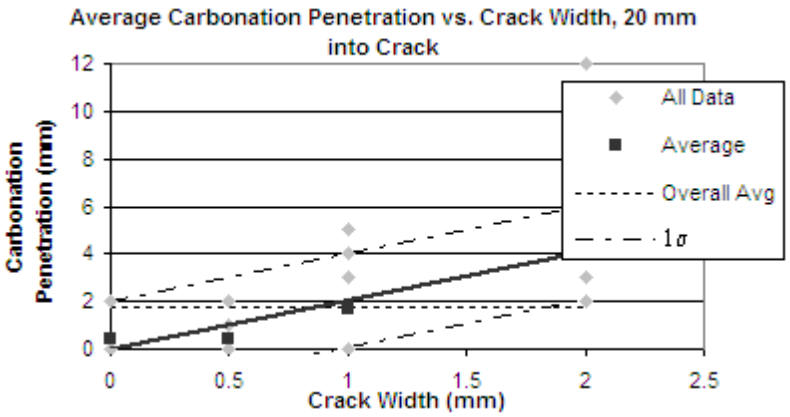

20 mm Depth- Maximum Carbonation Penetration

Crack Width	Reading	Linear Best Fit	Variance
0	0	2.2222	0.1593
0	0	2.2222	0.1593
0	7	2.2222	0.73637
0	15	2.2222	5.26684
0	1	2.2222	0.04819
0	0	2.2222	0.1593
0.5	1	4.66665	0.43369
0.5	0	4.66665	0.7025
0.5	10	4.66665	0.91757
0.5	6	4.66665	0.05735
0.5	3	4.66665	0.0896
0.5	4	4.66665	0.01434
0.5	6	4.66665	0.05735
0.5	6	4.66665	0.05735
0.5	4	4.66665	0.01434
1	0	7.1111	1.63122
1	0	7.1111	1.63122
1	7	7.1111	0.0004
1	6	7.1111	0.03982
1	0	7.1111	1.63122
1	0	7.1111	1.63122
1	9	7.1111	0.11509
1	5	7.1111	0.14377
1	11	7.1111	0.48786
2	5	12	1.58065
2	6	12	1.16129
2	10	12	0.12903
2	10	12	0.12903
2	12	12	0
2	25	12	5.45161
2	20	12	2.06452
2	20	12	2.06452
		sum	28.7658
n =	32	std	5.36338

Width	Average	Overall Avg.	Linear	1 s	1 s
0	3.8333	6.53125	2.2222	7.5856	-3.1412
0.5	4.4444	6.53125	4.66665	10.03	-0.6967
1	4.2222	6.53125	7.1111	12.474	1.74772
2	13.5	6.53125	12	17.363	6.63662

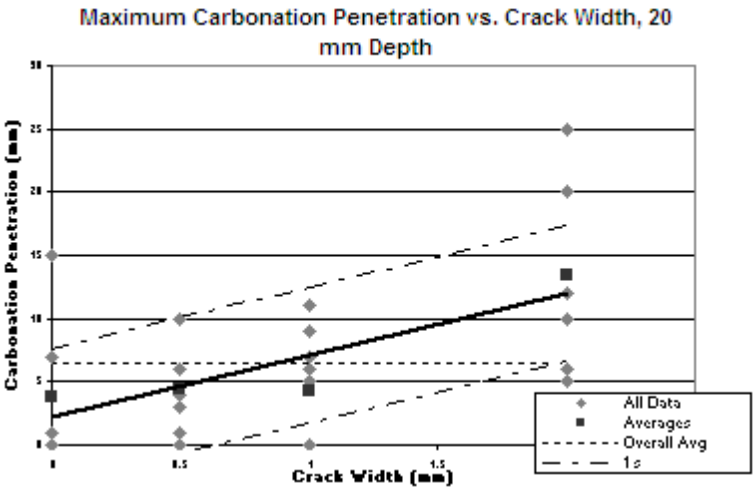

Depth Profiles Round 1

0 mm	10	20	35
	6	0	0
	1	0	0
	5	0	0
	0	0	0
	8	2	0
Avg.	4	0.4	0

0.5 mm	10	20	35
	0	0	0
	8	1	0
	5	0	0
	4	0	0
	3	0	0
	3	0	1
	2	0	0
	7	2	0
	9	2	0
	2	0	0
	1	0	0
Avg.	4	0.45	0.091

1 mm	10	20	35
	5	4	0
	5	0	0
	6	3	0
	7	5	0
	7	0	0
	5	0	0
	6	0	0
Avg.	5.86	1.71	0

2 mm	10	20	35
	6	3	0
	5	2	0
	9	5	2
	10	4	0
	7		0
	11		0
	7		
	8	3	0
	6	3	0
	7	3	0
	18	12	8
Avg.	8.55	4.38	1

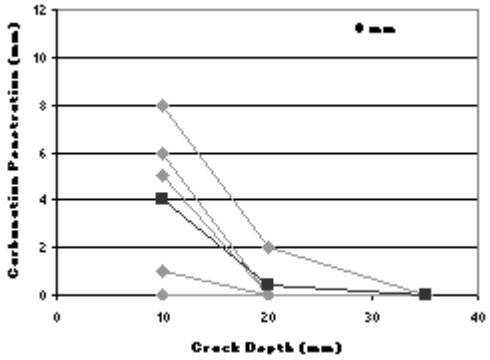

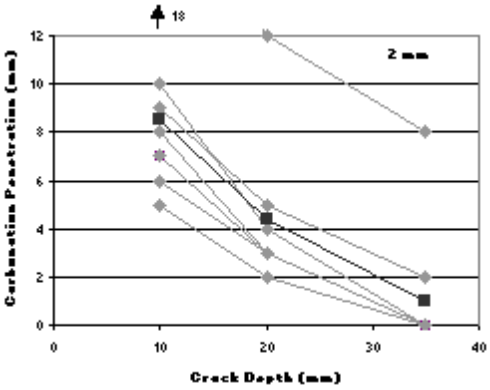

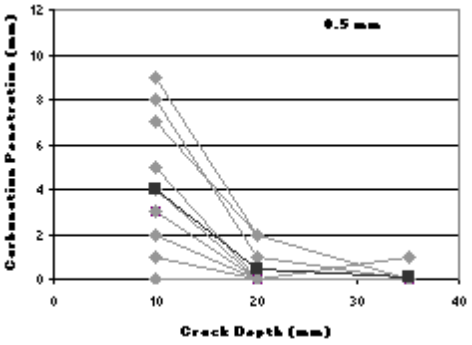

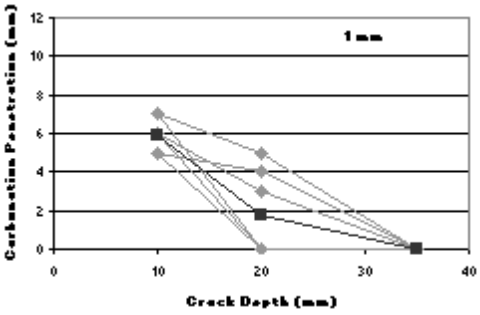

Carbonation Area Calculations

Width	Sample	Section	Area-C	Area-T	Percent	linear	Variance
0	3	3	400	1213	32.98%		
0		4	288	955	30.16%		
0	5	1	260	899	28.92%		
0		2	419	1314	31.89%		
0		3	198	1397	14.17%		
0		4	128	989	12.94%		
0	13	1	440	1487	29.59%		
0	46	3	273	1439	18.97%		
0		4	252	1157	21.78%		
0		1	178	1295	0.13745	0.179	3.1E-05
0		2	97	1306	0.07427	0.179	0.0002
0	2	3	100	1259	0.07943	0.179	0.00018
0.5		4	140	1147	0.12206	0.179	5.9E-05
0.5		1	212	653	0.32466	0.179	0.00039
0.5		2	192	577	0.33276	0.179	0.00043
0.5	23	3	248	1299	19.09%	0.179	2.6E-06
0.5		4	315	1377	0.22876	0.179	4.5E-05
0.5		1	134	1223	0.10957	0.179	8.8E-05
0.5		2	95	1247	0.07618	0.179	0.00019
0.5	24	3	66	1318	0.05008	0.179	0.0003
0.5		4	310	1474	0.21031	0.179	1.8E-05
0.5		1	239	1093	0.21866	0.179	2.9E-05
0.5		2	280	1165	0.24034	0.179	6.8E-05
0.5	26	1	229	1285	0.17821	0.179	1.1E-08
0.5		2	289	1305	0.22146	0.179	3.3E-05
0.5	35	3	175	1355	0.12915	0.179	4.5E-05
0.5		4	164	1353	0.12121	0.179	6.1E-05
0.5		1	111	1190	0.09328	0.179	0.00013
0.5		2	347	1271	0.27301	0.179	0.00016
0.5	44	3	114	1397	0.0816	0.179	0.00017
0.5		4	65	1224	0.0531	0.179	0.00029
0.5		4	250	1160	0.21552	0.205	2E-06
0.5		1	332	1370	0.24234	0.205	2.5E-05
0.5		2	294	1470	0.2	0.205	4.5E-07
1	20	1	211	1260	0.16746	0.205	2.6E-05
1		2	246	1366	0.18009	0.205	1.1E-05
1	42	3	281	1238	0.22698	0.205	8.8E-06
1		4	321	1179	0.27226	0.205	8.2E-05
1		1	405	1300	0.31154	0.205	0.00021
1		2	184	1212	0.15182	0.205	5.1E-05
1	45	3	338	1221	0.27682	0.205	9.4E-05
1		4	325	1312	0.24771	0.205	3.3E-05
1		1	437	1524	0.28675	0.205	0.00012
1		1	522	1101	0.47411	0.2571	0.00086
1	47	2	379	1393	0.27207	0.2571	4.1E-06
1	9	3	583	1258	0.46343	0.2571	0.00077
2		4	380	1091	0.3483	0.2571	0.00015
2		1	255	1241	0.20548	0.2571	4.8E-05

2		2	402	1251	0.32134	0.2571	7.5E-05
2	12	3	207	1280	0.16172	0.2571	0.00017
2		4	190	1290	0.14729	0.2571	0.00022
2		1	147	1209	0.12159	0.2571	0.00033
2		2	216	1303	0.16577	0.2571	0.00015
2	25	3	464	1291	0.35941	0.2571	0.00019
2		4	609	1483	0.41065	0.2571	0.00043
2		1	222	1364	0.16276	0.2571	0.00016
2		2	240	1366	0.1757	0.2571	0.00012
2	36	3	192	1228	0.15635	0.2571	0.00018
2		4	188	1239	0.15174	0.2571	0.0002
2		1	300	1078	0.27829	0.2571	8.2E-06
2		2	246	1320	0.18636	0.2571	9.1E-05
2	41	3	224	1240	0.18065	0.2571	0.00011
2		4	243	1099	0.22111	0.2571	2.4E-05
2		3	224	1240	0.18065	0.2571	0.00011
2		4	243	1099	0.22111	0.2571	2.4E-05
						sum	0.00801
			n	56		std	0.08951

Width	Avg.	Overall Avg.	σ1	σ1
0				
0.5	16.12%	21.37%	26.85%	8.94%
1	23.16%	21.37%	29.45%	11.55%
2	24.82%	21.37%	34.66%	16.76%

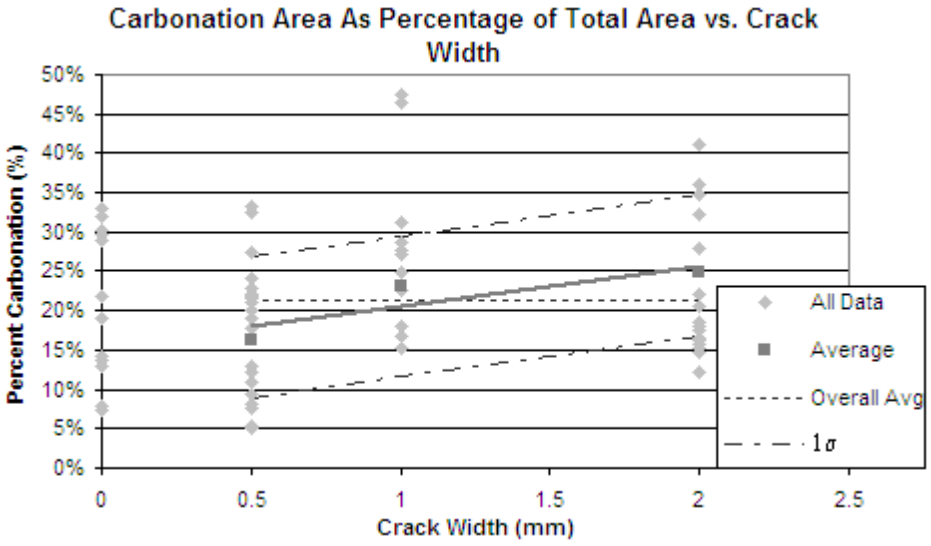

b. Round 2 Data

0 mm and 3 mm Crack Depth

Sample	Crack Width	Avg-0	Linear Best Fit	Variance	Avg-3	Linear Best Fit	Variance
1	0	13.42	7.81	0.92501	5.58	3.26	0.158365
2	0	0.67	7.81	1.50021	0.00	3.26	0.313133
3	0	10.42	7.81	0.20006	4.42	3.26	0.039152
4	0	13.25	7.81	0.87085	6.42	3.26	0.292537
6	0	1.50	7.81	1.17054	0.83	3.26	0.173612
8	0	13.92	7.81	1.09731	5.25	3.26	0.116134
9	0	5.00	7.81	0.23201	1.42	3.26	0.100252
12	0	9.08	7.81	0.04779	4.42	3.26	0.039152
14	0	0.00	7.81	1.79336	0.00	3.26	0.313133
16	1	7.00	7.28	0.00235	4.00	3.65	0.003692
17	1	8.83	7.28	0.07075	3.83	3.65	0.001035
18	1	8.08	7.28	0.01887	4.83	3.65	0.041484
19	1	14.08	7.28	1.36037	3.92	3.65	0.002159
20	1	5.00	7.28	0.15322	2.92	3.65	0.015632
21	1	8.67	7.28	0.05636	3.50	3.65	0.000624
22	1	8.67	7.28	0.05636	4.83	3.65	0.041484
23	1	8.67	7.28	0.05636	3.92	3.65	0.002159
24	1	5.83	7.28	0.06176	2.25	3.65	0.057293
25	1	5.50	7.28	0.09344	4.00	3.65	0.003692
26	1	9.58	7.28	0.15571	4.50	3.65	0.021466
27	1	7.67	7.28	0.00434	3.00	3.65	0.012263
28	1	5.83	7.28	0.06176	4.17	3.65	0.007983
29	2	5.58	6.76	0.04046	2.17	4.03	0.101954
30	2	6.33	6.76	0.00526	2.00	4.03	0.121024
31	2	4.50	6.76	0.14972	2.83	4.03	0.042012
32	2	9.75	6.76	0.26361	7.83	4.03	0.425787
33	2	6.67	6.76	0.00024	4.25	4.03	0.001443
34	2	11.58	6.76	0.68533	5.00	4.03	0.027759
35	2	4.58	6.76	0.13886	2.50	4.03	0.068715
36	2	2.38	6.76	0.56456	2.13	4.03	0.106568
37	2	3.17	6.76	0.37896	1.83	4.03	0.141728
38	2	1.58	6.76	0.78702	1.17	4.03	0.240885
39	2	2.92	6.76	0.43359	1.92	4.03	0.131172
40	2	16.58	6.76	2.84037	11.08	4.03	1.463843
41	2	7.83	6.76	0.03412	4.75	4.03	0.015311
			sum	16.3109		sum	4.644639
			std	4.03867		std	2.155143
		Linear	σ_1	σ_1	Linear	σ_1	σ_1
	0	7.81	11.849	3.77133	3.26	5.4151	1.104857
	1	7.28	11.319	3.24133	3.65	5.8051	1.494857
	2	6.76	10.799	2.72133	4.03	6.1851	1.874857

5 and 10 mm Crack Depth

Sample	Crack Width	Linear Avg-5	Best Fit	Variance	Linear Avg-10	Best Fit	Variance
1	0	2.00	1.06	0.02	0.00	0.06	0.000116
2	0	0.00	1.06	0.03	0.00	0.06	0.000116
3	0	1.00	1.06	0.00	0.25	0.06	0.000993
4	0	1.50	1.06	0.01	0.00	0.06	0.000116
5	0	0.00	1.06	0.03	0.00	0.06	0.000116
6	0	0.00	1.06	0.03	0.00	0.06	0.000116
8	0	2.33	1.06	0.05	0.08	0.06	1.11E-05
9	0	0.08	1.06	0.03	0.00	0.06	0.000116
12	0	2.67	1.06	0.07	0.25	0.06	0.000993
14	0	0.00	1.06	0.03	0.00	0.06	0.000116
16	1	2.75	1.70	0.03	0.83	0.56	0.002133
17	1	1.17	1.70	0.01	0.00	0.56	0.008963
18	1	2.50	1.70	0.02	1.25	0.56	0.013599
19	1	2.50	1.70	0.02	0.58	0.56	1.54E-05
20	1	1.00	1.70	0.01	0.00	0.56	0.008963
21	1	1.42	1.70	0.00	0.17	0.56	0.004423
22	1	2.92	1.70	0.04	0.25	0.56	0.002747
23	1	1.92	1.70	0.00	0.17	0.56	0.004423
24	1	0.83	1.70	0.02	0.25	0.56	0.002747
25	1	2.42	1.70	0.01	1.42	0.56	0.020963
26	1	2.58	1.70	0.02	1.17	0.56	0.010512
27	1	1.00	1.70	0.01	0.17	0.56	0.004423
28	1	1.83	1.70	0.00	1.17	0.56	0.010512
29	2	0.83	2.33	0.06	0.58	1.06	0.006399
30	2	0.67	2.33	0.08	0.25	1.06	0.018589
31	2	1.25	2.33	0.03	0.00	1.06	0.031897
32	2	4.58	2.33	0.14	2.33	1.06	0.046573
33	2	2.75	2.33	0.01	1.08	1.06	2.04E-05
34	2	2.92	2.33	0.01	1.33	1.06	0.002188
35	2	1.50	2.33	0.02	1.50	1.06	0.005617
36	2	1.25	2.33	0.03	0.00	1.06	0.031897
37	2	1.08	2.33	0.04	0.17	1.06	0.022628
38	2	1.33	2.33	0.03	0.75	1.06	0.002686
39	2	0.75	2.33	0.07	0.17	1.06	0.022628
40	2	4.88	2.33	0.18	4.50	1.06	0.338772
41	2	2.50	2.33	0.00	1.00	1.06	9.15E-05
		sum		1.24	sum		0.627215
		std		1.11166	std		0.791969
					avg.		0.60

Linear	σ_1	σ_1		Linear	σ_1	σ_1	
1.06		2.18	0.00	0.06	0.85197	-0.73197	
1.70		2.81	0.59	0.56	1.35197	-0.23197	
2.33		3.44	1.22	1.06	1.85197	0.279	

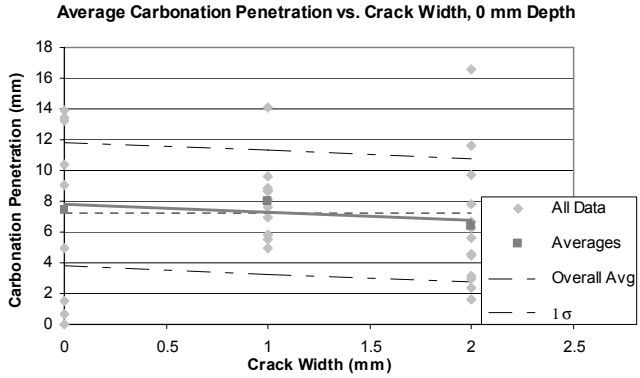
Average Carbonation Penetration vs. Crack Width, 0 mm Depth
Carbonation Penetration (mm)
Crack Width (mm)
All Data
Averages
Overall Avg
1σ

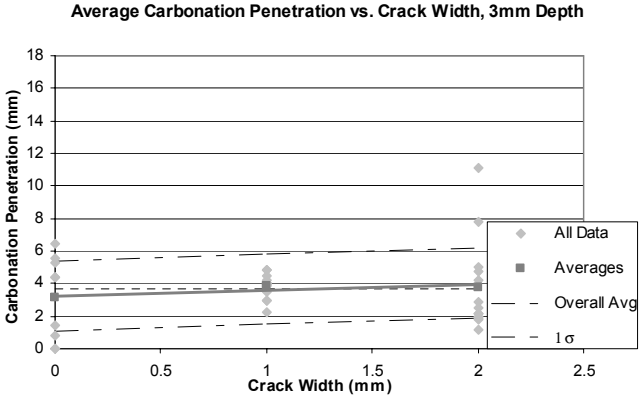
Average Carbonation Penetration vs. Crack Width, 3mm Depth
Carbonation Penetration (mm)
Crack Width (mm)
All Data
Averages
Overall Avg
1σ

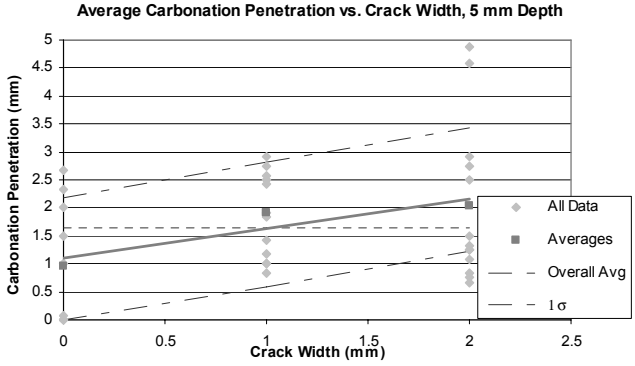
Average Carbonation Penetration vs. Crack Width, 5 mm Depth
Carbonation Penetration (mm)
Crack Width (mm)
All Data
Averages
Overall Avg
1σ

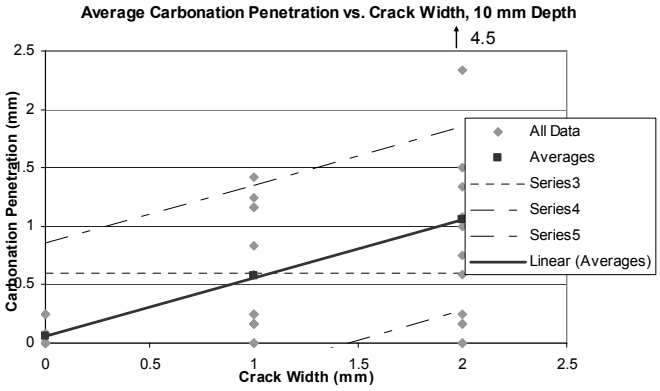
Average Carbonation Penetration vs. Crack Width, 10 mm Depth
4.5
Carbonation Penetration (mm)
Crack Width (mm)
All Data
Averages
Series3
Series4
Series5
Linear (Averages)

Carbonation Penetration Data

Sample	Crack Width	Avg-Max	Linear Best Fit	Variance
1	0	5.25	5.16	0.00025
2	0	0.83	5.16	0.53385
3	0	6.25	5.16	0.0342
4	0	6.58	5.16	0.05822
5	0	4.83	5.16	0.00297
6	0	0.67	5.16	0.57581
8	0	6.17	5.16	0.02919
9	0	2.75	5.16	0.16538
10	0	9.42	5.16	0.51869
12	0	8.17	5.16	0.25899
14	0	0.00	5.16	0.75952
16	1	10.50	7.64	0.23298
17	1	6.92	7.64	0.01513
18	1	12.00	7.64	0.54204
19	1	8.50	7.64	0.02092
20	1	7.17	7.64	0.00652
21	1	7.50	7.64	0.0006
22	1	7.17	7.64	0.00652
23	1	7.67	7.64	1.4E-05
24	1	6.58	7.64	0.03217
25	1	12.75	7.64	0.74478
26	1	8.25	7.64	0.01048
27	1	6.00	7.64	0.07726
28	1	9.00	7.64	0.0525
29	2	7.83	10.13	0.15109
30	2	6.00	10.13	0.48802
31	2	5.00	10.13	0.75276
32	2	17.08	10.13	1.38024
33	2	11.50	10.13	0.0534
34	2	10.58	10.13	0.0058
35	2	10.50	10.13	0.00385
36	2	6.13	10.13	0.45895
37	2	8.83	10.13	0.04825
38	2	11.33	10.13	0.04117
39	2	4.67	10.13	0.85371
40	2	16.17	10.13	1.04018
41	2	9.25	10.13	0.02227
			sum	9.97867
			std	3.1589

Linear	σ_1	σ_1
5.16	8.3148	1.997
7.64	10.8033	4.4855
10.13	13.2918	6.974

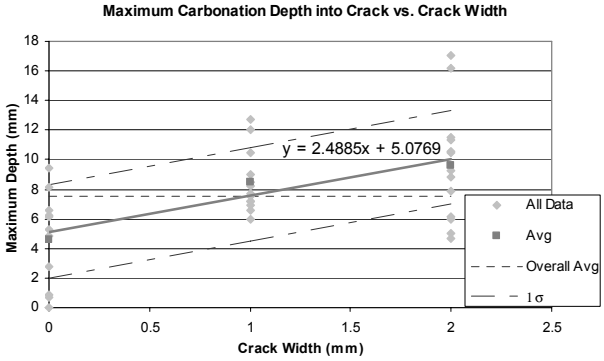

Depth Profiles

Sample	Crack Width	Crack Depth 0	3	5	10
1	0	13.42	5.58	2.00	0
2	0	0.67	0.00	0.00	0
3	0	10.42	4.42	1.00	0.25
4	0	13.25	6.42	1.50	0
6	0	1.50	0.83	0.00	0
8	0	13.92	5.25	2.33	0.08
9	0	5.00	1.42	0.08	0
12	0	9.08	4.42	2.67	0.25
14	0	0.00	0.00	0.00	0
	Average	7.47	3.15	0.96	0.06
16	1	7.00	4.00	2.75	0.83
17	1	8.83	3.83	1.17	0
18	1	8.08	4.83	2.50	1.25
19	1	14.08	3.92	2.50	0.58
20	1	5.00	2.92	1.00	0
21	1	8.67	3.50	1.42	0.17
22	1	8.67	4.83	2.92	0.25
23	1	8.67	3.92	1.92	0.17
24	1	5.83	2.25	0.83	0.25
25	1	5.50	4.00	2.42	1.42
26	1	9.58	4.50	2.58	1.17
27	1	7.67	3.00	1.00	0.17
28	1	5.83	4.17	1.83	1.17
	Average	7.96	3.82	1.91	0.57
29	2	5.58	2.17	0.83	0.58
30	2	6.33	2.00	0.67	0.25
31	2	4.50	2.83	1.25	0
32	2	9.75	7.83	4.58	2.33
33	2	6.67	4.25	2.75	1.08
34	2	11.58	5.00	2.92	1.33
35	2	4.58	2.50	1.50	1.5
36	2	2.38	2.13	1.25	0
37	2	3.17	1.83	1.08	0.17
38	2	1.58	1.17	1.33	0.75
39	2	2.92	1.92	0.75	0.17
40	2	16.58	11.08	4.88	4.5
41	2	7.83	4.75	2.50	1
	Average	6.42	3.80	2.02	1.05

Width	Depth	Linear	σ_1	σ_1
0 mm	3	2.5618	4.113	1.01
	5	1.7796	3.331	0.228
	10	-0.1759	1.376	-1.73
1 mm	3	3.3801	4.166	2.595
	5	2.5271	3.313	1.742
	10	0.3946	1.18	-0.39
2 mm	3	3.0196	4.17	1.869
	5	2.6479	3.799	1.497
	10	0.8729	2.024	-0.28

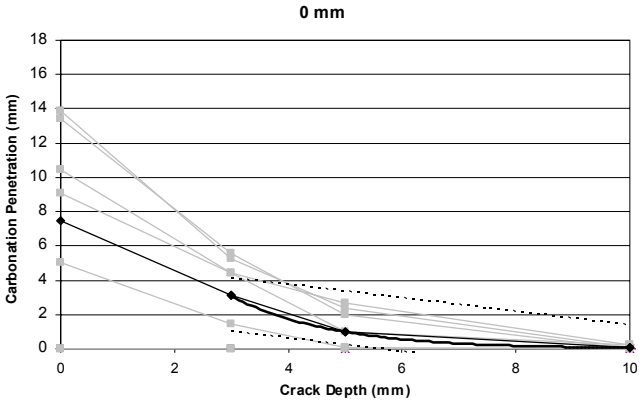
0 mm
Carbonation Penetration (mm)
Crack Depth (mm)
0
2
4
6
8
10
12
14
16
18

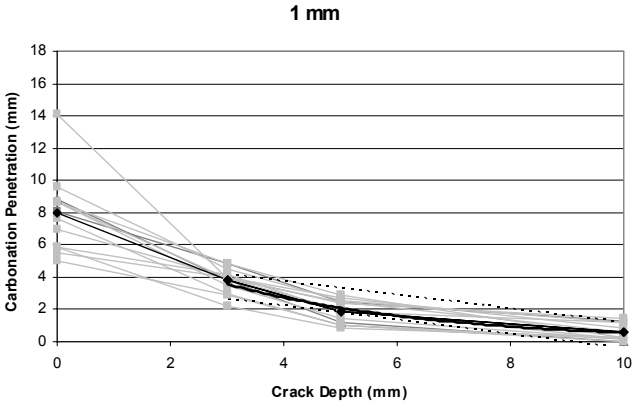
1 mm
Carbonation Penetration (mm)
Crack Depth (mm)
0
2
4
6
8
10
12
14
16
18

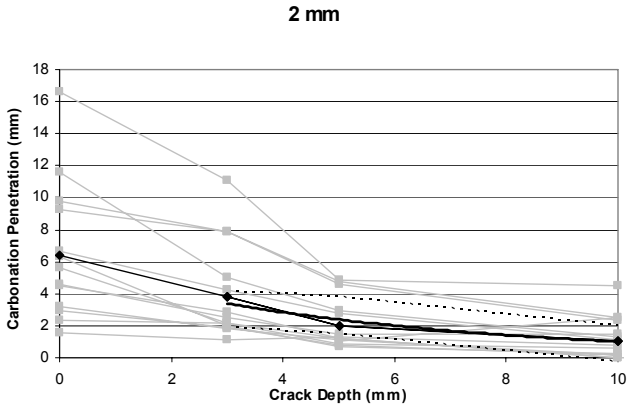
2 mm
Carbonation Penetration (mm)
Crack Depth (mm)
0
2
4
6
8
10
12
14
16
18

c. Relative Humidity Data

Round 1

Date	Reading
29-Mar	70%
30-Mar	88%
31-Mar	89%
2-Apr	87%
3-Apr	85%
5-Apr	80%
6-Apr	81%
8-Apr	81%
10-Apr	83%
12-Apr	85%
13-Apr	83%
14-Apr	82%
15-Apr	85%
16-Apr	84%
18-Apr	83%
19-Apr	85%
20-Apr	85%
21-Apr	85%
22-Apr	85%
23-Apr	85%
26-Apr	85%
27-Apr	85%
28-Apr	85%
29-Apr	85%
30-Apr	85%
1-May	85%
3-May	85%
4-May	85%
5-May	85%
6-May	85%
8-May	85%
10-May	85%
11-May	85%
13-May	85%

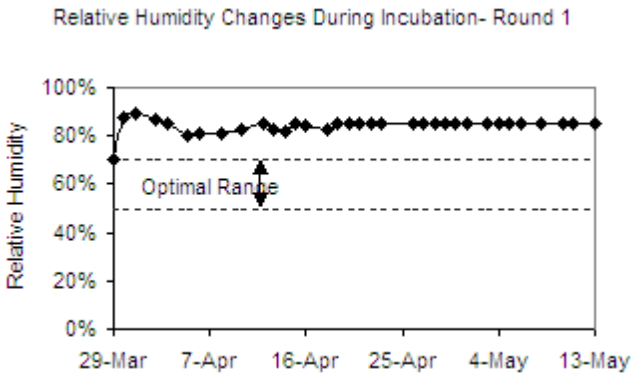

Round 2

Date	Reading
1-Jul	93%
14-Jul	93%
14-Jul	71%
29-Jul	87%
29-Jul	70%
11-Aug	79%
11-Aug	68%
15-Aug	51%

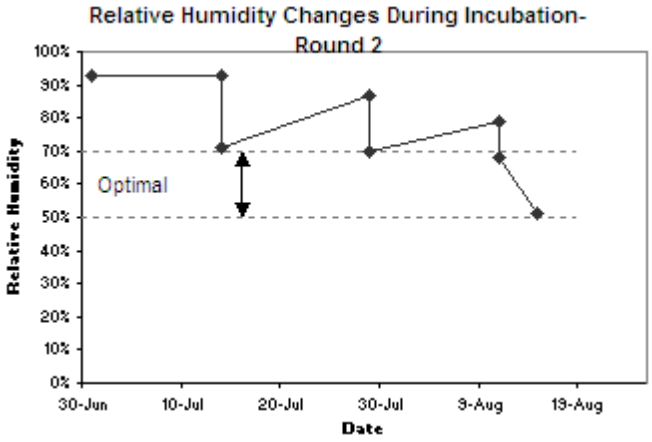

d. Gas Chromatography Data

% CO_2	% Air	Reading
100	0	13075760
100	0	13426672
100	0	13782152
90	10	12688264
90	10	12349960
80	20	11286360
80	20	11410392
70	30	10040312
70	30	9981734
60	40	8201501
60	40	8968154
50	50	7188865
50	50	6894085
40	60	5436282
40	60	5862013
30	70	4132778
30	70	4451267
20	80	3045768
20	80	2908706
10	90	2081660
10	90	1886443
0	100	16893
0	100	181954

% CO_2	Average
100	13428195
90	12519112
80	11348376
70	10011023
60	8584828
50	7041475
40	5649148
30	4292023
20	2977237
10	1984052
0	99423.5

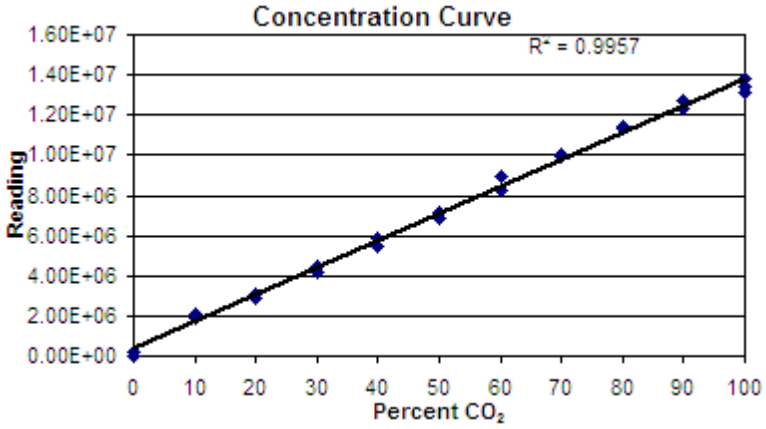

Date	Reading	Percent	0
26-Apr	13166344	0.9805	98.05
0	12015648	0.894807	89.84
0	13642880	1.015988	101.06

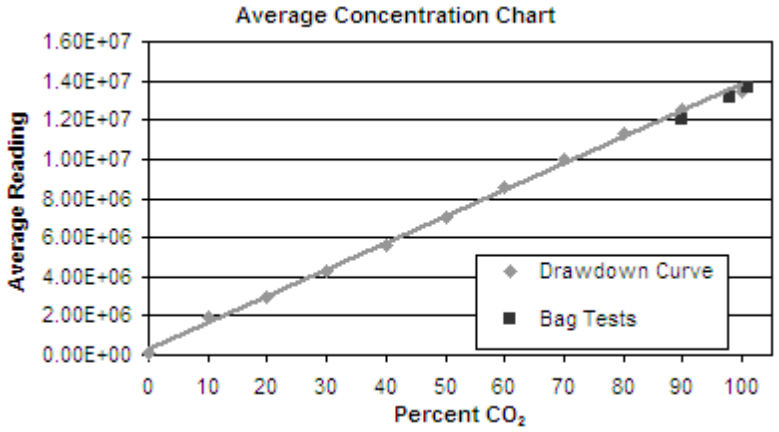

e. Concrete Strength Data

Concrete Strength

2" cubes tested in compression at 32 days

Fly ash %		35%	50%
Sample		lbs	lbs
1		23,072	16,201
2		24,494	17,024
3		21,108	18,537
4		--	17,282
Avg. Load	lbs	22,891	17,261
Strength	psi	5723	4315
	MPa	34.46	29.75

Accuracy to +/- 110 lbs (0.1% of 110 kips)

Loaded at 3000 lbs/min